Iraq Republic
Ministry of H. E. and S. R.
University of Babylon
College of Engineering
Environmental Department

HYDRODYNAMIC AND WATER QUALITY MODEL FOR EUPHRATES RIVE (FROM HINDIYA TO KUFA BARRAGE)

A THESIS

SUBMITED TO THE DEPARTMENT OF ENVIRONMENTAL ENGINEERING OF THE COLLEGE OF ENGINEERINGIN UNIVERSITY OF BABYLON AS PARTIAL FULFILLMENT OF THE

REQUIREMENTS FOR THEDEGREE OF MASTER IN ENGINEERING ENVIRONMENTAL ENGINEERING

By

Zainab Nadhum Hadi Al-Husseiny

(B.Sc. Environmental Eng., 2012)

Supervisor

Prof. Dr. Nisren Jassim Hussien Al-Mansori

1443 AH **2021 AD**

بسم الله الرحمن الرحيم

قَالَ رَبِّ ٱشۡرَحۡ لِي صَدۡرِي (25) وَيَسِّرۡ لِيٓ أَمۡرِي (26) وَٱحۡلُلۡ عُقۡدَةٗ مِّن لِّسَانِي (27) يَفۡقَهُواْ قَوۡلِي (28)

صدق الله العلي العظيم

سورة طه

الآيات (25، 26، 27)

Supervisors' Certificate

I certify that the thesis entitled " ***HYDRODYNAMIC AND WATER QUALITY MODEL FOR EUPHRATES RIVE (FROM HINDIYA TO KUFA BARRAGE) "*** *was prepared by "Zainab Nadhum Hadi ", under my supervision at the Environmental Engineering Department/ College of Engineering/ University of Babylon, as a partial fulfillment of the requirements for the degree of Master in Engineering/ Environmental Engineering.*

Signature:

Name: Prof. Dr. Nisren Jassim Hussien Al-Mansori

Date: / /2021

DEDICATION

To

How do I get the description and words that embody your struggle in life…? I dedicate this fruit to efforts that gave me strength and patience… To dear my heart… My Father and Mother … I ask God to protect they for us.

To

Who have the widest hearts which always give…

My Sisters and My brothers.

Zainab

2021

ACKNOWLEDGEMENT

"In the Name of Allah, the Most Gracious, the Most Merciful"

Praise to Allah his Majesty before anything and after anything and to the prophet "Mohammed and Ahl-Al-Bait" for the strength, courage, and wisdom that Allah gave me to complete this humble work and lengthy journey this degree.

I would like to express my deepest gratitude and respect to my thesis supervisor Prof. Dr. Nasreen Jassim Al-Mansori. I am very grateful for her precious time spent and useful suggestions which provided valuable guidance and important role in the completion of thesis as well as the moral support continued for the duration of the search, calling God richly rewarded him.

I would like to thanks to President of Environmental Engineering Department Asst. Prof. Dr. Hussein Ali Al-Zubaidi. For his help and he never saved an effort to help us and others.

I would like to thanks to Asst. Prof. Dr. Ahmed Nasih Hamdan. For him assistance throughout this work.

I would also like to thank the staff of Environmental Engineering laboratory at the University of Babylon for their assistance in providing laboratory equipment's through this work.

I would like to express my sincere thanks and gratitude to Eng. Ahmad T. Jaiad. Which had a great role by extending a helping hand to me throughout this work. I hope you, the Mighty Galilee to live up the highest echelons of scientific and practical.

Zainab

2021

ABSTRACT

The HEC-RAS Program was used to analyze one-dimensional unsteady flow in open channel and water quality analysis for the Euphrates River (from Hindiya Barrage to Kufa Barrage) in this thesis. The water quality model can be used to track the path of pollutants along the study area, While the hydraulic model developed herein can be used to analyze, monitor, and map river flows. It provides a means for understanding and representing the hydraulics characteristics for river. It has been successfully applied to the Euphrates River network, which consists of a main reach with 65 cross sections. The following is the order in which this work was completed:

In the hydrodynamic side and using the HEC-RAS model the calibration of the direct routing model for the Euphrates River over the period (1/1-30/6/2020) The accuracy of calculated Manning's roughness coefficient (n) is crucial in making exact predictions in this work based on observed regular stage and flow data. As a result, the roughness coefficient values (0.045) and (0.047) are optimal for the main channel and floodplain, respectively, as well as the time weighting factor (θ), which was introduced herein as a unity. To determine the degree of agreement between observed and computed outcomes, measurable parameters such as the root cruel square mistake (RMSE) and coefficient of assurance (R2= 0.056, 7.453) were utilized.

For analysis water quality data, the samples for laboratory work were collected along four months (January, February, March, April). The studied parameters, for water quality, were [Temperature (T), Acidity Function(pH), Total Dissolved Solids (TDS), Dissolved Oxygen (Do)]. After that, these parameters were fed to the HEC-RSA program, in addition to the meteorological data, which were

obtained from the Meteorological Directorate (Baghdad). The measured and calculated parameters were compared for each component, and the results showed an acceptable agreement between the calculated and observed values.

Highest temperature T =34.1C recorded at 13:30 noon, the highest value of DO was at 18:45 at noon, while the lowest value of DO was at 15:415 pm at night.DO= 4.9 mg/l , DO= 2.45 mg/l, the highest pH value was at 16:45 in the morning, while the lowest value was at 1:45 pm. pH= 8.03 , 6.9 ,the highest value reached by the total dissolved solids was at 9:00 noon, while the lowest value was at 1:30 at night .TDS= 1054 mg/l , 736 mg/l.

Table of CONTENTS

Table of CONTENTS

List of FIGURES

List of FIGURES

List of TABLES

List of SYMBOLS

Symbol	Description	Unit
v	Instantaneous velocity in the y-direction	L/T
u	Instantaneous velocity in the x-direction	L/T
q	channel length of the total lateral seepage flow and lateral overland flow	m^3/s
S_f	friction slope	L/L
Sb	the bed slope	L/L
n	Manning coefficient	-
h	the hydrograph stage value	l
Fn	Rate of transfer of substance per unit area of section	L/T
D_T	Lateral dispersion coefficient	L^2/T
D_L	Longitudinal dispersion coefficient	L^2/T
C	Concentration of pollutant	M/L^3
g	Acceleration due to gravity	L/T^2
H	Average flow depth	L
K	Turbulence kinetic energy	L^2/T^2
Q	Discharge	M^3/T
R	Hydraulic radius	L
S	Slope of bed channel	L/L
t	Time	T
T	Top width of water	L
U	Stream velocity	L/T
U_*	Shear velocity	L/T
u^-	Time-averaged velocity in the x-direction	L/T
Greek Symbols		
μ*	Function of channel geometry and crosssectional velocity distribution	-
μ	Dynamic fluid viscosity	M/L.T
β	Proportionality constant	
p	Fluid's density	M/L^3
υ	Kinematic viscosity	L_2/T

CHAPTER ONE

INTRODUCTION

1.1 Introduction

Open channels are found in natural rivers, basins and estuaries. Several problems in water resources, river dynamics and environmental hydraulics need an accurate definition of the characteristics of the flow system parameters of these channels, making water resource analysis, development and management one of the key concerns of engineers.

The increasing demand for limited water resources, the need to conserve the quality of water suitable for human, industrial and agricultural uses, and the dynamic interactions between the various components of the human-water environment have led to the use of more advanced forecasting techniques. In the planning, design and management of the water resources system, This forecast is important for forecasting criteria cover a number of topics, such as surface or ground water prediction, resources and their quality.

In the assessment of surface water quality in Iraq, the Euphrates River is of particular significance because anthropogenic and recreational activities result in significant changes in the quality of river water and pose a serious threat to the quality of river water. In order to describe and predict the observed and future effects of a change in the river system, modelling the quality of a river system is usually done. Therefore, modeling can be used as an aid to decision-making on quality control for resource distribution to achieve designated targets for water quality. For the selection of the position of water intakes for different uses such as agricultural, industrial water supply purposes, the prediction of the distribution of pollutant concentrations in the river is significant.

1.2 Problem Statement

The basis for the conservation and fair use of water resources is an accurate measure of the degree of water pollution. Water quality in rivers is continuously impaired by natural processes resulting from eutrophication and for anthropogenic causes, so there is a need for successful decision-making approaches that can be implemented to address problems with water quality management.

Four issues are the most common problems with water quality in rivers: -

1. Siltation refers to the deposition on the bottom of the river of small sediment particles (silt), the suffocation of fish eggs and the degradation of aquatic insect habitats, and the depletion of the food system sustaining fish and other wildlife. Siltation can occur as a result of construction, agriculture and forest operations.
2. Pathogenic surface water pollution can cause problems with human health, ranging from basic skin rash to acute gastroenteritis. Inadequately treated urban wastewater, wildlife fecal material and agricultural, the major sources of pathogens.
3. Nutrient contamination refers to large levels of nitrogen and phosphorus in the water. Increased plant and algae growth are caused by inadequate quantities of nutrients, resulting in decreased oxygen levels and diminished fish and other desirable aquatic populations. The primary sources of nutrients are urban and industrial wastewater discharges and drainage from agricultural land and forestry operations.
4. The discharge into rivers and streams of oxygen-demanding content triggers a loss of dissolved oxygen downstream from the discharge site. This poses problems for marine life and has a serious effect on a river or stream 's natural biota. Municipal and municipal waste water and agricultural and urban runoff are the origins of oxygen-demanding pollutants.

1.3 Objectives of The Research

The primary aim of the research is to build a one-dimensional water quality model using the Hydrodynamics and Water Quality Model (HEC-RAs) software for the Euphrates River system (from Hindiya to Kufa Barrage). This involves collecting data on water quality and flow channels for the scheme of the Euphrates River. The current research is split into two parts:

❖ **Hydrodynamic Modelling**

- To calibrate the value of Mannnig's "n" coefficient by using HEC-RAS unsteady flow model for Euphrates River by comparing water surface profiles with the observed one.

❖ **Water Quality Modelling**

- To test certain water quality improvement management scenarios in the Euphrates River
- To estimate the water quality components such as the Euphrates River's Temperature (T), total dissolved solids (TDS), dissolved oxygen (DO) and acid function (pH) by taking samples from the water and undergoing certain laboratory tests and then using the HEC-RAs (5.0.7) simulation software for simulation.

1.4 Thesis Layout

The dissertation is broken down into five chapters and arranged as follows:

1. **Chapter One: Introduction**

   An introduction to the research and the aim of this study in addition to the determinants and the study plan.

2. **Chapter Two: Theoretical concept & Literature review**

   A general study of hydraulic techniques, flood characteristics and processes for water quality throughout review of literatures is given

3. **Chapter Three: Data Collection &Experimental Work**

   The practical side of the study includes sites for taking samples from the river, methods of measurement, and devices used.

4. **Chapter Four: Results & Discussions**

   This chapter focuses on the study area and uses the HEC-RAS software to prepare the hydraulic model for this study area and evaluate the model using the calibration and verification process in the addition water quality model using the simulation for each parameter.

5. **Chapter Five: Conclusions & Recommendations**

CHAPTER TWO

THEORY AND LITERATURE REVIEW

2.1 Introduction

Interest in using unsteady models directly for river modeling has grown in recent years, as hydrology and hydraulics have become a major concern for predictions of river flow in open channels. It is possible to outline the establishment of the modern analysis of unstable flow in open channels to the latter half of the nineteenth century, when the French engineer Saint-Venant introduced the partial differential equations of continuity and momentum governing free surface flow in open channels.

2.2 Hydraulic flow routing model

The method of hydrological routing depends on the solution of mass equation conservation and the relationship between storage and discharge in a stream or reservoir range. The system simulates stage and discharge to account for storage as Water flows into the stream channel and the system of water control. In general, the system of hydrological flood routing consists of two parts, the first dealing with the change of rainfall into runoff and the second with the routing of that runoff to the outlet of catchments. The flood routing method based on hydrological modeling methodology is constrained in that the catchment parameter is lumped together in a simplistic way that results in surface profile misrepresentations. The system of hydrological flow routing also neglects the impact of back water and is not accurate for fast rising hydrographs routed through mild to flat inclined rivers (Sibanda, 2015). By using hydraulic flow routing methods such as the dynamic

model, several of the limitations of hydrological modeling listed as stated above can be addressed.

Previous studies have verified the functional validity of the flood routing hydraulic model, despite the fact that it is not economically feasible to collect cross-sectional data covering more than one hundred kilometers of flood routing operation. Hydraulic flow routing models were used in the assessment of flood plain depth, required altitudes of structures such as bridges or levees, real-time forecasts of river floods and flood maps for dam break contingency planning, according to Fread (1992).

2.2.1 Saint-Venant Equations

The Saint-Venant equations representing mass and momentum conservation for one-dimensional open channel flow were based on assumptions used in their derivation. The following assumptions were made when the Saint-Venant equations were extracted from (Litrico and Fromion,2009):

1. The flow is one-dimensional, i.e., across the cross section, the velocity is uniform and the water level is horizontal over the section.
2. The effects of boundary friction and turbulence can be considered similar to those used for steady-state flow via the resistance law.
3. The average slope of the channel bed is slight, so that unity can alter the angle of cosine it makes with the horizontal.
4. Streamline curvature is minimal and vertical accelerations can be insignificant, so the strain is hydrostatic.
5. The variations in the width of the channel along x are minimal.

   We assume that there is negligible distributed lateral inflow and outflow. A longitudinal axis indexed by the x-coordinate is shown in the Figure lengthwise (2.1).

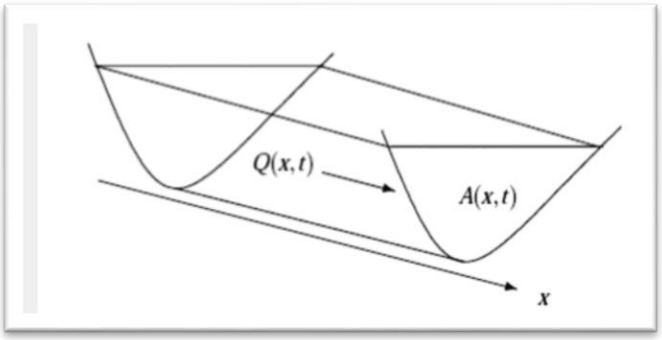

Figure (2.1): Flow of open channels along the longitudinal axis

Governing Equations:

The discharge Q (x, t) is defined as:

$$Q(x,t) = \mathrm{A(x,t)v(x,t)} \qquad (2\text{-}1)$$

The equations in Saint-Venant are two partial deferential equations combined. The first equation is the equation of mass conservation [Chow (1959); Henderson (1966); Chow et al. (1988); Chanson (2004); Litrico and Fromion (2009)]:

$$\frac{\partial A(x,t)}{\partial \mathrm{t}} + \frac{\partial Q(x,t)}{\partial \mathrm{x}} - q = 0 \qquad (2\text{-}2)$$

Which is the q per channel length of the total lateral seepage flow and lateral overland flow. The momentum conservation equation is the second equation:

$$\frac{\partial v}{\partial \mathrm{t}} + v\frac{\partial \mathrm{v}}{\partial \mathrm{x}} + g\frac{\partial y}{\partial x} - g\left(S_0 - S_f\right) = 0 \qquad (2\text{-}3)$$

v velocity gradient, S_0 slope of the channel bottom, with the classical Manning formula modelled on the friction slope S_f:

$$\mathrm{S_f} = \frac{Q^2 n^2}{A^2 R^{4}/_{3}} \qquad (2\text{-}4)$$

Which:

n = is the Manning coefficient, and R the hydraulic radius (L), defined by:

$$R = \frac{A}{B} \quad (2\text{-}5)$$

P = is the wetted perimeter.

2.2.2 Numerical Solution of Governing Equation

In order to describe these equations in numerical solutions, such as finite difference methods, the governing equations are carried out in two steps. Earliest step, the equations are replaced by an equation of algebraic finite difference, and secondly step, through solving linear equations, the solution of differential equations is achieved. A range of numerical techniques can be developed depending on how the procedure is performed in one or both of the steps (Zhan, 2003). The channel is split into a number of reaches. At discrete times, computations were carried out. The (x-t) plane is divided into a row, commonly referred to as the computational grid, Figure (2-2), (Chow et al., 1988).

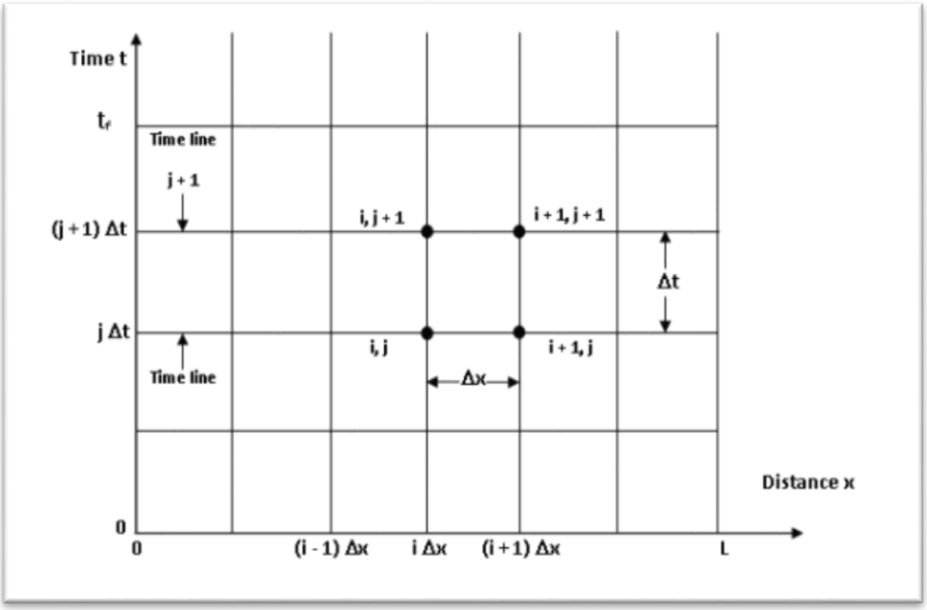

Figure (2-2): Grid of points [After Chow et al., 1988] on (x-t) plane

The explicit and implicit arrangements are further categorized by all finite difference arrangements used in the direct and characteristic methods. The finite difference equations were usually linear algebraic equations in the explicit scheme, from which the unknowns can be directly determined. The implicit scheme of the unknown exists implicitly in equations of finite differences that are normally nonlinear algebraic equations. The implicit method is mathematically more complicated, but it is stable, efficient and much faster from the explicit method, especially when treating long-term unsteady flow phenomena such as floods in Major River. Moreover, the implicit method can also handle channel geometry varying significantly from one channel cross section to another (Chow et al., 1988).

According to above reasons, the implicit method is adopted herein to solve routing problem of Euphrates River (from Hindiya to Kufa Barrages)

The weighted four-point finite difference approximations appear most advantageous and stable among different implicit finite difference arrangements that have been advanced because they can be used with imbalanced distance and time steps (Gündüz,2004).

2.2.3 Formulation of Saint Venant Equations by Finite Difference Method

In this section, the finite difference formulation of the dynamic flood routing equation (2.1) will be detailed. In the implicit creation, all derivative terms and other parameters were approximated by use the unknown at the forward time line (j+1) as shown in the x-t grid shown in Figure (2.3) below. The tacit methods of finite differences advance solutions simultaneously from one time line to the next at all points in the time line.

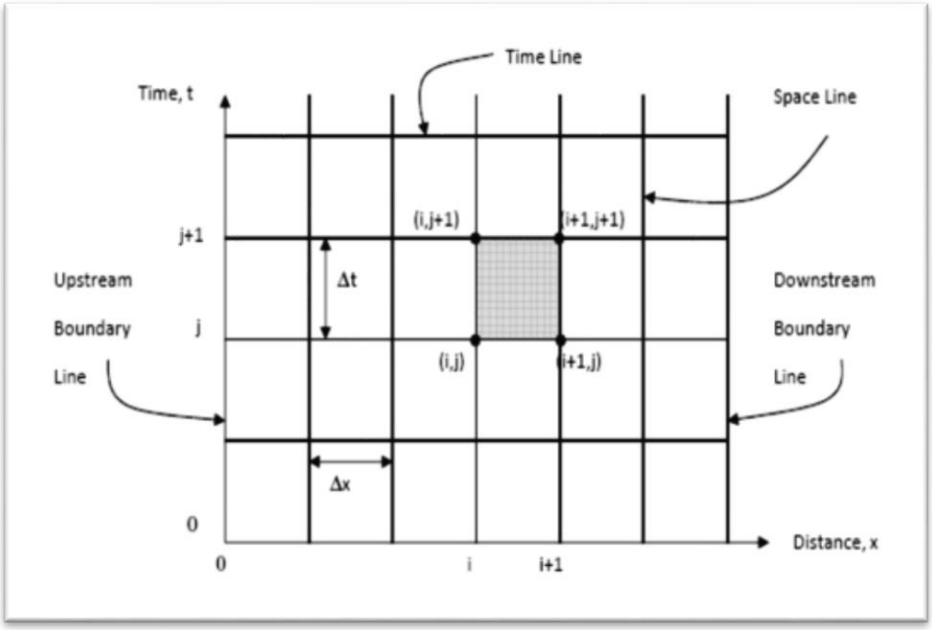

Figure (2-3): The time grid of distances used to formulate the implicit scheme of finite differences [After Gündüz, 2004]

The net points were determined by the intersections of straight lines, these parallel to the x axes and t axes, on a distinct rectangular net of points on the (x, t) plane. The lines drawn parallel to the t-axis represent points in the channel and times are drawn parallel to the x-axis. Spacing (Δx_i) draws the position lines, while spacing (Δt_j) draws the time lines. While Δx and Δt are assumed to be constant for simplicity in this development, in practice Δx and Δ t will differ as needed in space and time. The t-axis can be used as the boundary location of the upstream channel, and the last line drawn parallel to the t-axis can be used to symbolize the boundary of the downstream channel, to be designated the N^{ith} line. Two indices mark each point of the network, a subscript (i) to denote the x-positions of the point, and a superscript (j) to designate the time value as shown in the above Figure (2.4). Another important aspect of the Pressman's scheme is the applicability of an equal time stage, mainly in the case of hydrograph routing, where flood waters will usually increase relatively rapidly and leave gradually over time. The four points of the grid from the $(j)^{th}$ and $(j+1)^{th}$ time lines are used in this arrangement to approximate the term in the differential equations. In order to change the effect of the points (i) and (i+1), a weighing factor, θ, is used in the measurement of all terms of the equations except for the time derivative. For the dummy parameter F, the approximations of the derivative and constant terms in the four-point weighted difference schemes are given as follows.

Time derivative $\left(\frac{\partial F}{\partial t}\right)$:

$$\frac{\partial F}{\partial t} = \varphi \frac{F_{(i+1)}^{(j+1)} - F_{(i+1)}^{j}}{\Delta t^{j}} + (1-\varphi)\frac{F_{i}^{(j+1)} - F_{i}^{j}}{\Delta t^{j}} \qquad (2\text{-}6)$$

Space derivative $\frac{\partial F}{\partial x}$:

$$\frac{\partial F}{\partial x} = \theta \frac{F_{(i+1)}^{(j+1)} - F_{(i)}^{(j+1)}}{\Delta x^{i}} + (1-\theta)\frac{F_{(i+1)}^{j} - F_{i}^{j}}{\Delta x^{i}} \qquad (2\text{-}7)$$

$$F = \theta \frac{F_{(i+1)}^{(j+1)} - F_{(i)}^{(j+1)}}{2} + (1-\theta) \frac{F_{(i+1)}^{j} - F_{i}^{j}}{2} \quad (2\text{-}8)$$

Where I and j were subscripts on the x and t axes, φ and θ are weighing factors between 0 and 1, respectively, and Δ x and Δ t are incremental duration and time of reach, respectively. If the value of θ is chosen between 0.5 and 1.0, the weighted four-point implicit scheme is unconditionally stable for any time stage. Examination of the effect of the weighing factor on the accuracy of computations, in addition to stability parameters, showed that the accuracy decreases as 0.5 departs from and approaches 1.0. When the magnitude of the computational time step increased, this effect became more pronounced. In addition, analysis also revealed that unconditional stability and good accuracy were provided by a θ value of between 0.55, 0.6, making this scheme superior compared to the explicit scheme that requires time steps of less than a critical value determined by the Courant condition.

2.2.4 The Boundary Conditions

The two additional equations needed for the system to be calculated derive from the external limits. At the upstream and downstream locations of the range. At the upstream boundary, two kinds of boundary conditions can be specified:

1. Discharge Hydrograph,
2. Stage Hydrograph,

It is possible to specify one of the five available conditions at the downstream boundary given as:

1. Discharge Hydrograph,
2. Stage Hydrograph,
3. Single-Valued Rating Curve,
4. Looped Rating Curve,

5. Manning's eq .

2.2.4.1 Upstream Boundary Condition

Discharge or a stage hydrograph may be the upstream boundary conditions. It defines a discharge hydrograph as:

$$Q_1^{\,j+1} - Q(t) = 0 \qquad (2\text{-}9)$$

Similarly, it defines a stage condition as:

$$h_1^{\,j+1} - h(t) = 0 \qquad (2\text{-}10)$$

Where $Q_1^{(j+1)}$ and $h_1^{(j+1)}$ are the discharge and stage to be measured at the node of the upstream boundary, Q(t) and h(t) are the hydrographs entered into the model.

2.2.4.2 Downstream Boundary Condition

A discharge or a phase hydrograph may be the downstream boundary state. A single or looped rating curve that determines the relationship between step (or depth) and discharge may also be used. Furthermore, a critical flow segment may also be the downstream boundary. The equations corresponding to these conditions are given as follows:

1. Discharge Hydrograph: -

The following equation is obtained when a discharge hydrograph is used at the downstream boundary:

$$Q_N^{\,j+1} - Q(t) = 0 \qquad (2\text{-}11)$$

In which $Q_N^{(j+1)}$ is the discharge at the downstream boundary to be measured and Q(t) is the hydrograph discharge value.

Inappropriate use of a discharge hydrograph can result in gross errors at the downstream boundary. The imposed flow which exceed the channel's capacity to supply the node with water. In addition, if at the upstream boundary, a discharge condition is also defined, any mistake in the values of these flows is expressed in

the water levels that may often cause the stream to be partially or fully dry. In this respect, in unsteady flow simulations, a discharge condition at the downstream boundary is seldom used.

2. Stage Hydrograph: -

If at the downstream boundary, a stage hydrograph is defined, one can obtain:

$$h_N{}^{j+1} - h(t) = 0 \qquad (2\text{-}12)$$

In which $h_N^{(j+1)}$ is the stage at the downstream boundary to be measured and h(t) is the hydrograph stage value.

3. Single-Valued Rating Curve: -

If the downstream boundary condition is used as a single-valued rating curve, the boundary condition equation is written as:

$$Q_N{}^{j+1} - Q'(t) = 0 \qquad (2\text{-}13)$$

In which $Q_N^{(j+1)}$ is the discharge at the downstream boundary to be measured and $Q'(t)$ is the discharge value calculated from the rating curve. Any intermediate discharge is computed by linear interpolation between the two data sets if the rating curve is expressed in a tabular, piecewise linear manner:

$$Q'(t) = Q_k + \frac{Q_{k+1} - Q_k}{h_{k+1} - h_k}\left(h_N{}^{j+1} - h_k\right) \qquad (2\text{-}14)$$

In which the rating curve $h_N^{(j+1)}$ is the stage at the downstream boundary, and $Q_k, Q_k^{(k+1)}, h_k, h^{(k+1)}$ is consecutive tabular data sets.

2.3 Mechanisms of Mass Transport in Rivers

When a mass of material is introduced into a stream, it will move down the stream as a concentrated mass. It will undergo mixing and dispersion so as to occupy an ever increasing volume. Hence, the average and the maximum concentrations within occur in the three different mechanisms. (Plawsky, 2001).

1. **Advection:** Is the transfer of mass from one point to another in a current and moving, Advection refers to the movement in any of three directions of dissolved or very fine particulate material and the present velocity (longitudinal, lateral or transverse, and vertical). Advective transport in rivers is the consequence of the volumetric flow rate and mean concentration, as shown in Figure (2.4) (Schnoor, 1996)

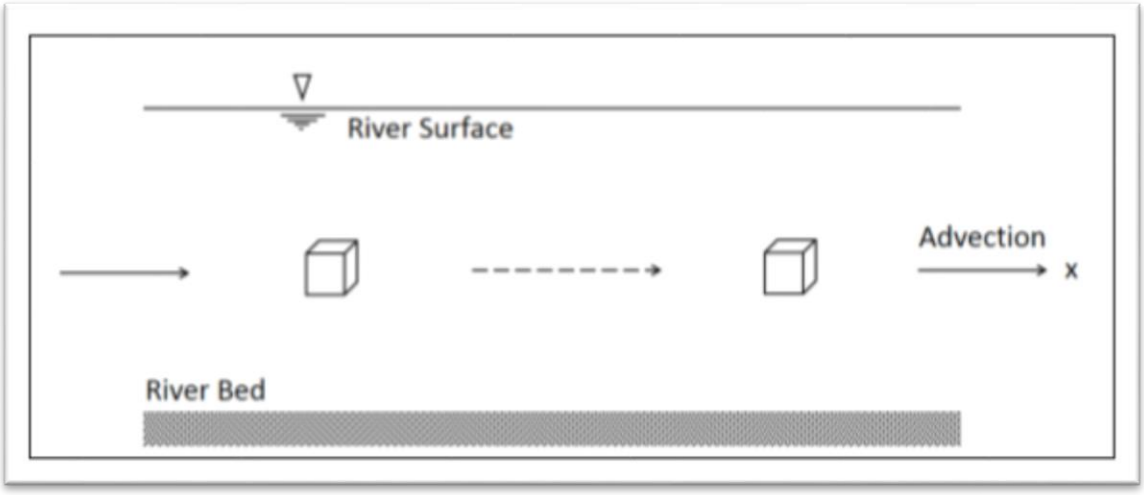

Figure:(2.4) Phenomena of advection (Schnoor, 1996)

2. **Diffusion:** There two type of diffusion:

a. The Diffusion (molecular): By random molecular motions, the dispersion of particles.

b. Diffusion (turbulent): The dispersion of particles by turbulent motion, considered approximately analogous to molecular diffusion, but with coefficients of "eddy" diffusion, which are much larger than coefficients of molecular diffusion and can be neglected in turbulent flow (Roberts and Webster, 2005), as shown in the Figure (2.5).

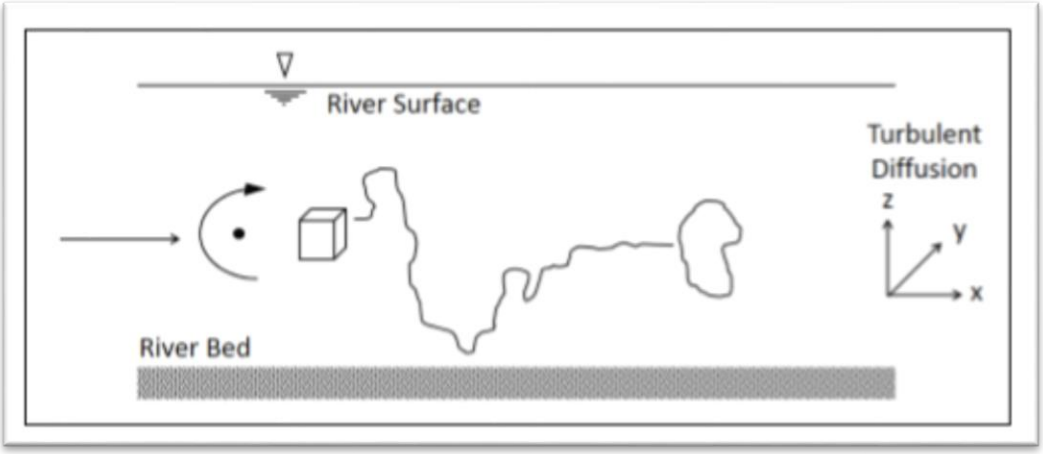

Figure:(2.5) Phenomena of diffusion (Schnoor, 1996)

3. **Dispersion:** A still greater degree of mixing known as dispersion is caused by the interaction of turbulent diffusion with velocity gradients induced by shear forces in the water body. The transport of toxic substances in streams and rivers is mainly by advection, but dispersion-controlled transport in lakes and estuaries is often (Czernuszenko, 1987). Velocity gradients, such as vertical profiles due to wind shear at the air-water interface and vertical and lateral profiles due to shear stresses at the sediment-water and bank-water interface, are induced by shear forces at the boundaries of the water body, as shown in the Figure (2.6). The mixing of dissolved and fine particulate matter is referred to as turbulent or eddy diffusion. There can be turbulent diffusion in all three directions, but it is typically anisotropic (Schnoor, 1996).

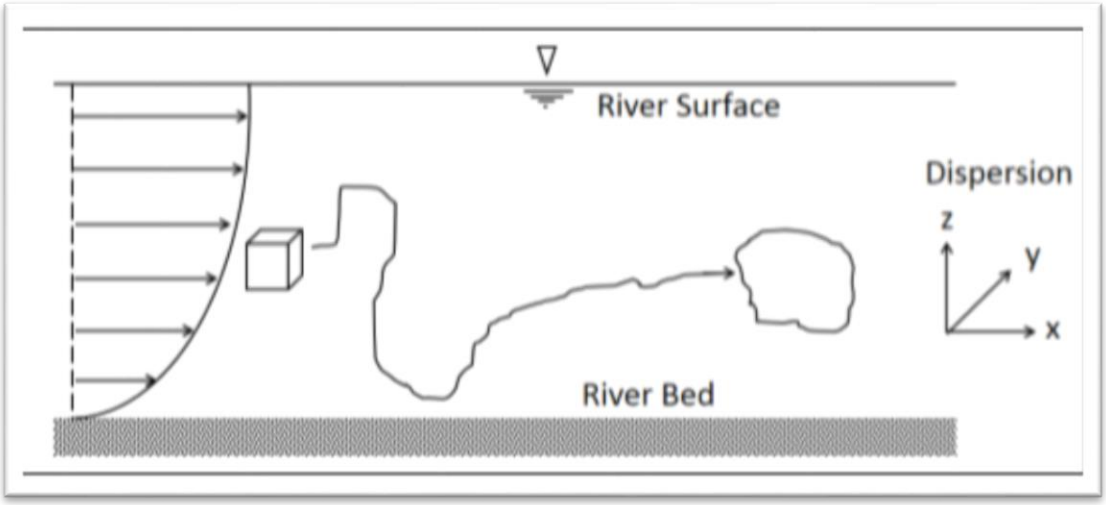

Figure (2.6) Dispersion phenomena (Schnoor, 1996)

2.3.1 Advection Dispersion Equation

The approach of Fickian advection-dispersion used in this study is based on convective-diffusive mass transport in flowing water. The basic advection-dispersion equation (ADE) for pollutant transport in running water is the mathematical method employed. ADE is a partial differential (PDE) equation derived from the mass balance applied in the river to a mass volume unit.

The rate of spread of type A in an arbitrary direction 'n' as a result of molecular diffusion is mathematically expressed by Fick's first law of diffusion, when an element of fluid type A is inserted into a mass of fluid type B (Aswed, 2000):

$$F_n = -M_{NB}\frac{\partial c}{\partial n} \qquad (2\text{-}15)$$

where: (Fn) is the rate of substance transfer per unit area from section normal to (n), (MAB) is the coefficient of fluid (A) molecular diffusion into (B), whilst (C) the fluid concentration is (A).

For the diffusion of fluid B into fluid A, a similar equation will, of course, hold. When the fluid added varies only in its concentration from the recipient one, the coefficient of diffusion is called the coefficient of self-diffusion M and Eq. (2.16) transforms into:

$$F_n = -M\frac{\partial \mathrm{c}}{\partial \mathrm{n}} \tag{2-16}$$

The expression for mass preservation of a preservative material may be stated as follows from the above description of the preservation of mass for component (A) in the fluid element:

$$\begin{pmatrix}\text{The net flux of mass A}\\ \text{through the fluid element}\\ \text{(inflow minus out flow)}\end{pmatrix} = \begin{pmatrix}\text{The time}\\ \text{accumulation}\\ \text{the}\end{pmatrix}\ \begin{matrix}\text{rate of}\\ \text{with}\\ \text{fluid}\end{matrix}\ \begin{matrix}\text{mass A}\\ \text{in}\\ \text{element}\end{matrix}$$

The above expression can be described in equation form as (Aswed, 2000) by applying the above principle in Cartesian coordinates (x,y,z) for incompressible fluid and dilute solutions in which the density and the diffusion coefficient are essentially constant:

$$\frac{\partial \mathrm{c}}{\partial \mathrm{t}} + u\frac{\partial \mathrm{c}}{\partial \mathrm{x}} + v\frac{\partial \mathrm{c}}{\partial \mathrm{y}} + w\frac{\partial \mathrm{c}}{\partial \mathrm{z}} = M\left[\frac{\partial^2 c}{\partial x^2} + \frac{\partial^2 c}{\partial y^2} + \frac{\partial^2 c}{\partial z^2}\right] \tag{2-17}$$

Where: x: the longitudinal direction, y: the side direction and z: the vertical direction (L).U, v and w: speeds in the x, y and z directions (L/T), respectively.C: Material concentration, x, y, z function and time (M/L^3).T: Time (T), and M: Coefficient of Self-diffusion (L^2/T).

2.3.2 Dispersion Coefficient Equation

Dispersion is an essential mechanism which helps to reduce the concentration of pollutants. Rivers with a high dispersion coefficient have a high potential to

minimize the concentration of pollutants, so several experiments have been carried out to study the dispersion phenomenon in rivers and to measure its effects on the quality of water. Dispersion has been characterized by the combined action of velocity distribution and turbulent fluctuation as the distribution of known components (Kefay, 2000).

2.3.2.1 Longitudinal Dispersion Coefficient Equation

After the total cross-sectional mixing has taken place, temporarily varying source situations. To present simple formulas for its estimation, several studies have been carried out. However, due to the uncertainty of the phenomenon, it could not always result in precise prediction (Sahay and Dutta, 2009).

Fischer is known as one of the earlier researchers researching water longitudinal dispersion. During the years of 1966, 1967 and 1968, he carried out continuous research. In 1968, Fischer found in his experiments that when the discharge (Q) increases depending on the resulting form of the velocity distribution, the longitudinal dispersion coefficient (DL) value increases (Hashim, 2007).

Fischer et al. (1979) derived the following simple and approximate expression for streams' longitudinal dispersion coefficient in open channel flow:

$$DL = 0.011 \frac{U^2 T^2}{H U_*} \qquad (2\text{-}18)$$

Where: - U: Stream velocity (m/s). DL: Longitudinal dispersion coefficient (m2/s). H: Cross-sectional average flow depth (m). T: Top width of water (m). U_*: $U_* = \sqrt{RSg}$ Shear velocity (m/sec). g: Acceleration due to gravity (L/T2). S: Slope of bed channel (m/m). R: Hydraulic radius (in a wide river R=depth of flow (Fisher, 1981)).

Equation (2.18) is commonly used,for its simplicity and theoretical context, but the significant deviation between the expected values and measured values now made the equation unpopular (Rajeev, 2013). The deviation may be because the assumptions inherent in the creation of this equation are not fully fulfilled by either stream. Liu (1977) stressed the position of lateral velocity gradients in dispersion after analyzing several dispersion data from US rivers and derived an expression for (DL) as:

$$DL = M\ \frac{U^2T^2}{HU_*} \qquad (2\text{-}19)$$

The parameter (μ) is a function of channel geometry and distribution of cross-sectional velocity. An approximate value of (μ) was obtained (Godfrey and Frederick, 1970) as:

$$M* = 0.18\left(\frac{U*}{U}\right)^{1.5} \qquad (2\text{-}20)$$

(McKeefer and Quivey ,1974) successively resolved the continuity equation with the dispersion equation to represent the following dispersion coefficient form:

$$DL = 0.058\ \frac{Q}{ST} \qquad (2\text{-}21)$$

Where: DL: Longitudinal dispersion coefficient (m2/sec). S: Slope of bed channel (m/m). T: Top width of water (m). Q: Discharge (m3/sec).

Using dimensional and regression analyses on reported river data, (Falconer and Kashefipour 2002) defined the following definition for DL in natural streams:

$$DL = 10.612(\frac{H}{U*})U^2 \qquad (2\text{-}22)$$

where:

As stated before, DL, U, H and U*.

2.3.2.2 Lateral Dispersion Coefficient Equation

Lateral blending is much slower, but within a few kilometers downstream, it is normally complete. The coefficient of lateral dispersion in the river described by certain representative properties of the water body is taken into account.

(Fischer et al., 1979) note that river dispersion is commonly correlated with the river's characteristics using the following relationship (Schnoor, 1996):

$$D_T = \beta H U_* \quad (2\text{-}23)$$

Where: -

DT: Lateral dispersion coefficient (m2/sec).

H: Cross-sectional average flow depth (m).

U*: Shear velocity (m/sec).

β: Proportionality constant (dimensionless).

A number of values for (β) have been identified by researchers. (β) varies in the laboratory flumes from (0.5 to 2.4). Fischer (1967) proposes (β=0.6) for practical purposes. The dispersion coefficient in the lateral direction used by the riverine variable is given by combining the equation (2.19) with (β= 0.6) (Schnoor, 1996):

$$D_T = 0.6 H U_* \quad (2\text{-}24)$$

where: - As stated before, DT, H and U* .

2.4 General Philosophy of the Modeling System in HEC-RAS

HEC-RAS is an integrated software system intended to be used interactively in a multi-task environment. A graphical user interface (GUI), separate components of research, data storage and management capabilities, graphics and reporting facilities compose the framework. The HEC-RAS system comprises four elements of one-dimensional river analysis for:

1. steady flow water surface profile computations.

2. unsteady flow simulation.
3. movable boundary sediment transport computations.
4. water quality analysis.

A key aspect is that all four components use a shared representation of geometric data and common routines for geometric and hydraulic computation. The system includes many hydraulic design features, in addition to the four river analysis modules, which can be invoked once the basic water surface profiles are computed.

The new HEC-RAS version supports of the Steady and Unsteady flow water surface profile calculations; sediment transport/mobile bed computations; and analysis of water quality. In future updates, new features and additional functionality will be included.

2.4.1 Unsteady Flow Simulation

This HEC-RAS modeling system part is capable of simulating one-dimensional unstable flow through a complete open channel network. The unsteady flow equation solver was adapted from the UNET model of Dr. Robert L. Barkau (Barkau, 1992 and HEC, 1997). For subcritical flow regime calculations, the unsteady flow portion was mainly developed. However, with the release of Version 3.1, in the unstable flow computation module, the model can now perform mixed flow regime calculations (subcritical, supercritical, hydraulic leaps, and drawdowns).

The hydraulic calculations were integrated into the unsteady flow module for cross-sections, bridges, culverts, and other hydraulic structures that were developed for the steady flow portion.

Special features of the unsteady flow portion include: study of dam breaks; breaching and overtopping of levees; pumping stations; operations of navigation dams; and systems of pressurized pipes.

2.4.2 Water Quality Analysis

This part of the modeling system is designed to allow the user to perform analyses of riverine water quality. Detailed temperature analysis and transport of a small number of water quality constituents can be done in the current version of HEC-RAS (Algae, Dissolved Oxygen, Carbonaceuos Biological Oxygen Demand, Dissolved Orthophosphate, Dissolved Organic Phosphorus, Dissolved Ammonium Nitrate, Dissolved Nitrite Nitrogen, Dissolved Nitrate Nitrogen, and Dissolved Organic Nitrogen). The ability to transport many additional water quality elements will be included in future versions of the program.

2.5 Previous Studies:

Numerous analysts have examined Hydrodynamic and water quality of the Euphrates Waterway. A rundown of a few of these thinks about is recorded underneath.

Shaymaa.A.M et al., (2012) carried out the analysis using nineteenth criteria to determine the physical, chemical and biological quality of the drinking and irrigation water of the Euphrates River by selecting the fourteenth sampling sites along the river from Al-Qaim to Al-Qurnah stations during the period from April 1998 to April 2001. The observed values of these physico-chemical parameters were correlated with Iraqi and WHO criteria. The results showed that for drinking and irrigation use, the WQI of the Euphrates river ranged from "good"

to "very bad" quality. The analysis was then needed as it would give the preliminary judgment on the value of each water quality parameter at the Euphrates river for WQI calculation. The statistical analysis was carried out by measuring the matrix coefficient of correlation between the various pairs of parameters. To exclude independent variables that show the lowest contribution in variance, multiple linear regression (MLR) was applied. After eliminating the variables with low variance, the DWQI was calculated based on ten variables out of twelve parameters. Based on three variables from ten parameters with correlation coefficients of (0.95) and the IWQI, this model with correlation coefficients of the IWQI was predicted (0.907). These models are checked by comparing their findings with the experimental data gathered from October 2009 to September 2010 for the same stations along the river. The comparison results suggest a strong agreement between the WQI values.

Emad A. Mohammad et al., (2012) demonstrated the utility of the cluster analysis (CA)approach for analyzing and interpreting surface water datasets in order to evaluate the temporal and spatial variations in the parameters of water quality and to optimize the sampling network for regional water quality. Use of 16 parameters at 11 sampling sites for the 2008-2009 period for the Euphrates River. The 8 months were divided into three cycles (I, II and III) by the Hierarchical CA and the 11 sampling sites were categorized into two classes (I and II) on the basis of similarities in water quality characteristics. The temporal trend suggests that April has higher levels of emissions compared with the other months. Sampling site 7 (S7) has a lower level of pollution in spatial terms, whereas other sampling sites have a higher level of pollution.

Luay Kadhim.H et al., (2013) Estimated of Manning's roughness coefficient Hilla River through calibration using the HEC-RAS model.The HEC-RAS unstable flow model was applied to the river Hilla (upstream city of Hilla) to predict the value of the coefficient of Manning. The data is collected for the period from 20 August 2008 to 12 September 2008 and is divided equally into two sets, the first for calibration purposes and the second for verification purposes. The value of the roughness coefficient (n) of Manning for the Hilla river, which shows strong agreement between observed and computed hydrographs, is found to be (0.027).

Ameera Mohamad. A. (2015) used HEC-RAS to develop a hydraulic model and determine the Manning Roughness Value for Shatt Al-Rumaith, it is important to calibrate the channel roughness coefficient for open channels, whether natural or artificial. By comparing the computed water surface profiles with one observed, using the HEC-RAS steady flow model for the shatt al-Rumaith channel in Al-Muthanna (Iraq), the value of Mannnig's 'n' coefficient is attempted to calibrate.Flows for the year 2014 have been considered for this calibration.The value of Manning's roughness coefficient for shatt al-Rumaith is found to indicate a strong agreement between the measured water surface profiles, n=0.023 and n=0.04 for the main channel and floodplain, respectively.

Abdul Hussain.A (2016) used one dimension and unstable case to study river water hydrodynamic and TDS simulation using HEC-RAS in Shatt Al-Arab River and related rivers. The data of discharge, stage and TDS was taken daily for the year of 2014 at different sections along Shatt Al-Arab river and Tigris-Euphrates confluence. These data were used to calibrate and validate the Model. The results of the model were compared with the data found on these actual rivers.

The result indicates a very good agreement with the minimum correlation (R)was equal to (0.825) between observed and simulated data being.

Mohammed Ali et al., (2017) used the Water Quality Index (WQI) and Geographical Information System (GIS) were used to determine the quality of the raw water of the Kufa river for drinking water due to its significance in Najaf province. From July 2013 to June 2014, water samples were obtained from seven separate stations along the Kufa river for twelve months. Eleven parameters of water quality including [(TH), (pH), (Ec), (TDS), (Alk.), (Cl), (Ca), (Na), (Mg) and (K)] were analyzed. In order to determine the quality of Kufa River water for human use, the application of the Water Quality Index (WQI) with several physicochemical water quality parameters was carried out. Throughout the study period, the average annual general WQI for drinking water was found to be (77.895).The quality of the Kufa River is rated as very low quality from this study. The high WQI obtained is due to the numerous human activities taking place along the banks of the river. The results indicate that the use of methods (GIS) and the Water Quality Index (WQI) will provide a very useful and powerful tool for demonstrating river contamination for various uses and for managing water supplies.

Zainab Ali.O.et al., (2018) studied the Shatt Al-Hilla river for 51,100 km length and discharge equal to 70 and 170 m3/sec was applied to the HEC-RAS software by using the steady flow. The results of this study: Shatt Al-Hilla is an alluvial river, ffor discharge 70 m3/s from upstream to downstream measured by HEC-RAS, be slow velocities ranging from 0.71 to 0.27 m/s with low shear stress of 0.60 N/m2 and low Froude No. ranging from 0.18 to 0.05 (13) ensuring that the river was at risk of high sedimentation loads cumulative. In the case of discharge 170 m3/s the results do not differ much from the first, as The velocities ranged

from (1.08 to 0.42) m/s, Slow velocity was considered, too,low shear stress 1.22 N/m2 and low Froude No. (0.22 to 0.06).High likelihood of erosion of embankments and can cause natural sequences of regularly changing bends. It can be noted that when the river passes within the center of Al-Hilla city, the speed increased from the beginning of the specific research field.

Jumana Hadi.S. (2018) Calculated the roughness coefficient of Manning's channel by using the remaining verification data, which is the model test with real data. The area was studied at the upstream of the Al-Meshkab Barrage, where data were collected in 2010, through the adoption of the mathematical one-dimensional mathematical model using the HEC-RAS program. The value of the roughness coefficient (n) of Manning for Al-Meshkab River, which demonstrates good agreement between observed and computed data, is found to be (0.031).

Rafea H (2018) used Different frequency distributions models to fitted the monthly data of the water quality parameters of the southern Iraqi Shatt Al-Hilla River.For the time, five water quality parameters were studied (2000-2013). The monthly series for magnesium, alkalinity, total hardness, sulfate and calcium are the data obtained. The equipped distribution models are the Gamma form of Normal, Log-normal, Weibull, Exponential and Two parameters. The Kolmogorov-Smirnov test was used to assess the accuracy of fit. The fittings were done for the 9-year data span (2000-2008)..For the first three parameters, the best suited distributions were used to forecast three sets of monthly data for each and compared to the observed data sets for the last 5 years (2009-2013).The results of the Kolmogorov-Smirnov test show the ability of these models to generate data with the same frequency distribution as the observed frequency. For Sulphate and

Calcium, no distribution of the tried ones will match. Therefore, (Lag Correlation) analysis was for all the variables, performed to examine the reasons for the Sulphate and Calcium non-fit. This study reveals that these two variables have relatively high lag-correlation and thus low randomness behavior compared to the other three variables.

Nassrin Jassim .H et al., (2019) used on the Saint-Venant Equations, with one-dimensional hydrodynamic model that Described the various unstable flows found in natural channels. The model consists of the mass and momentum conservation equations. With the Newton-Raphson iteration method with an updated Gaussian elimination strategy, the formulas, kept up by the four-point implicit finite difference scheme, solve the nonlinear system of equations. Using data on the Euphrates River during the early spring flood in 2015, the model is calibrated. It is confirmed by its application to the ideal channel and to the range chosen by the River Euphrates. The feasibility of our methodology and the accuracy of results (R2 = 0.997) are demonstrated by a comparison between model results and field data, indicating that the model is ready for future use once field observations are available.

Sarmad A. Abbas et al., (2020) presented the results of the hydraulic model proposal to calculate the Tigris River roughness coefficient (Manning's coefficient n) along 3.5 km within the Maysan Governorate, south of Iraq. The simulation method used in this study was HEC-RAS software. By using two sets of observed water levels, the HEC-RAS model was adopted, calibrated, and validated. Findings from this investigation showed that a Manning coefficient value of 0.025 provided an appropriate agreement between water level values observed and simulated.

2.6 The Summary

On the hydrodynamic side, and through previous studies by some researchers, it was found that the value of the roughness coefficient (Manning's coefficient n) for the Hilla River (0.027) [Luay.(2013)], the Rumaitha Shatt (0.023) and (0.04) for the channel and flood plains, respectively, [Ameera .(2015)], the River Al-Mashkhab (0.031) [Jumana.(2018)], the Tigris River in Maysan Governorate (0.025) [Sarmad . (2020)].

In the aspect of water quality, where the water quality ranged between good and bad for the Euphrates River, [Shaymaa. (2012)],[Emad. (2012)], [Rafea (2018)].

In the present research, the Euphrates river (from Hindiya Barrage to Kufa Barrage) were adopted as study area for calibrate the value of Mannnig's "n" coefficient Using data for the year 2020.After that, we proceed study to process of transporting pollutants. This study, it is considered one of the studies that used HEC-RAS in the field of pollutant transport simulation.

CHAPTER THREE

MATERIALS & METHODS

3.1 Introduction

This chapter is concerned with the field work of the hydrodynamic and water quality aspects. The data were collected at different various locations along the Euphrates River (from Al-Hindiya to Al-Kufa Barrages). It was necessary to put a working program for performing field and laboratory measurements to collect the data required for application, calibration, and verification of the model.

Unfortunately, such data is not available and/or not enough. Therefore, for the purpose of calibration and verification of the water quality model applied to the Euphrates river (from Hindiya Barrages to Kufa Barrages) Flow, all the data used in this analysis was collected and carried out. While the data is available on the hydrodynamic side.

3.2 Study Area

The Euphrates River is the longest river in South-western Asia. The Euphrates River has its source in the highlands of Eastern Turkey and its mouth at the Arabian Gulf. And it passes through Turkey, Syria and Iraq on its way, and enters Iraqi lands at Al-Qaim City in Al-Anbar Province, then enters Babel Governorate and branches of Shatt Al-Hillah, then enters the Euphrates River into Karbala Governorate, then Najaf Governorate, Diwaniyah Governorate, then Muthanna Governorate, then Dhi Qar Governorate, to extend to form the marshes, and to unite with it in Iraq the Tigris River to form the Shatt al-Arab, Its waters flow into the Arabian Gulf for 90 miles (120 km). From its source in Turkey to its mouth in the Shatt al-Arab in Iraq, the length of the Euphrates River is approximately 2,940 km, of which 1,176 km in Turkey, 610 km in Syria and 1,160

km in Iraq, and its width varies between 200 and more than 2000 meters at the mouth.

In this study river reach has a length of 73 km, starting from the Hindiya Barrages and up to the Kufa Barrages. During the study period, the flow rates were (120-100) m^3/s. Tables (3-1 and 3-2), as well as Figures (3-1 and 3-2), include both hydraulic and spatial data for the Hindiya and Kufa Barrages, respectively.

The Figure (3-3) shows the zone of the study for the Euphrates River (from Hindiya to Kufa Barrages). (Ministry of Water Resources, MOWRB,2021).

Table (3.1): Some hydraulic information about Hindiya barrage(MOWRB)

Details	Value
Date of construction	1984
Completion date	1989
Location	Euphrates river
No. of gates	6
Dimension of slots	(6.75×16) m
Type of gates	Radial
Methods of gates operation	Manually and Electrically
Maximum designed discharge	250 m^3/s
Maximum designed level U/S	32.55 m a.s.l.
Normal operation discharge U/S	200 m^3/s
Hydroelectric power	15 MW

Table (3.2): Some hydraulic information about Kufa barrage (MOWRK)

Kufa Barrage	
Details	**Value**
Date of construction	1984
Completion date	1988
Location	Euphrates river
No. of gates	7
Dimension of slots	(6.30×12) m
Type of gates	Radial
Methods of gates operation	Manually and Electrically
Maximum designed discharge	1400 m^3/s
Maximum designed level U/S	25.7 m a.s.l.
Normal operation discharge U/S	(50-250) m^3/s
Hydroelectric power	5 MW

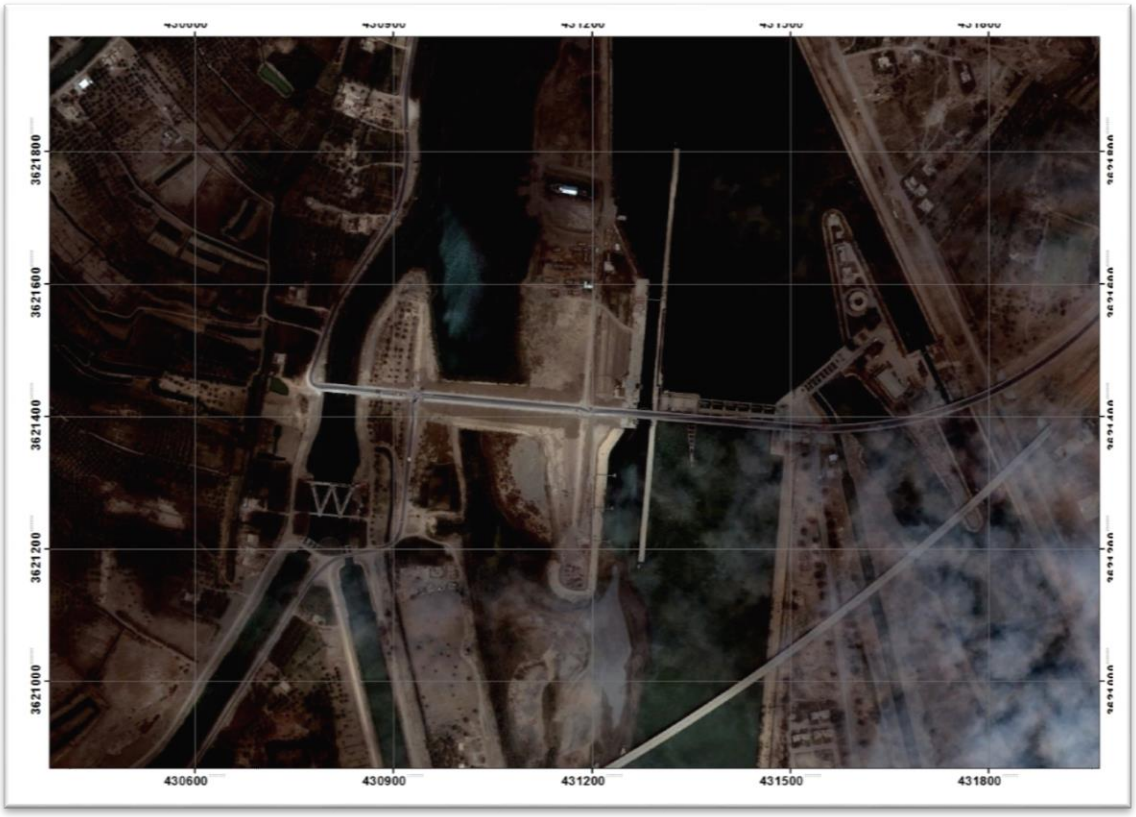

Figure (3.1): Hindiya Barrages [QWRB], Iraq

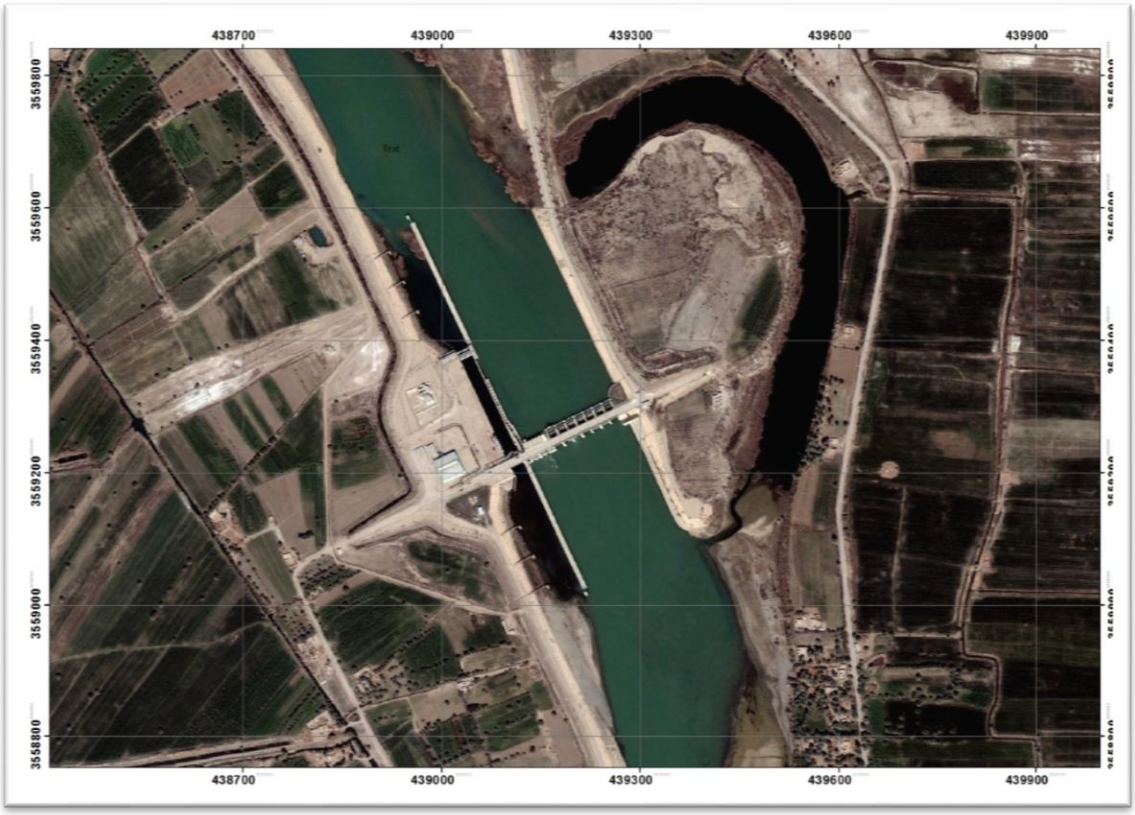

Figure (3.2): Kufa Barrages [QWRB] ,Iraq

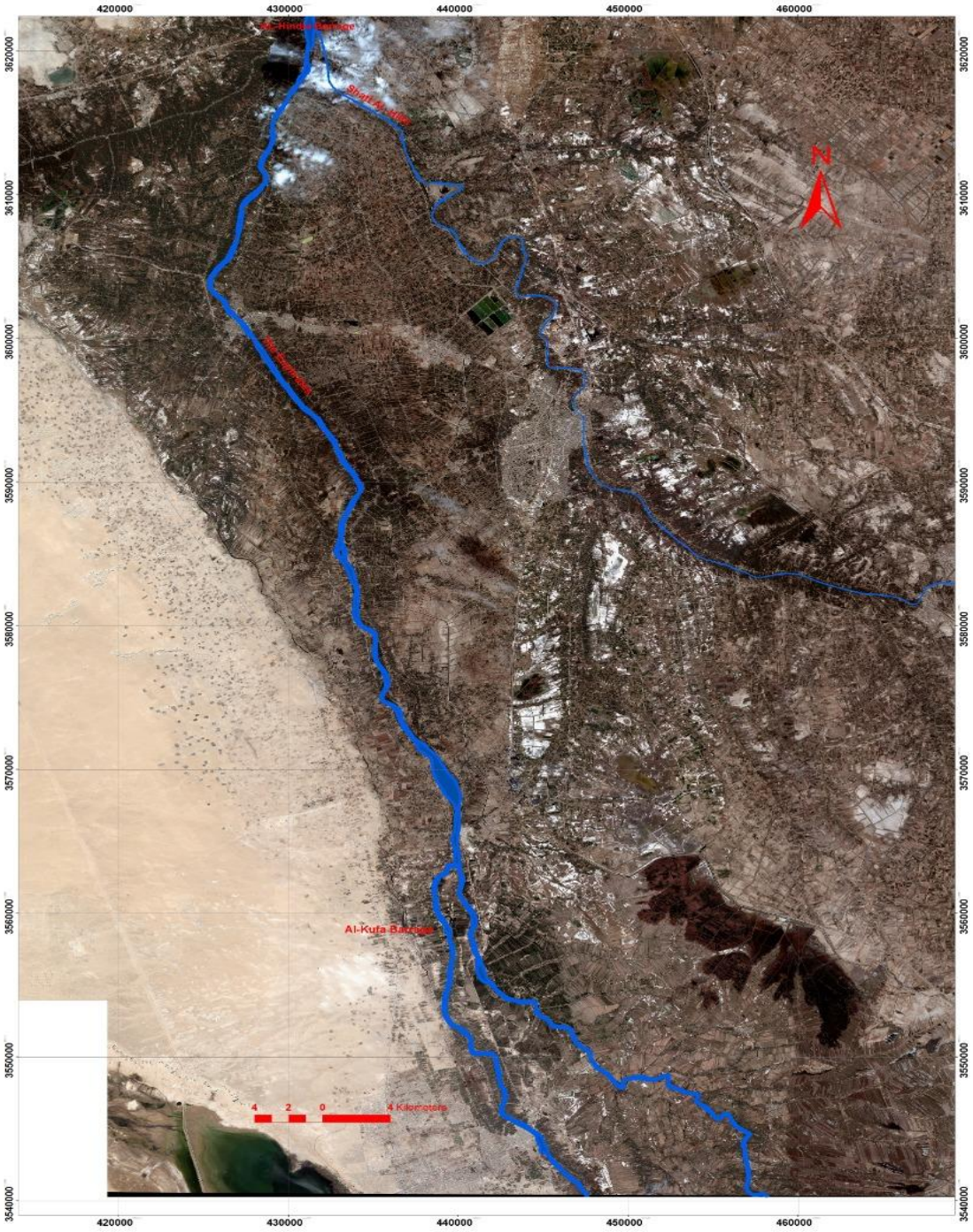

Figure (3.3): The Euphrates River schematization [QWRB] ,Iraq

Iraq, since it is far from the sea, is part of the tropical zone (semi hot). The properties that are most significant are:

1. The great difference in temperatures between day and night and between summer and winter.
2. Low annual precipitation in winter and spring.
3. The evaporation of water is high.

The climate property in Iraq is the rise in summer temperature. The hottest months are June, July, and August when the temperature is (40-50 C°) and the relative humidity at 2 p.m. at that time (15-18 percent). Although December, January and February are the coldest months of the year, where temperatures often drop below the freezing point and the air moisture content average is around (50 percent).

The expected amount of rain for each year is witnessing a marked variation, as the rate of rainfall for the period for Babel Governorat (2015-2020) ranges (1058.5) mm. (MORB,2020).

3.3 Data Collection

3.3.1 Flow –Stage Data

The hydraulic side data were obtained from the General Authority for Surveying (Baghdad), which is represented in 65 cross-sections along the Euphrates River (from Hindiya to Kufa Barrages), the positions of which are shown in the Tables (3-3) and (3-4).

Table (3-3): The location of the cross-sections the Euphrates River (from Hindiya Barrage to Kufa Barrage) [QWRD]

River station No.	Location (km)	Sub reach length (m)	River station No.	Location (km)	Sub reach length (m)
1	0+00	1000	15	13+450	1000
2	1+00	1000	16	14+450	1000
3	2+00	950	17	15+450	950
4	2+950	950	18	16+450	1000
5	3+900	1000	19	17+400	1000
6	4+900	850	20	18+400	950
7	5+750	900	21	19+400	1000
8	6+650	1000	22	20+350	850
9	7+650	1000	23	21+350	950
10	8+650	1000	24	22+200	900
11	9+650	900	25	23+150	700
12	10+550	1000	26	24+050	9550
13	11+550	1000	27	24+750	1000
14	12+550	900	28	34+300	950
29	35+300	800	48	53+200	950
30	36+100	1000	49	54+150	1000
31	37+100				

		1000	50	55+150	
32	38+100	1000	51	56+150	1000
33	39+100	1000	52	57+150	1000
34	40+100	900	53	58+000	850
35	41+000	1000	54	58+950	950
36	42+000	1000	55	59+950	1000
37	43+000	1000	56	60+950	1000
38	44+000	800	57	61+950	1000
39	44+800	950	58	65+950	4000
40	45+750	1000	59	66+950	1000
41	46+750	800	60	67+950	1000
42	47+550	850	61	68+950	1000
43	48+400	1000	62	70+100	1150
44	49+400	1000	63	71+000	900
45	50+400	850	64	72+000	1000
46	51+250	1000	65	73+150	1150
47	52+250	950			

Table (3-4): Schematic representation by HEC-RAS of the Euphrates River (from Hindiya Barrage to Kufa Barrage)

	Reach	River Sta. No.		Reach	River Sta. No.
Euphrates River	Hilla	1	Euphrates river	Hilla	36
		2			37
		3			38
		4			39
		5			40
		6			41
		7			42
		8			43
		9			44
		10			45
		11			46
		12			47
		13			48
		14			49
		15			50
		16			51
		17			52
		18			53
		19			54
		20			55
		21			56
		22			57
		23			58
		24			59
		25			60
		26			61
		27			62
		28			63
		29			64
		30			65
		31			
		32			
		33			
		34			
		35			

As for the daily expenses and the real water depth, they were obtained from the Directorate of Water Resources of Babylon, which are shown in the Figures (3-4) and (3-5).

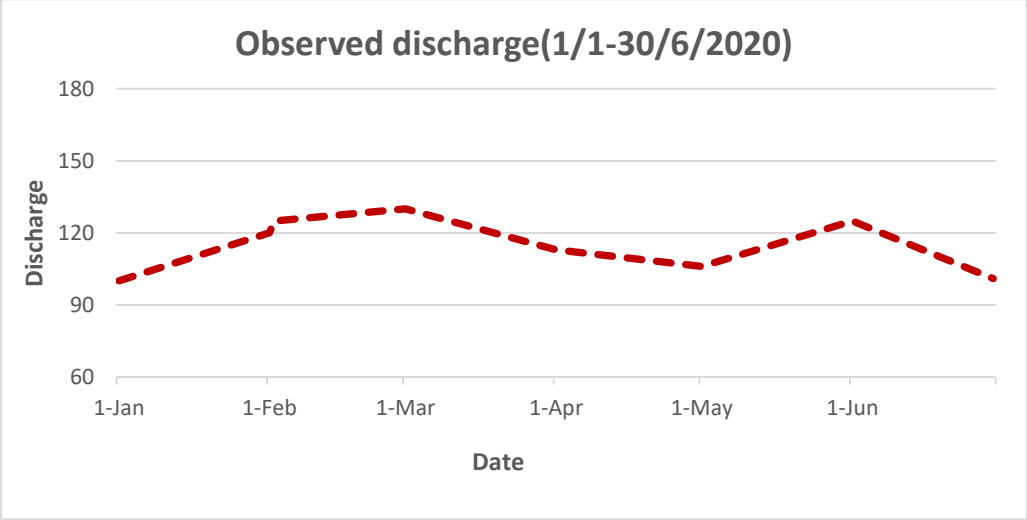

Figure (3-4): Inflow hydrograph for upstream boundary condition in station (1) (BWRB,2020)

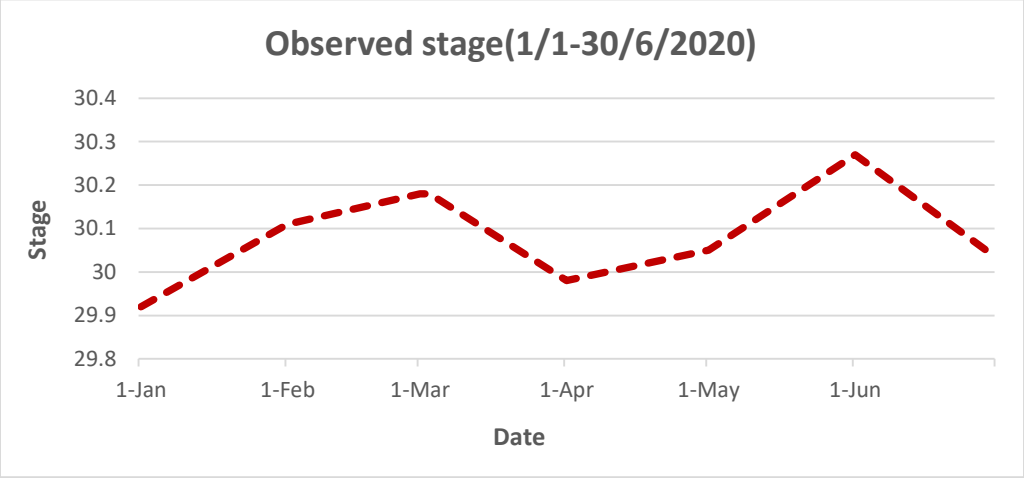

Figure (3-5): Stage hydrograph at station (65) (BWRB,2020)

3.3.2 Water Quality Data

The purpose of river sampling is to obtain a representative and accurate measure of the components of water quality along the river range. Because of the complex system of the river and subject to many variations, many stations with enough sample numbers to define the outcome are far more accurate than few stations with only few samples.

In current work, four variables were calculated, which are Total Dissolved Solids (TDS), Dissolved Oxygen (DO), Acid Function (pH), and Temperature].

In this study, the experimental work can be divided into two parts; field work and laboratory work. Three station for the Euphrates river were selected these points and their stations are shown in the Figure (3.6).

Figure (3.6): Sampling Location

Different field measurements were, these measurements were initiated on 1 November 2020 and were completed on 30 April 2021.

For the collection of samples from different Euphrates River locations, using a rod made of wood with a length of 4 meters, there is a bottle with a capacity of (1) litter at the end of it, as shown in Figure (3.7).

Figure (3.7) Sampling of collection

The table (3-5) shows the acceptable water quality limits of the river system according to the 1967 Iraqi River Maintenance Requirements No25 (for irrigation and drinking).

Table (3.5): allowable limits of Iraqi river maintenance for the river samples

Chemical Variables	Symbol	Measurement Unit	Iraqi River Water Standards for river samples
Total Dissolved Solids	TDS	mg/l	1500
Dissolved Oxygen	DO	mg/l	More than 5
Acid Function	pH	/	6.5-8.5
Temperature	T	C°	35 C°

(*) Source: DGOHE, 1967

River and outfall water samples were obtained monthly according to standard requirements and standard methods used to perform these tests. The studies are carried out in the Environmental Engineering Department/Faculty of Engineering Sanitary Laboratory.

Department of Engineering /University of Babylon. The name of the measurement method and its comparison are shown in the following table. In Appendix A1, the measurement methods are explained.

Table (3.6): The methods used in the analysis.

Parameter	Method name or device name	Reference
PH	PH meter (at location)	APHA, 2005
Total Dissolved Solid (TDS)	Lovibond device HM digital (COM-100)	APHA, 2005
Dissolved Oxygen(DO)	Winkler method	(Al-Tufaili,2015)
Temperature (T)	Mercury thermometer (at location)	APHA, 2005

The following Figures (3-8),(3-9),(3-10) and (3-11) show the results of the tests for the four water quality parameters (Temp,,PH,DO,TDS), respectively.

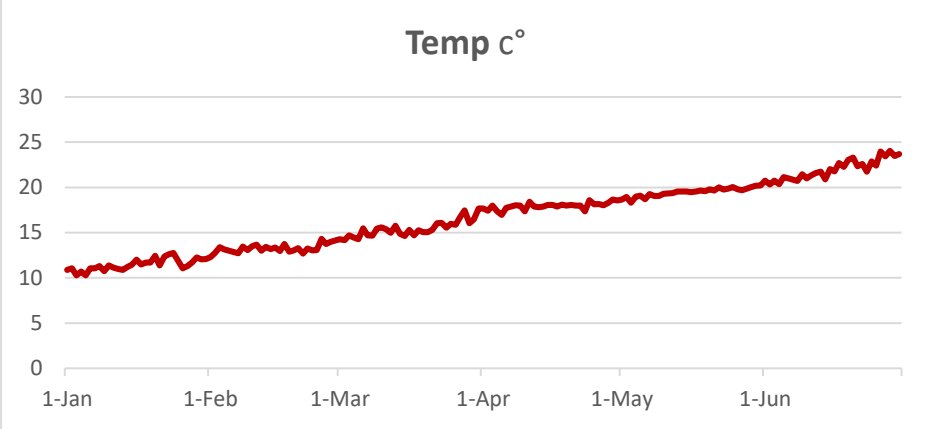

Figure (3-8) The measured temperature in practice

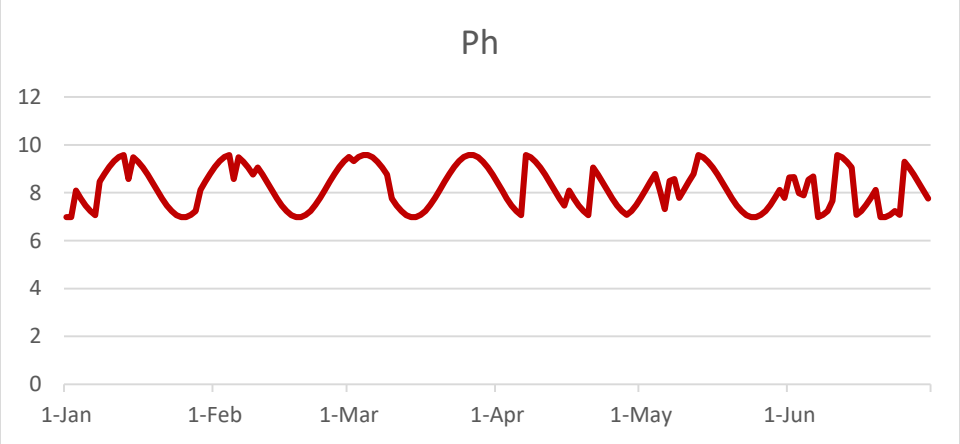

Figure (3-9) The measured PH in practice

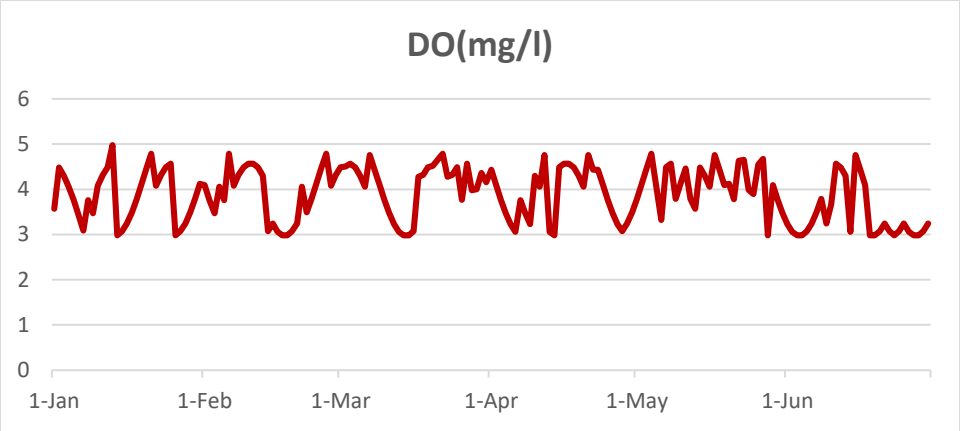

Figure (3-10) The measured DO in practice

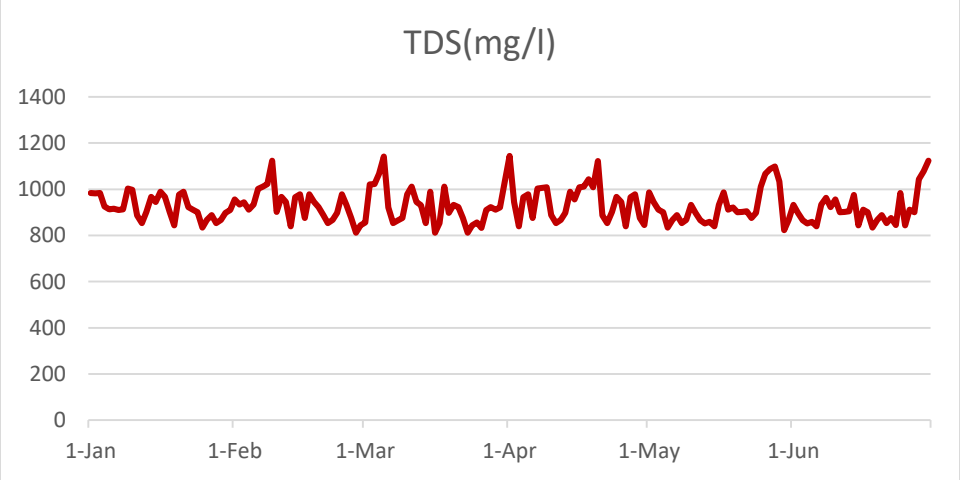

Figure (3-11) The measured TDS in practice

3.3.3 Meteorological Data

Meteorological data were obtained from the Meteorological Directorate (Baghdad) one full scale meteorological dataset was given to model the temperature of the water. For the required simulation duration, each meteorological dataset contains a time series of weather variation in the study area, including atmospheric pressure, air temperature, humidity, solar radiation, wind speed, and cloudiness. The air temperature and the shortwave radiation were included in the dataset based on the elevation and the latitude-longitude of the area. Was the wind speed 64.25 m/s , the cloudiness factor is to be 0.2,atmospheric pressure 1013 mb and humidity 49.7 mb, in the months of study, during which the simulation is carried out.

3.4 Methodology of The Study

Figure (3-12) shows the stages of implementing the research plan from the beginning, through data collection and entry into the program, and the most important results that have been reached.

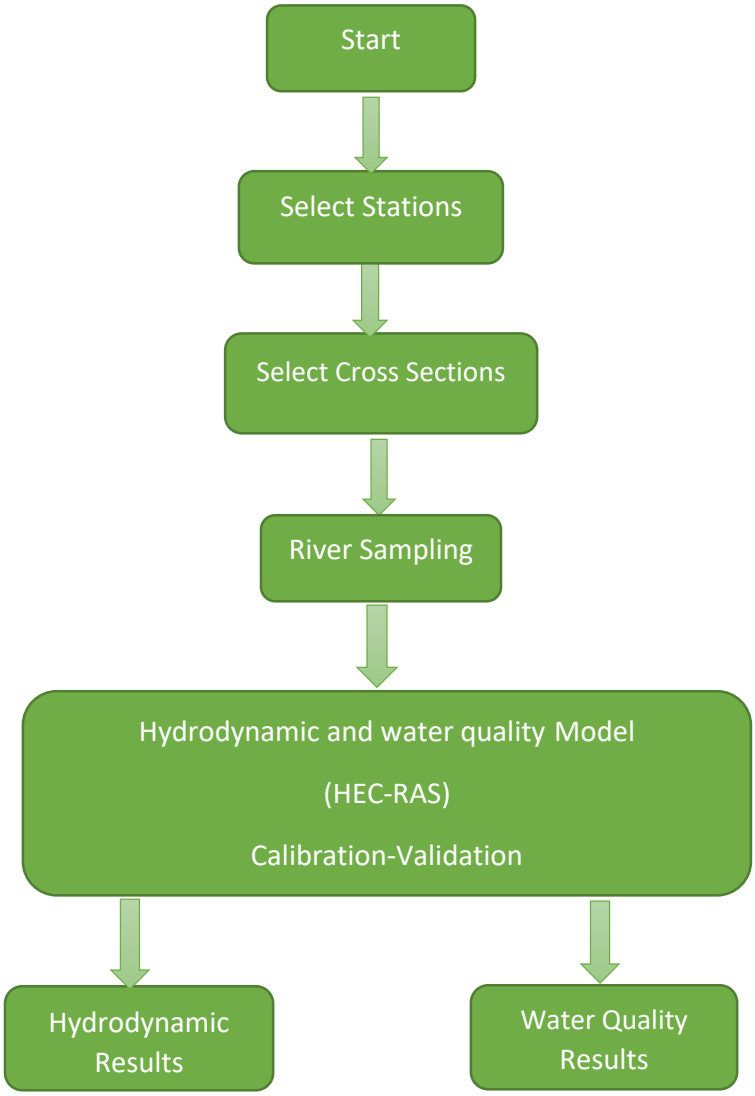

Figure (3.12) Methodology of study

CHAPTER FOUR

Results and Discussion

4.1 Introduction

This chapter is concentrated the procedures required to develop the HEC-RAS hydraulic and water quality models. Essentially, the next steps are concerned with the HEC-RAS model calibration process, which was carried out to document inputs and assumptions used in the simulation of the Euphrates river (from Hindiya to Kufa Barrages) using HEC-RAS to show that this model is sufficient to assess the hydraulic characteristics of the case study in relation to different operation scenarios as well as water quality.

4.2 HEC-RAS Model

A well-known river analysis system model HEC- RAS (V.5.0.7) was used in this study to perform analysis in the Euphrates river (from Hindiya to Kufa Barrages). The Hydrologic Engineering Center of the United States Army Corps of Engineers created and designed HEC-RAS for one-dimensional hydraulic calculations in natural and built channel systems. The HEC-RAS model allows for the simulation of both steady and unsteady flow in a single or branched channel structure. HEC-RAS is a software framework that is designed to be used interactively in a multi-tasking, multi-user network environment. The system is comprised of a graphical user interface (GUI), different hydraulic analysis modules, data storage and management features, graphics and reporting capabilities. Figure (4-1) depicts the main screen when the model is first started.

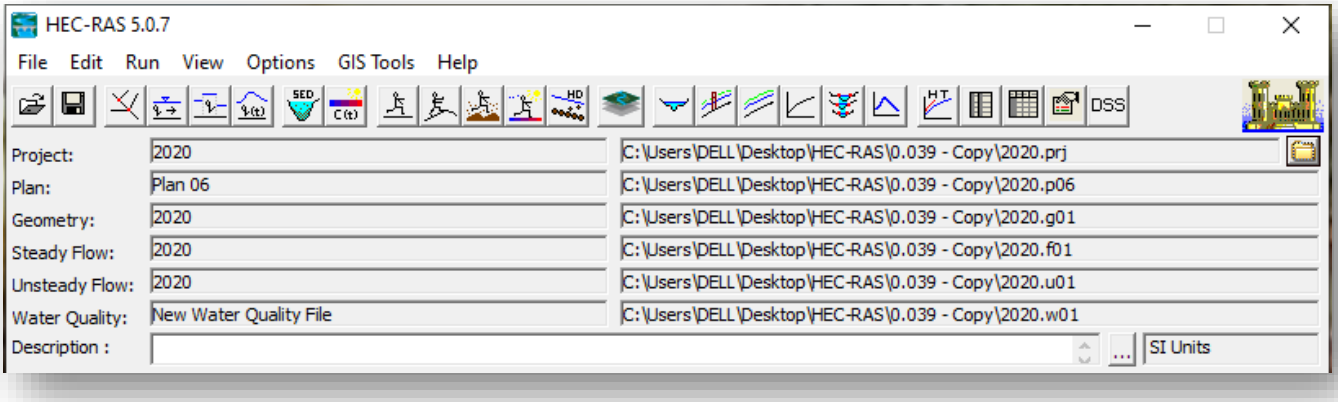

Figure 4-1: The HEC-RAS model's main screen

The HEC-RAS system includes four components for one-dimensional river analysis:

1. Water Surface Profiles for a steady Flow: This part of the modeling method calculates water surface profiles for a steady yet gradually varied flow. A single river reach, a dendritic system, or a complete network of channels may all be handled by the system. The steady flow portion can model water surface profiles in the subcritical, supercritical, and mixed flow regimes.
2. Simulation of an Unsteady Flow: This part of the HEC-RAS modeling framework will simulate one-dimensional unsteady flow through a complete network of open channels. The UNET model of Dr. Robert L. Barkau was used to build the 1-D unsteady flow equation solver (Barkau, 1992 and HEC,1997). This 1-D unsteady flow portion was designed primarily for calculations of subcritical flow regimes.
3. Sediment Transport/Movable Boundary Computations:This part of the modeling method is used to simulate one-dimensional sediment transport and movable boundary calculations caused by scour and deposition over long periods of time (typically years, although applications to single flood events will be possible).

4. Water Quality Analysis: This part of the modeling framework allows the consumer to conduct riverine water quality assessments.HEC-RAS can only perform comprehensive temperature analysis and transport of a small number of water quality constituents in its current version (Algae, Dissolved Oxygen, Carbonaceuos Biological Oxygen Demand, Dissolved Ammonium Nitrate, Dissolved Orthophosphate, Dissolved Organic Phosphorus, Dissolved Nitrite Nitrogen, Dissolved Organic Nitrogen and Dissolved Nitrate Nitrogen).

4.3 Modeling of the study area in Euphrates river

Two files are needed to prepare an unsteady flow model using the HEC-RAS model: the geometric data file and the unsteady flow data file.

4.3.1 Geometric Data File (GDF) of the study area

Drawing a schematic of the river system from upstream to downstream is the first step. The extension is defined by 65 cross-sections, the positions of which are shown in the Tables (3-2) and (3-3) on the Euphrates (from Hindiya Barrage to Kufa Barrage).

The schematic system for the Euphrates River (from Hindiya Barrage to Kufa Barrage) was drawn based on the plans for the Euphrates River mentioned above as shown in the Figure (4-2).

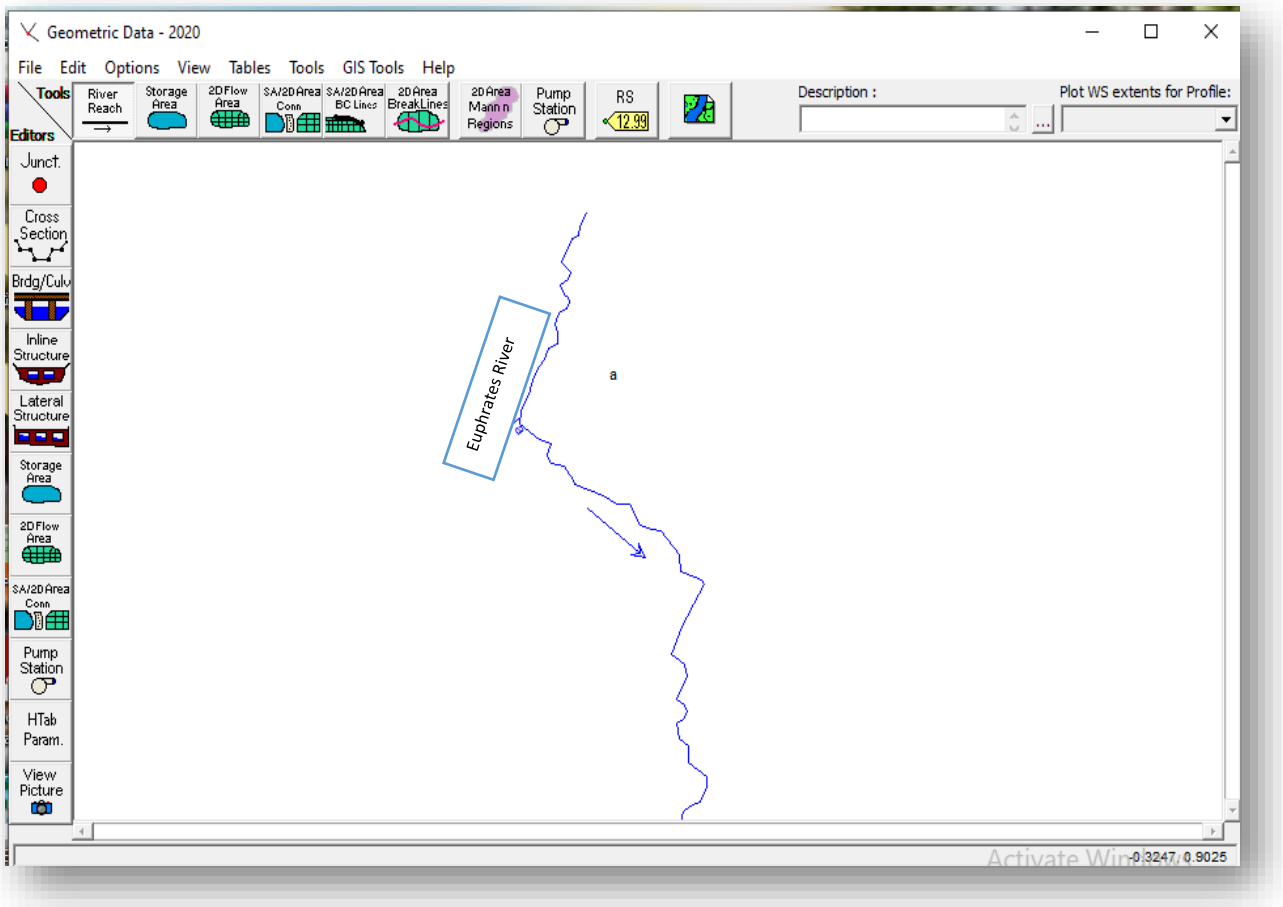

Figure (4-2): Schematic diagram of the Euphrates River (from Hindiya Barrage to Kufa Barrage) system by HEC-RAS.

The entire reach is drawn in the flow direction, from upstream to downstream. The Euphrates River (from Hindiya Barrage to Kufa Barrage) system schematic is then plotted, followed by the critical geometric data, which contains the streams system's connectivity information, i.e. geometric data for each reach and cross-sections. The geometric boundaries of the streams are defined by cross sections data. The rivers reach and rivers location identifier (station and elevation point), lengths of subreaches, chief channel bank station, and contraction and expansion coefficient are all required for a cross section. The cross sections data editors view all of the necessary information as shown in Fig. (4-3).

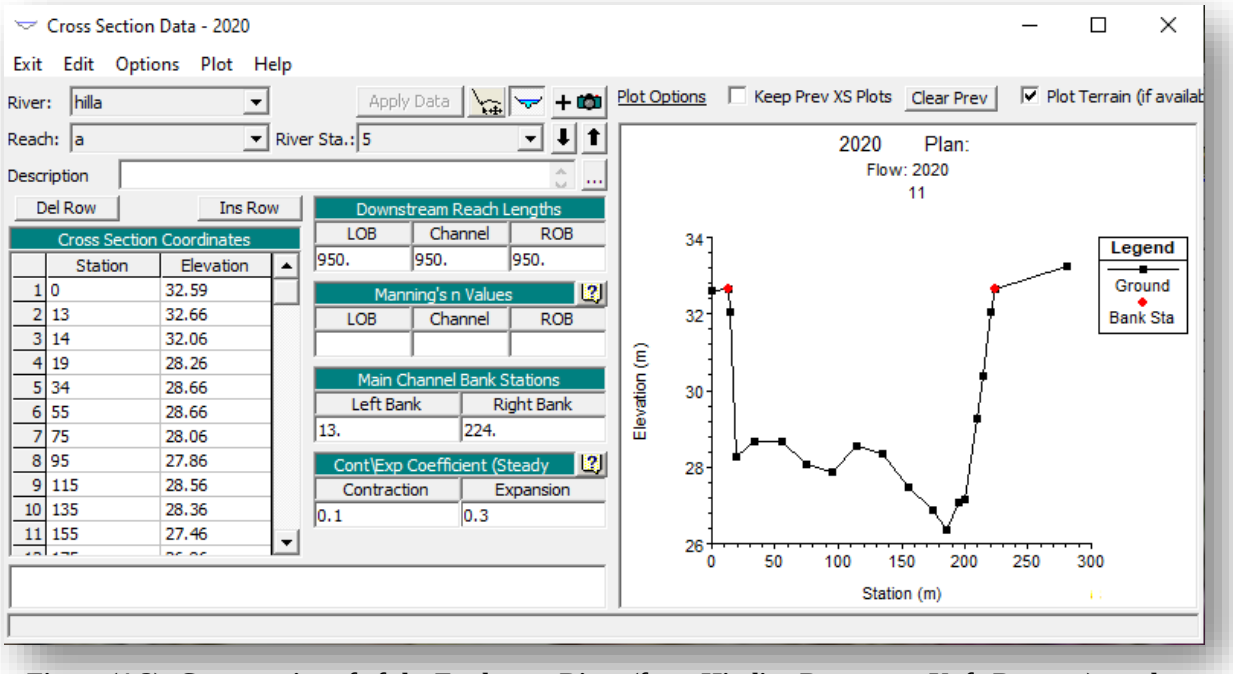

Figure (4-3): Cross section of of the Euphrates River (from Hindiya Barrage to Kufa Barrage) reach

Figures 4-4 to 4-8 display a 3-D plots of multiple cross sections in an XYZ plot interpolated by the HEC-RAS model along entire reach.

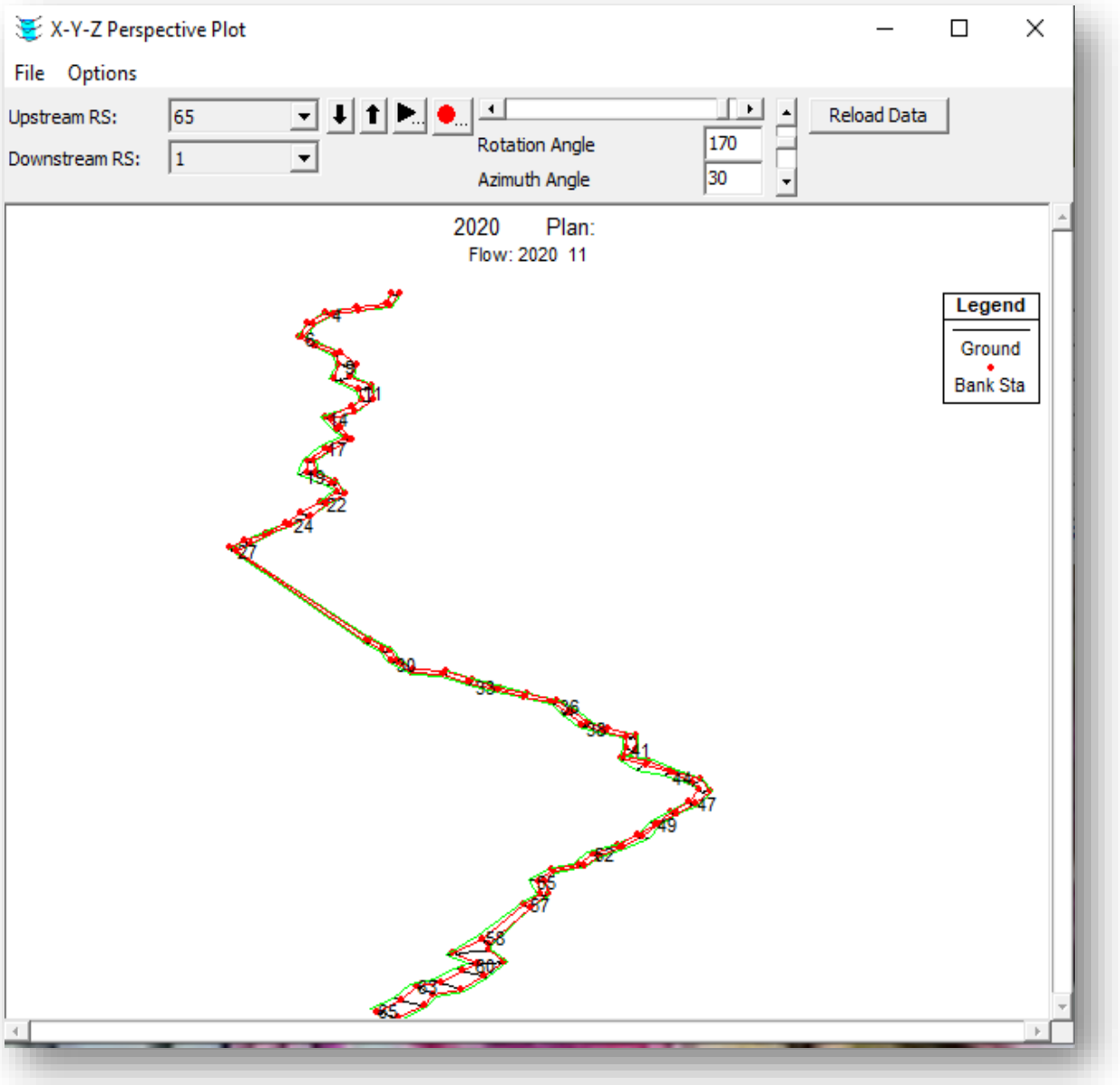

Figure (4-4): 3-D modeling plot of different cross areas from stations [0+00 to 73+150]

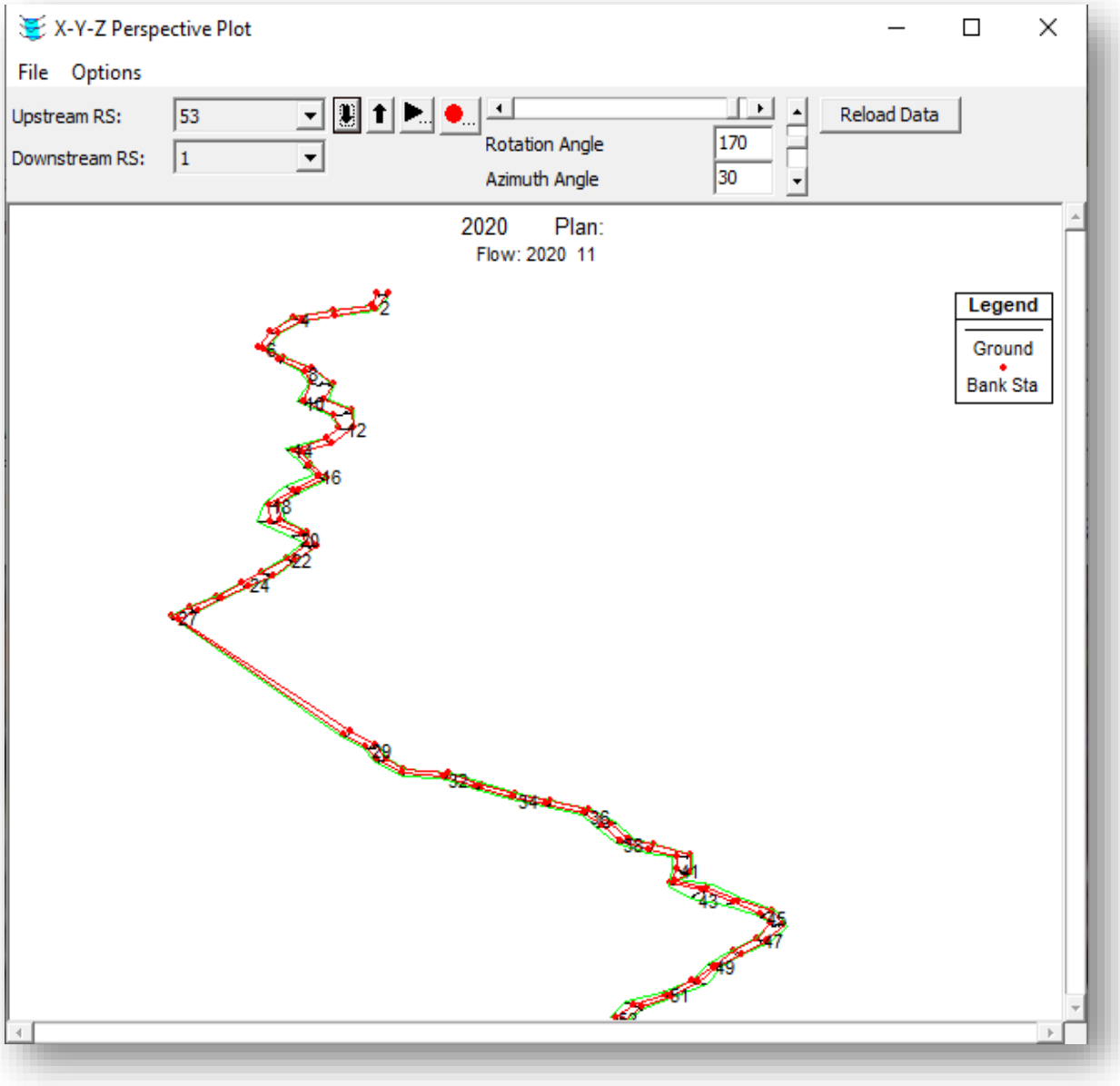

Figure (4-5): 3-D modeling plot of different cross segments from stations [0+00 to 58+000]

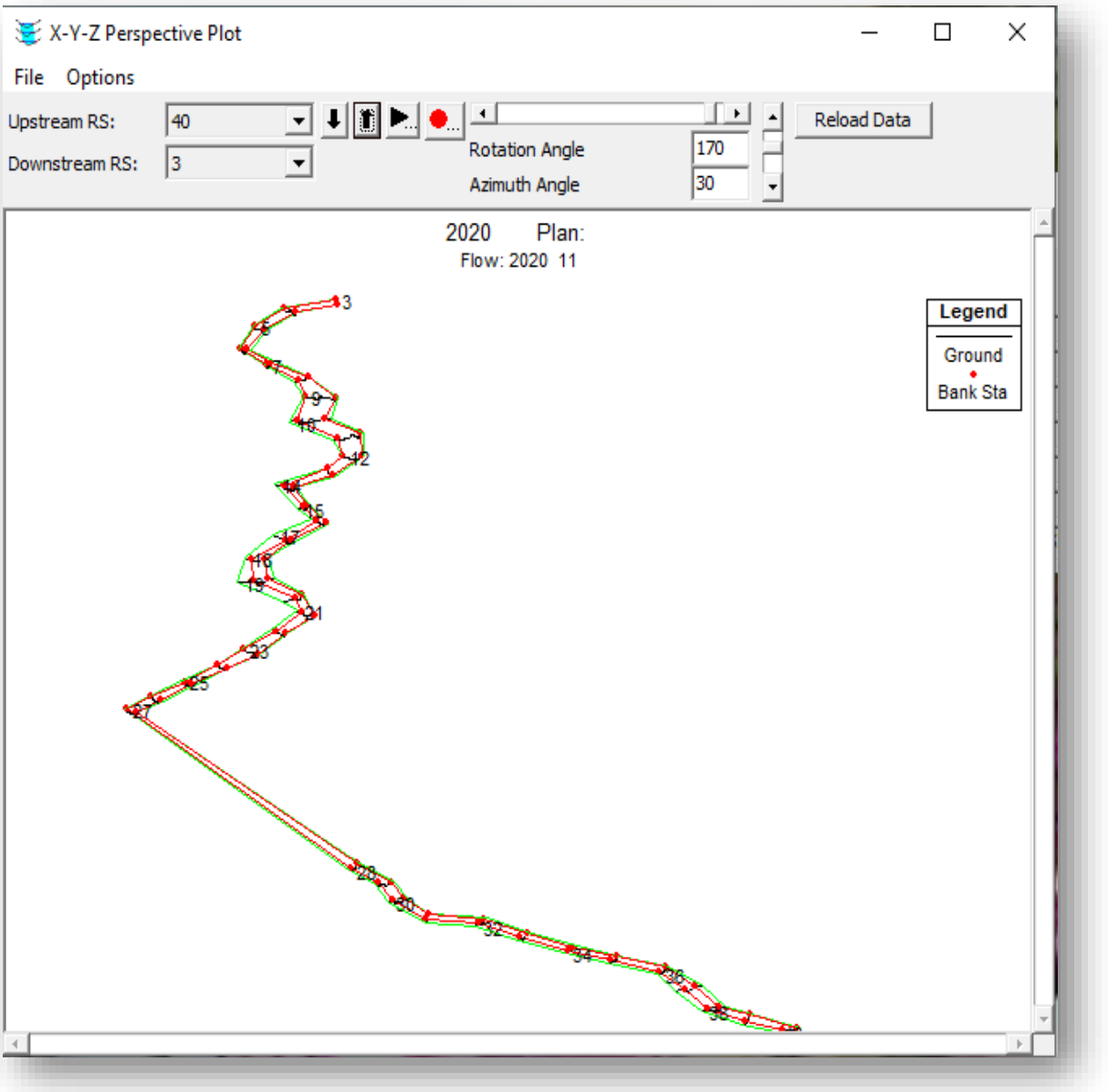

Figure (4-6): 3-D modeling plot of different cross areas from stations [0+00 to 45+750]

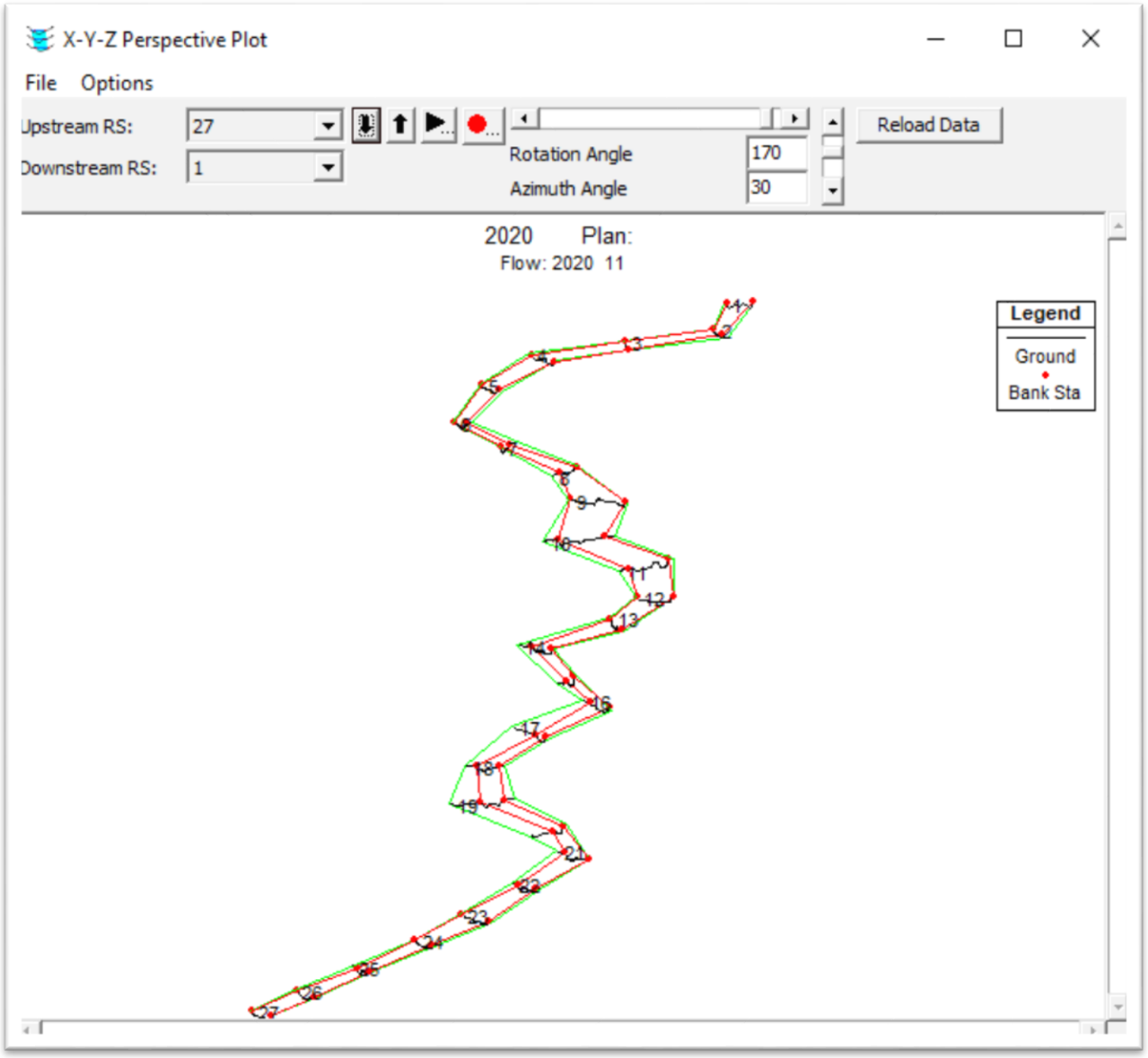

Figure (4-7): 3-D modeling plot of numerous cross segments from stations [0+00 to 24+750]

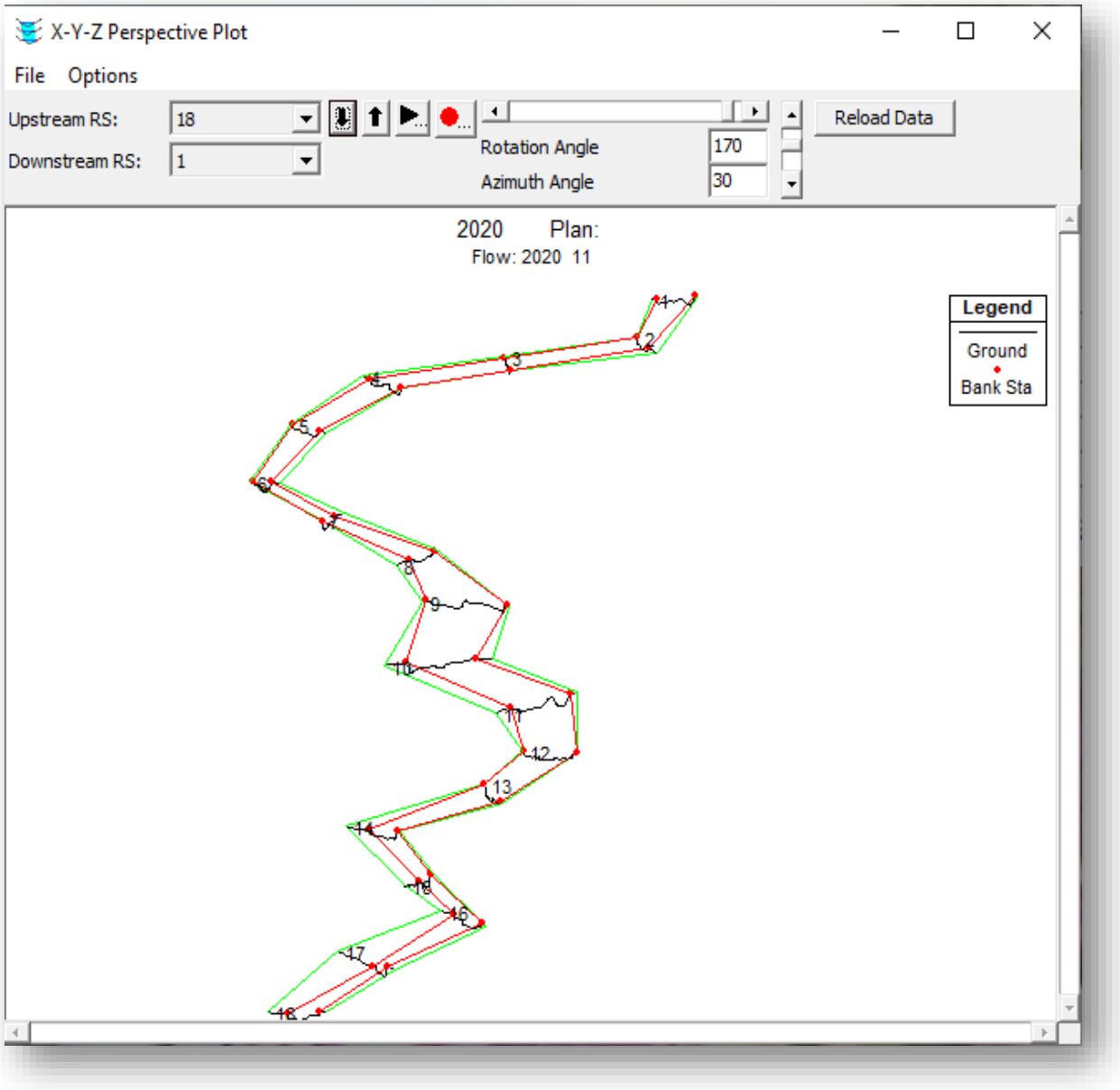

Figure (4-8): 3-D modeling plot of different cross segments from stations [0+00 to 16+450]

4.3.2 Boundary and Initial Conditions

To perform an unsteady flow analysis, it need steady flow data. The boundary condition and initial conditions are described in detail in unstable flow data. The flow in each segment at the start of the simulation, as well as the stage hydrograph, are among the initial conditions. At all open ends of the river system being modeled, a boundary condition must be defined. The following types of boundary / initial conditions can be used to model the upstream end of the channel system: inflow discharge hydrograph; stage hydrograph flow; and stage hydrograph. According to the available data for the model, the downstream end of the channel system can be modeled using the following types of boundary conditions: rating curve, normal depth (Manning's equations); stage hydrograph; flow hydrograph; stage and flow hydrograph. This data is entered into the form through the list of unstable flow data through the window shown in Figure (4-9), which was mentioned in the third chapter.

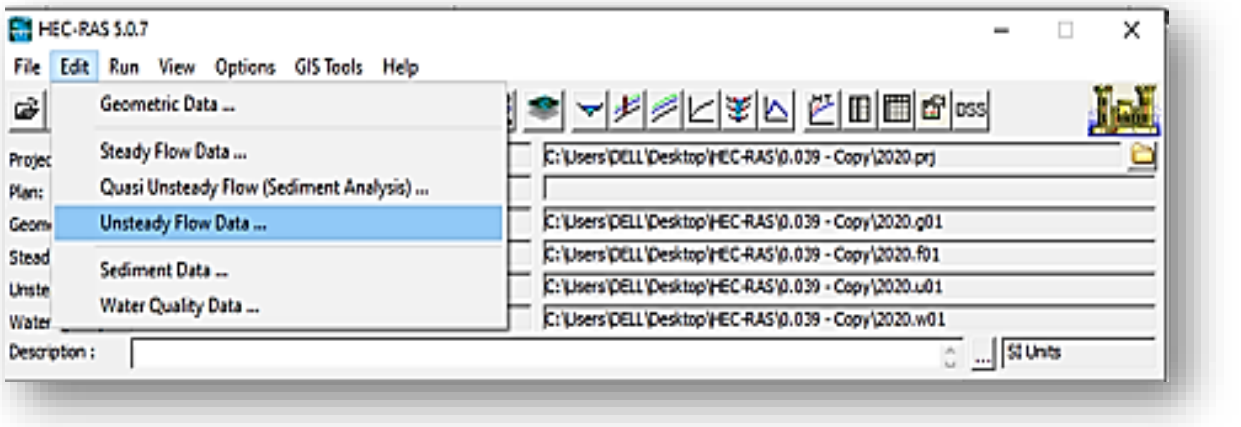

Figure (4-9): Unsteady Flow Data "Input Menu".

4.4 Calibration and Validation of the Hydraulic Model

Unsteady flow simulation must be calibrated and checked, which is possibly convenient for all models. Accurate prototype data is needed for these processes. Two independent, statistically accurate sets of prototype data were needed for calibration and validation.

According to French and Krenkel (1980), the first data set is used to determine the optimum coefficient value, and the second data set is used to demonstrate that the calibration processes determine optimal coefficient values. Many variables in unsteady flow models can't be calculated directly or aren't physically dependent in reality. In such models, the value of the roughness coefficient (Manning's n) is typically the focus of attention, which cannot be calculated explicitly and must be estimated.

In this analysis, Manning's coefficient values were assumed for each cross-section based on field investigations or previous studies in the study area (region of Euphrates River). Previous experiences of flow in an Iraqi natural river suggest that the Manning's coefficient value which range from 0.025 to 0.04 [cited by Hameed, 2011], Jumana(2018), and Al-Aboodi(2018) (2020). Ameera (2015) specified a channel roughness range of 0.023 to 0.03 and a floodplain roughness range of (0.03-0.04). According to the previous analysis, a Manning's coefficient range of (0.038 to 0.05) for the main channel and (0.039-0.052) for the floodplain is used to calibrate an appropriate Manning's coefficient value for the study area's river reach.

In this study, the data is based for the time span from January 1, 2020 to Jul 30, 2020, for calibration purposes, i.e., an approximation of Manning's coefficient, and for verification purposes, i.e., testing the model with real data to determine its predictive accuracy.

4.4.2 Initial Conditions

The initial conditions are represented in Figures (4-10) and (4-11), which are presented by discharges and stages determined using the HEC-RAS model using Default parameter flow conditions along the Euphrates River (from Hindiya Barrage to Kufa Barrage) reach.

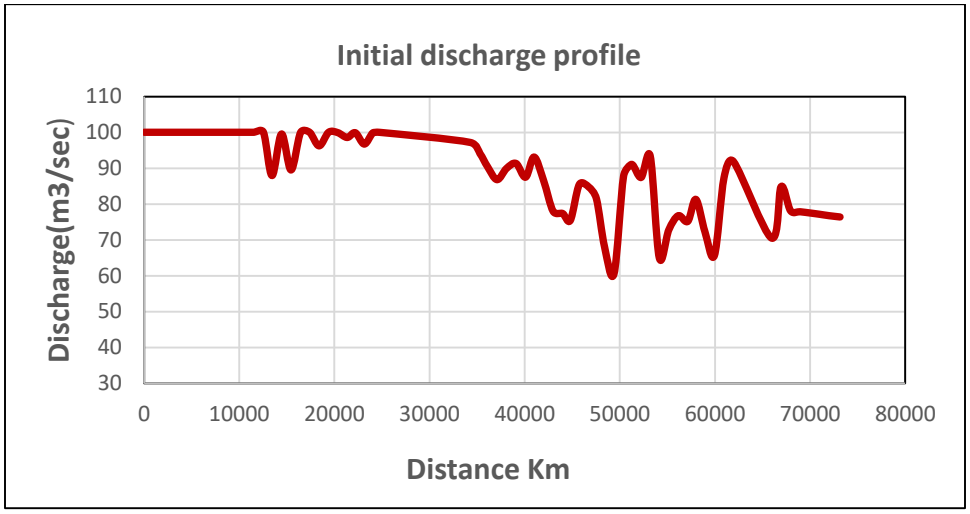

Figure (4-10): Computed Initial Discharge Profile in the Euphrates River (from Hindiya Barrage to Kufa Barrage)

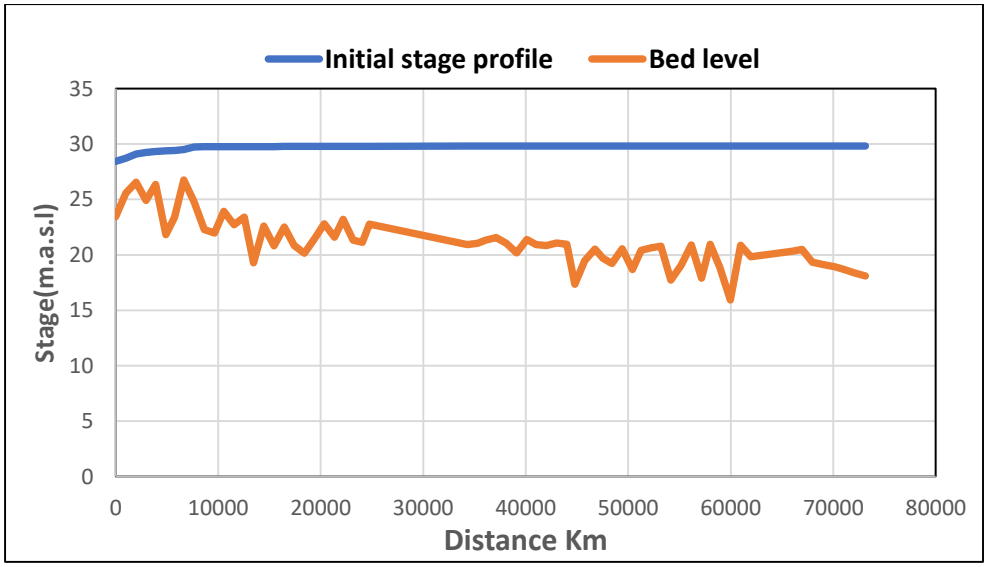

Figure (4-11): Computed Initial Stage Profile in the Euphrates River (from Hindiya Barrage to Kufa Barrage)

The Manning's roughness coefficients which used is ranged between (0.038 to 0.05) for the main channel and (0.039-0.052) for the floodplain. Figures (4-12) and (4-13) display the results predicted by the model for a given value of θ=1 and a time phase of one day duration, compared computed and observed stage hydrograph (measured) at section (65) .

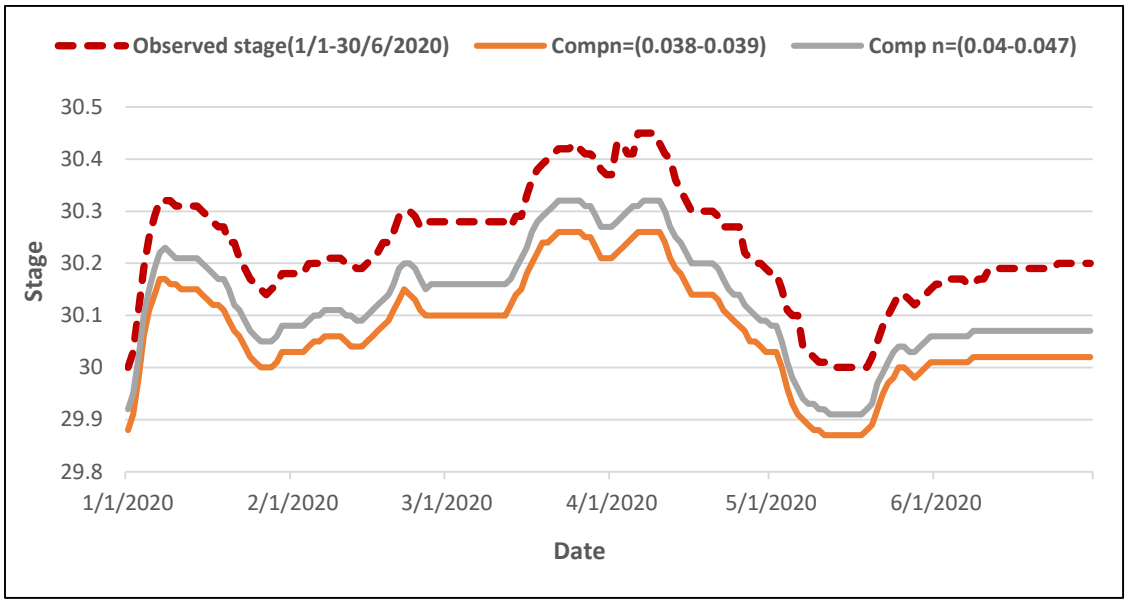

Figure (4-12): Computed and observed stage hydrograph at section (65) for different value of manning's

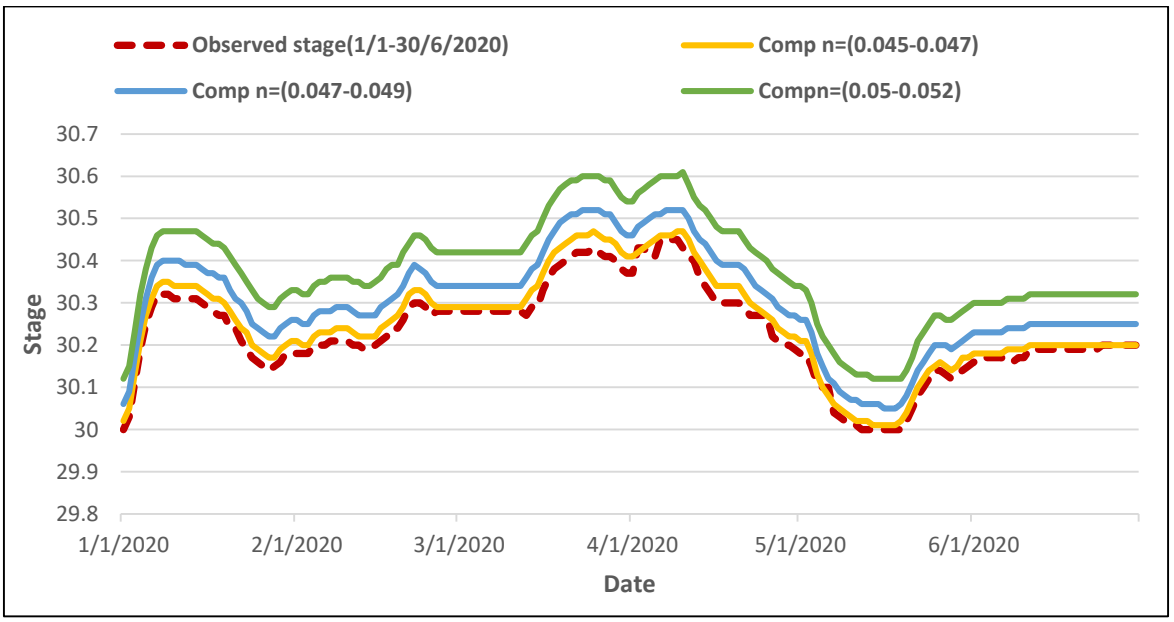

Figure (4-13): Computed and observed stage hydrograph at section (65) for different value of manning's

The time weighting factor θ, which is used in the finite difference approximation when solving the unsteady flow equation, is another parameter that must be calibrated due to its important effect on simulation stability. Practical values of θ tend to be in the range of ($0.6 \leq \theta \leq 1.0$). According to the obtained results, the value of θ=1.0 produces the most stable solution, which implies a more robust simulation, while the value of θ=0.6 provides more precision, but appears to cause oscillations in the solution. In HEC-RAS unstable flow models, the default value of is equal to unity (HEC- RAS, User's Manual, 2010).

Many scholars, including (Dronkers, 1969) and Schaffranek (1981), have noted that if θ =1 yields the best computational stability, the values of are set to unity in the current work. As Manning's coefficient is set, the following are general patterns that emerge. Except for the particular variables being calibrated, this trend assumes that all geometric data and variables will be kept constant (HEC,2010):

1. Where the Manning's n value is increased in the region, the stage will increase locally.
2. As the flood wave moves downstream, the peak discharge will decrease (attenuate).

In addition, to validate the hydraulics model performance, statistical test is used to compare predictors and observations. The root mean square error (R.M.S.E) criterion is a widely used statistical measure for evaluating the validity of numerical predictions.

$$\text{R .M .S .E} = \frac{\sum_{i=1}^{n}(Q_o - Q_p)^2}{n} \qquad (4\text{-}1)$$

where:

n: the total number of data sets

i: is the rank of data

Qo: is the observed values (discharge or stage) by the model.

Qp: is the predicted value of (discharge or stage) by the model.

Table (4-1) compares the observed and measured hydrographs for the stage at position No. (65) and the discharge at position No. (1). The corresponding value of R.M.S.E is the smallest in the case of time step (t=1 day), n=0.027, and θ=1.

Table (4-2) showing the values of (R.M.S.E) for the validated result obtained by hydraulic model for comparison with discharge and stage hydrographs at positions No. (1) and No. (65) of Hilla reach.

Table 4-1: R.M.S.E. Values for the Calibrated Result

Station no.	Δt	θ	n	∑RMS Stage
1	1	1	0.038-0.039	0.059
			0.04-0.047	0.0741
			0.045-0.047	0.0147
			0.047-0.049	0.0524
			0.05-0.052	0.0471
65	1	1	0.038-0.039	
			0.04-0.047	
			0.045-0.047	
			0.047-0.049	
			0.05-0.052	

Table (4-2): Values of R.M.S.E for the Verified Results between Observed and Computed Hydrographs

Data	For stage hydrograph at Sta. (1)
	∑R MS.
1Jul-31Des 2020	0.056

4.5 Water Quality Model

River water quality is affected a variety of natural and human pollutants. Geological, hydrological, and climatic pollution are the three types of natural pollution that are most prevalent. Water contamination occurs when a body of water is adversely impacted by the incorporation of harmful materials. It may come from a variety of sources. Computer simulation is one of the most effective methods for studying hydrodynamics and monitoring water quality. It is a strong and necessary tool for monitoring and making decisions about water quality parameters. To assess river water quality, we can compile and analyze hydrodynamic and water quality parameter data for a specific length of river.

Based on hydrodynamic simulation and unsteady flow, we conduct a water quality model of the Euphrates river from (Hindiya Barrage to Kufa Barrage) to evaluate the degree of pollution loading in the river and to provide various engineering solutions to prevent further degradation of the river water.

4.5.1 Model Description

The HEC-RAS water quality model solves one-dimensional advection dispersion equations with explicit numerical methods. For modeling the quality of river water, the model has three parameters: water quality data entry, water quality analysis menu, and finally output tools. The water quality data entry program

successfully enters all of the quality parameters in a time series format. The water quality data entry program successfully enters all of the quality parameters in a time series format Figure (4-14) shows the list of water quality data entry.

The water quality analysis menu then simulates and forecasts changes in water quality parameters over time and space, and the output tools present the simulated results to the user in the form of time series or spatial plots (HEC-RAS manual 2015).

Water samples will be collected at the following three sites. Water quality parameter tests on collected water samples were used to generate data for the water quality simulation. The pH, Dissolved Oxygen (DO), Total dissolved solids (TDS) and Temperature.

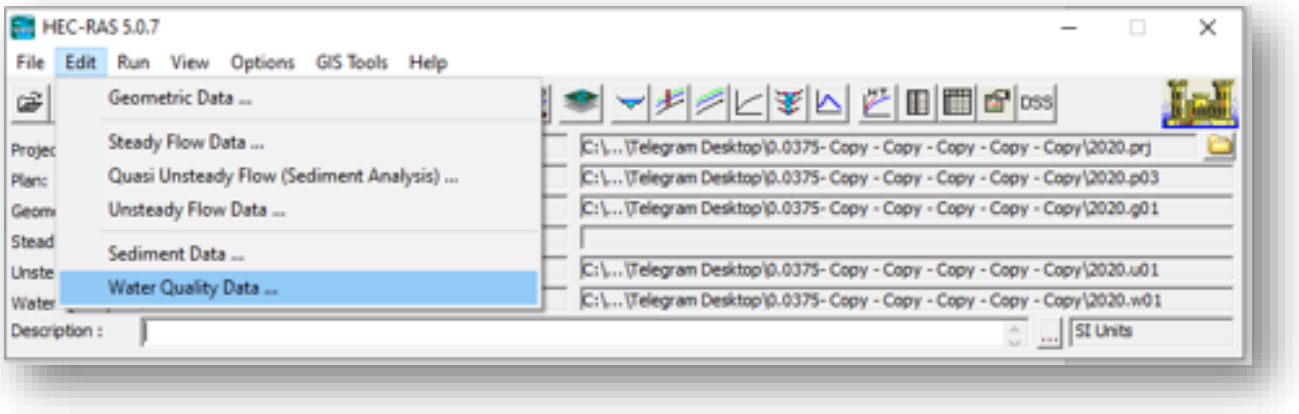

Figure (4.14): Water Quality Data "Input Menu".

4.5.2 Initial and the Boundary Conditions

pH, dissolved oxygen (DO), total dissolved solids (TDS), and temperature measurements were taken. The points of section 1 and section 65 were used as a boundary condition for the model in this analysis as shown in Figure (4-15). The

initial conditions were taken along Euphrates river from from (Hindiya Barrage to Kufa Barrage).

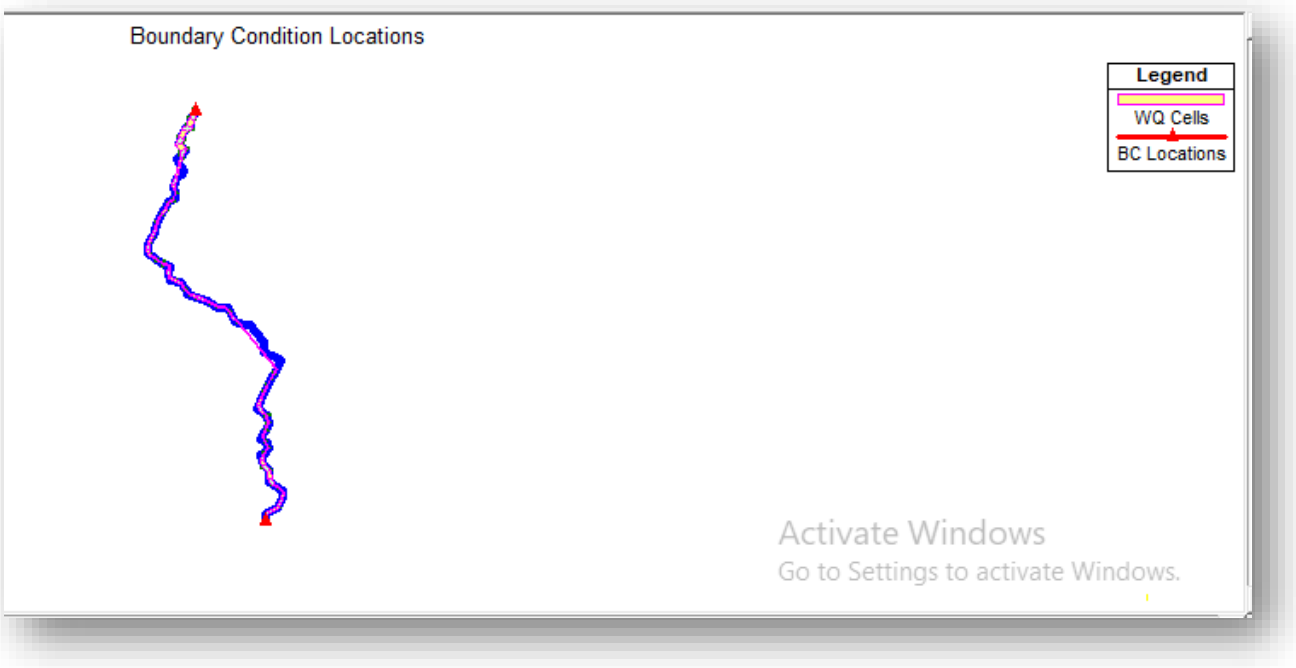

Figure (4.15). TDS, PH, T, DO boundary conditions

4.6 Model Simulation

The HEC-RAS model was used to compute the variations of river water quality parameters using the desired inputs for the current river system. The analysis is being carried out during the defined simulation period. The simulation results were given with a 1-hour output time interval so that the differences in the water quality parameters could be seen every 1 hour. The simulation's outcomes included a longitudinal and time series variance plot of the water quality parameters. Figures (4-16, 4-17, 4-18 and 4-19) Temp, pH, DO and TDS.

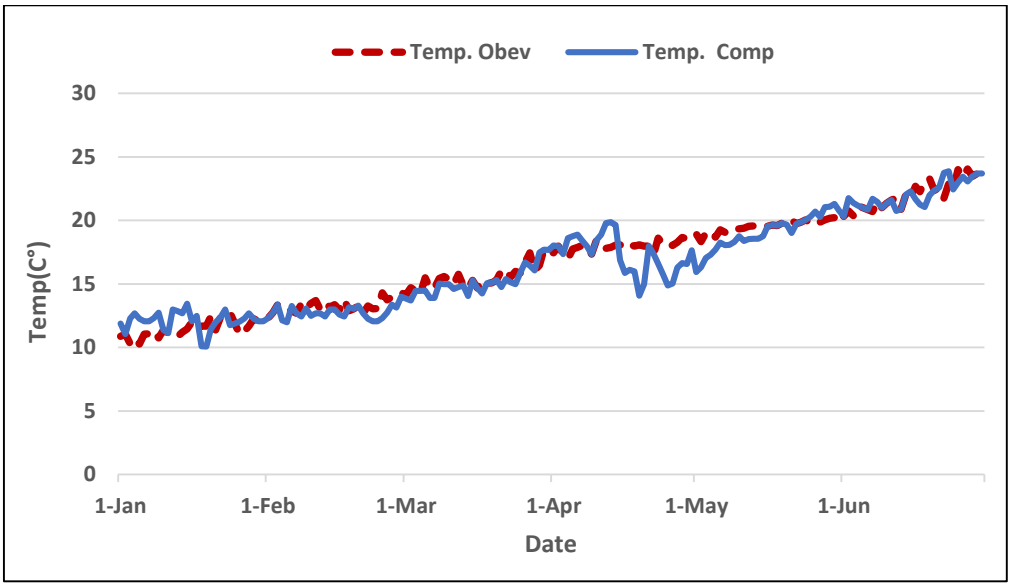

Figure (4.16) Compassion between simulated and observed Temp (C°)

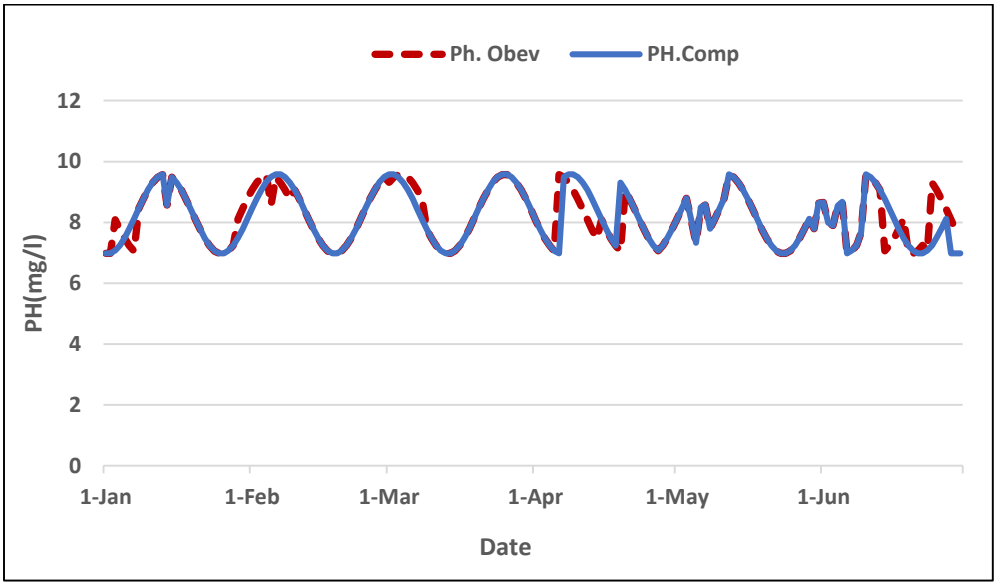

Figure (4.17) Compassion between simulated and observed PH (mg/l)

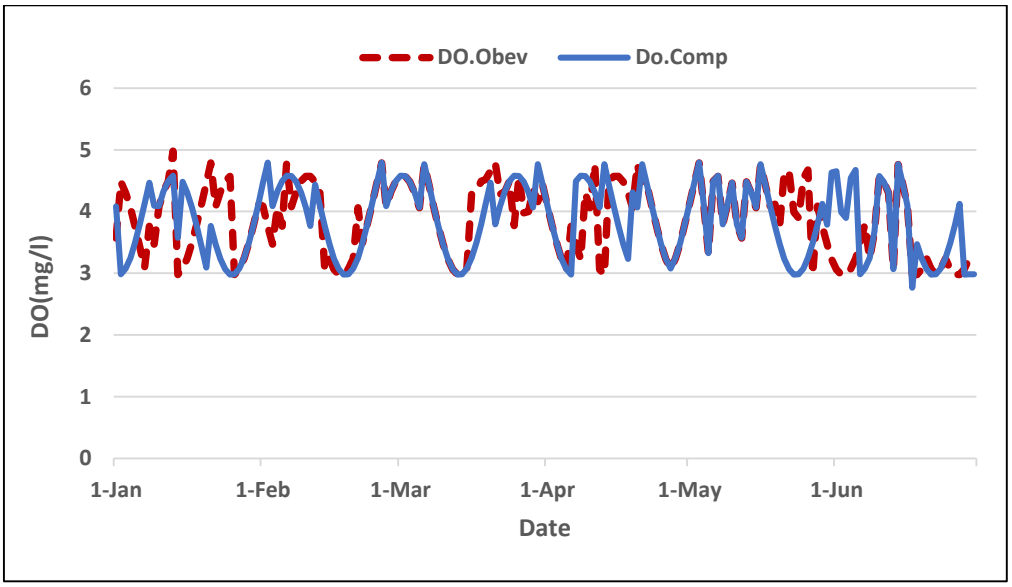

Figure (4.18) Compassion between simulated and observed DO (mg/l)

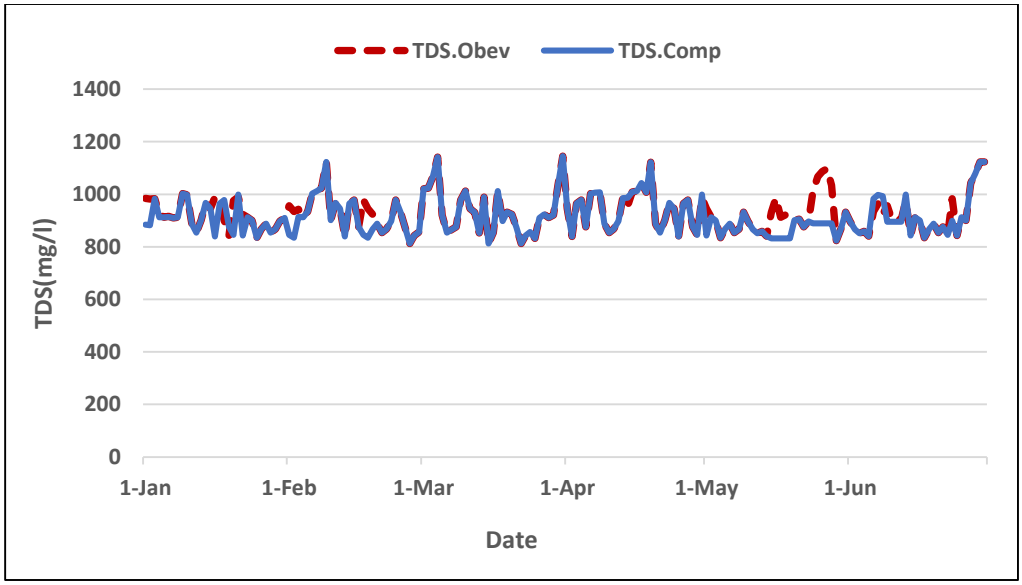

Figure (4.19) Compassion between simulated and observed TDS (mg/l)

4.7 Discussion of Water Quality Model.

Based on the results of model simulations for water quality parameters along the river stretch at various points in time. The following conclusions can be taken in order to determine the river's water quality:

- Temperature: Figure (4-20) depicts longitudinal temperature variations along the length of the river, with the highest temperature recorded on 25/6/2020 at 13:30 noon.
- DO: Figures (4 -21a,b) represents the longitudinal differences DO respectively along the length of the river, as it was observed that the lowest value of DO was on 3/1/2020 at 15:15 at night, while the highest value of DO was on 5/6/ 2020 at 18:45 pm .
- PH: Figures (5-22a,b) depict longitudinal pH differences along the river's length. It was discovered that
- TDS: Figures (5-23a,b) shows the longitudinal differences TDS respectively along the length of the river, as it was observed that the lowest value reached by the total dissolved solids was on13/1/2020 at 1:30 at night, while the highest value was on 25/5/2020 at 9:00 pm.

The key cause of changes in water quality parameters is a combination of factors, including temperature differences between summer and winter, night and day , unusual phytoplankton formation, and sewage discharge into the riverbed. As a result, these factors contribute to the depletion of significant quantities of dissolved oxygen in the water, the death of fish, the degradation of the river's aesthetics, the development of many lung diseases, hus having a significant hand in the degradation of the river water quality.

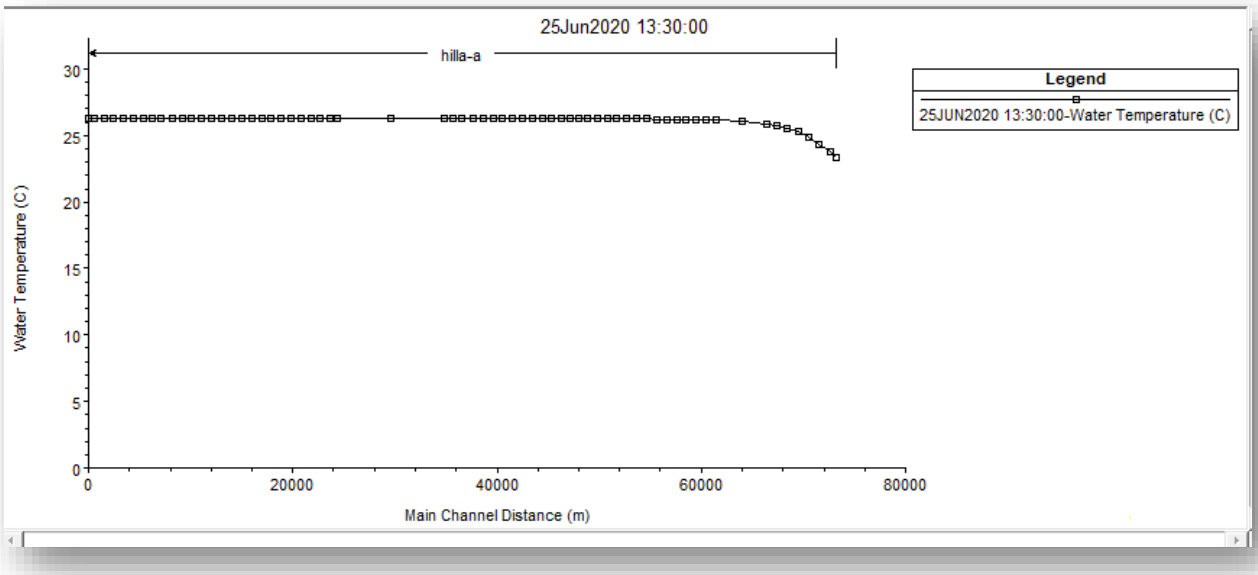

Figure (4.20) Temperature differences Euphrates river

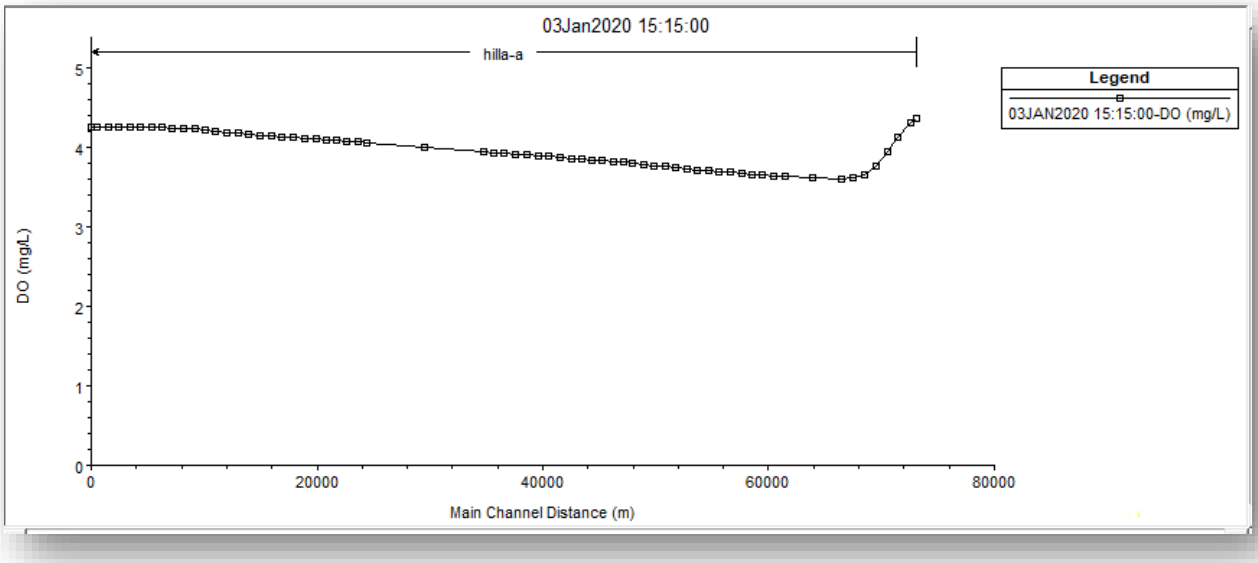

Figure (4.21a) DO differences Euphrates river

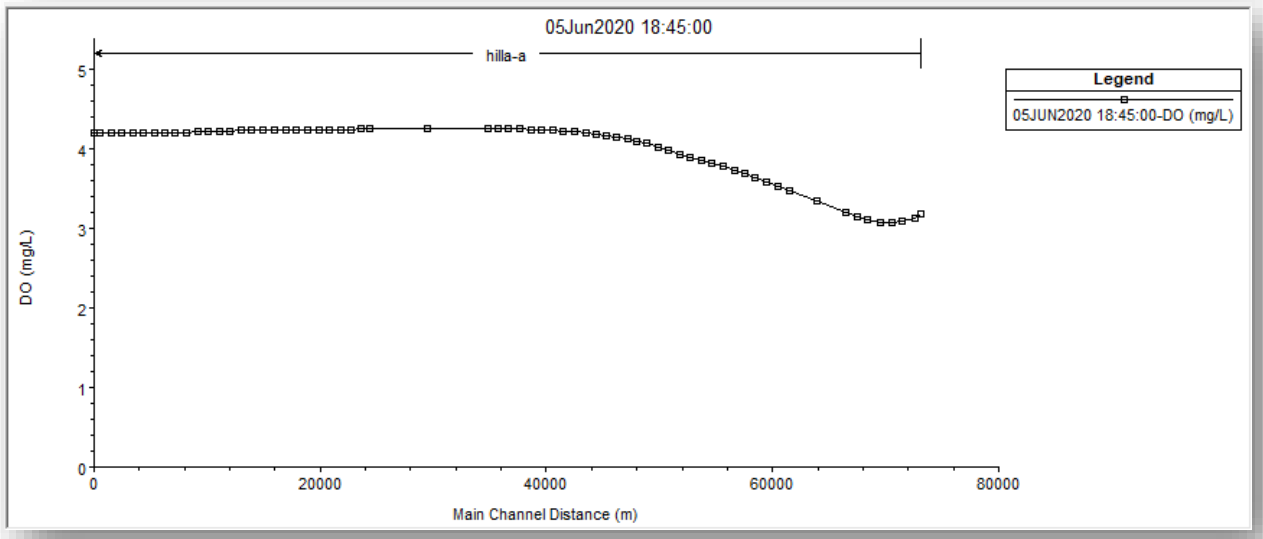

Figure (4.21b) DO differences Euphrates river

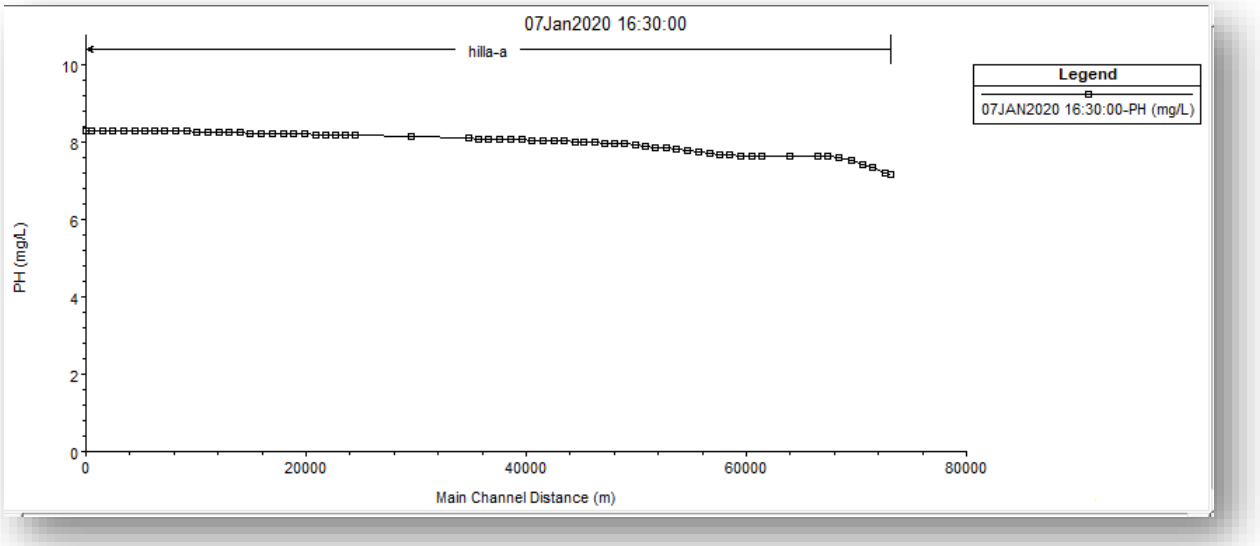

Figure (5.22a) pH differences Euphrates river

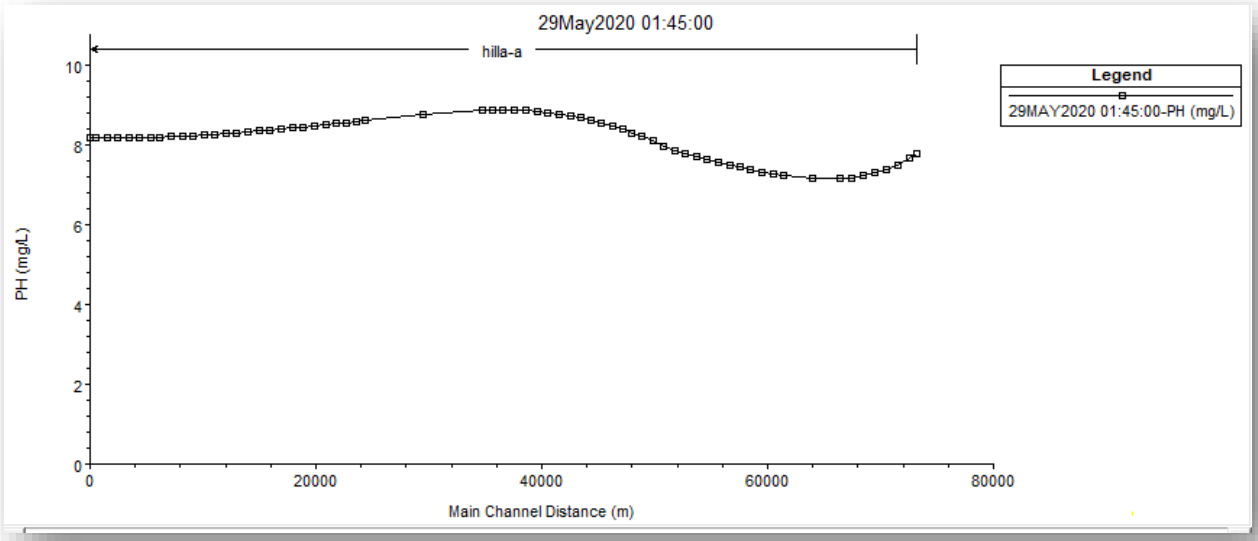

Figure (5.22b) pH differences Euphrates river

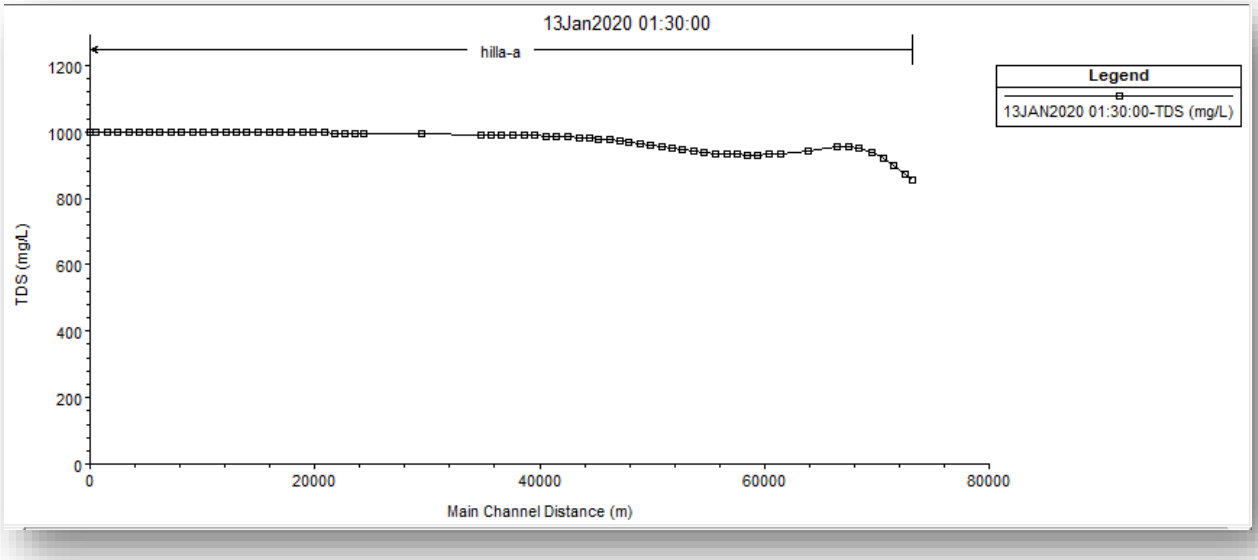

Figure (5.23a) TDS differences Euphrates river

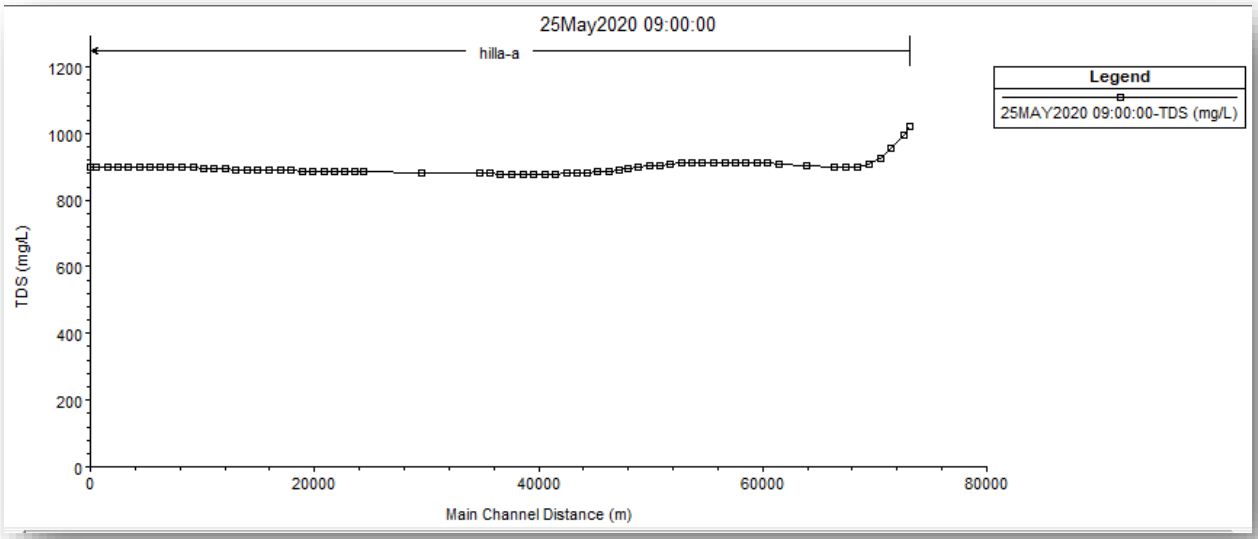

Figure (5.23b) TDS differences Euphrates river

Figures (4-24, 4-25 4-26 and 4-27) shows Schematic for Water Quality Parameters.

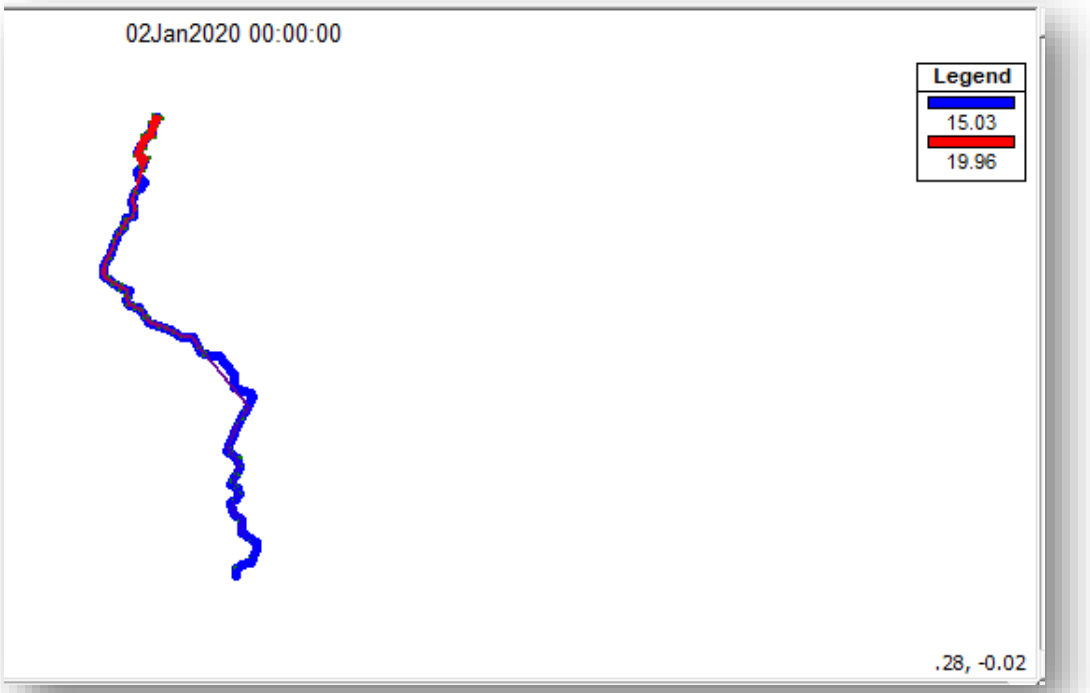

Figure (4.24): Schematic for Parameter Temperature

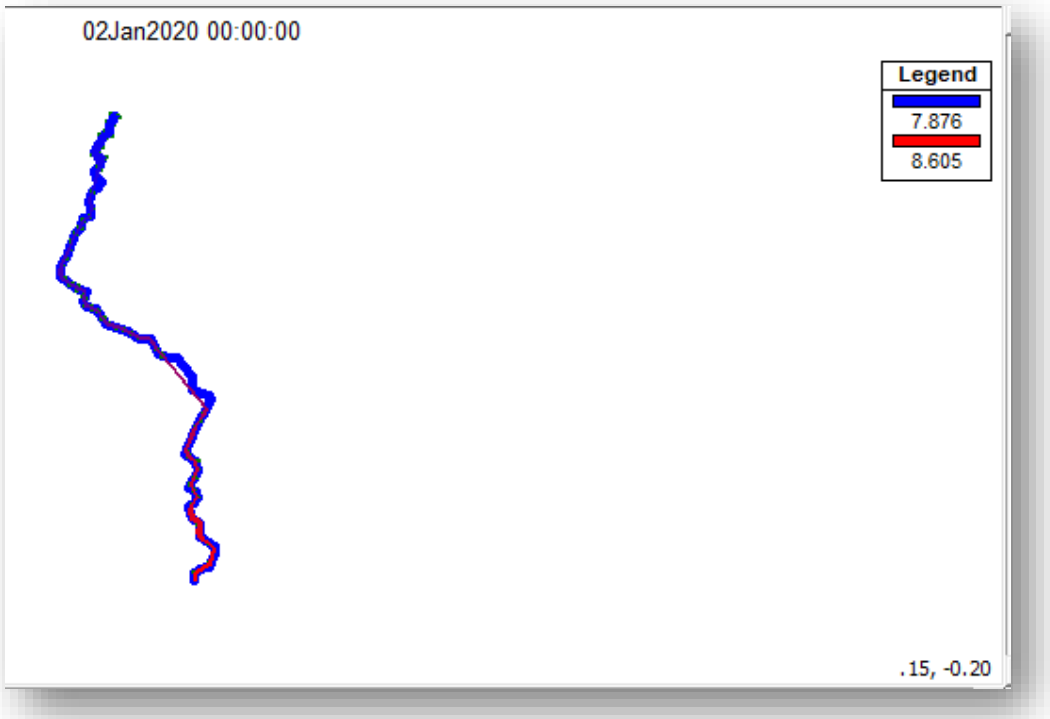

Figure (4.25): Schematic for Parameter PH

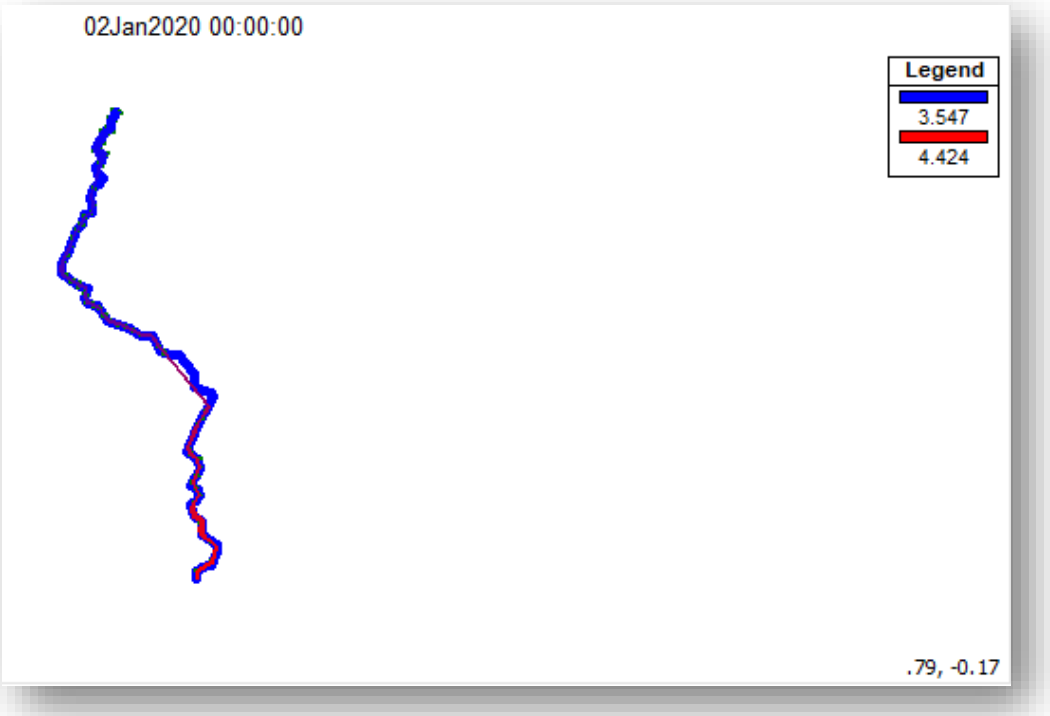

Figure (4.26): Schematic for Parameter DO

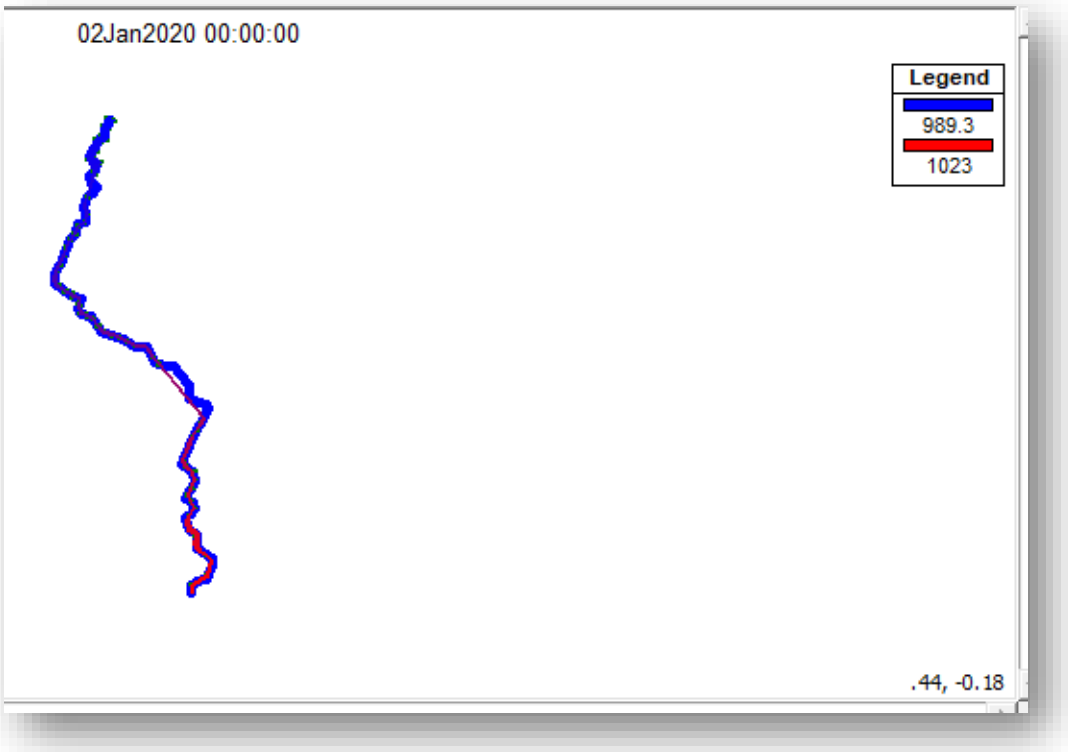

Figure (4.27): Schematic for Parameter TDS

CHAPTER FIVE

CONCLUSIONS & RECOMMENDATIONS

5.1 Conclusions

After analyzing the data provided by the HEC-RAS Model and laboratory work, the following conclusions were reached.

1. Weighting factor θ values that provide reliable and accurate solutions tend to be in the $\theta \leq 0.95$ range. When a weighting factor of $\theta = 1$ is used, accurate results are obtained.
2. Manning's coefficients (0.045) and (0.047) are suitable for the main channel and floodplain, respectively, since they provide fair agreement between computed and observed hydrographs.
3. The findings of the field data revealed that:
   a. The temperature of water for sources does not exceed the permitted Iraqi specifications of the temperature factor of (35 C°). With the highest temperature recorded on 25/6/2020 at 13:30 noon. While the lowest temperature was recorded on 16/1/2020 at 12:30 morning.
   b. The acidity function pH throughout the research time and the study scope, remained within acceptable limits (6.5-8.5). The lowest pH value was on 7/1/2020 at 16:30 in the morning, while the highest value was on 29/5/ 2020 at 1:45 pm.
   c. The concentration of dissolved oxygen (DO) in most of the stations was less than 5 mg/l, indicating that the water river is unhealthy. The lowest value of DO was on 3/1/2020 at 15:15 at night, while the highest value of DO was on 5/6/ 2020 at 18:45 pm .

d. Total Dissolved Solid (TDS) is not exceeds the allowable limits in all stations. as it was observed that the lowest value reached by the total dissolved solids was on13/1/2020 at 1:30 at night, while the highest value was on 25/5/2020 at 9:00 pm.

4. A model verification revealed that the calculated and predicted values were in full agreement.

5.2 Recommendations

1. Using a Two-dimensional model in the HEC-RAS software, run simulations for various parameters.
2. Measuring more parameter for water quality such as Tss , Calicum ,Potassium and Heavy metals.
3. Further studies concerning lateral outflows, seepage, and losses from the Euphrates river and its main branches should be recommended for the study region, which is primarily dependent on agriculture, in order to meet current and potential irrigation requirements and other requirements.
4. Using a finite element computational technique to solve the governing equations in two dimensions of flood wave diffusion (coupled flow and contaminant transport modeling).

REFERENCES

- Ardıçlıoğlu, M., Kuriq, A., 2019, "Calibration of channel roughness in intermittent rivers using HEC-RAS model: case of Sarimsakli creek, Turkey" , SN Applied Sciences (2019) 1:1080 | https://doi.org/10.1007/s42452-019-1141-9.
- Ivanescu, Veronica., Sandu, M., 2014, " Application of a hydrodynamic mike 11 model for argesel river" , STEF92 Technology Ltd., 1 "Andrey Lyapchev" Blvd., 1797 Sofia,Bulgaria . OI: 10.5593/sgem2014B31 .
- Omran, A.Z., Othman, Y.N., Saleh, A.Z., 2018, " STEADY FLOW ANALYSIS FOR SHATT AL- HILLA USING HEC-RAS PROGRAM" , International Journal of Civil Engineering and Technology (IJCIET) Volume 9, Issue 6, June 2018, pp. 525–533, Article ID: IJCIET_09_06_060 .
- Al-Mansori, H.J.N., Al-Zubaidi, A.S.L., 2019, " One-Dimensional Hydrodynamic Modeling of the Euphrates River and Prediction of Hydraulic Parameters" , Civil Engineering Journal vol. 6, No. 6, June.
- Hameed, K.L., Ali,T.S., 2013, " Estimating of Manning's Roughness Coefficient for Hilla River through Calibration Using HEC-RAS Model", Journal of Civil Engineering, volume 7,No.1.
- Patel, L.P., Timbadiya, V.P., 2012, " HEC-RAS BASED HYDRODYNAMIC MODEL IN PREDICTION OF STAGES OF LOWER TAPI RIVER", Journal of Hydraulic Engineering 17:2, 110-117, OI: 10.1080/09715010.2011.10515050.

REFERENCES

- Tunas, G.I., Arafat, Y., Azikin, H., 2019, " Integration of Digital Elevation Model (DEM) and HECRAS Hydrodynamic Model for flood routing", Materials Science and Engineering 620 (2019) 012026
  OI:10.1088/1757-899X/620/1/012026.
- Abbas, K.A.H.A., 2016, " Application of a Hydrodynamic HEC-RAS Model For Shatt Al-Arab River", JOURNAL OF ENGINEERING
  AND TECHNOLOGY (MJET) Vol.(4),No.(2),(2016),11-22.
- Salah , M.A.E., Al-Othman, M.E., Turki, M.A., 2012, " Assessment of Water Quality of Euphrates River Using Cluster Analysis", JOURNAL OF ENGINEERING Protection, 2012 3, 1629-1633.
- Al-Suhili, H.R., 2018, " Frequency Analysis of Some of Water Quality Parameters of
  Shatt Al-Hilla River, Iraq", JOURNAL OF ENGINEERING Research (AJER) Volume-7, Issue-6, pp-190-199.
- Dash, S., Vijay, R., 2017, " A MODELLING APPROACH FOR WATER QUALITY ASSESSEMNT OF PILI RIVER USING HEC-RAS", Annual Convention of IWWA on “Smart Water Management” January 19-21, 2017.
- Yang, Y., Wang, Y., Zhang, W., 2012, " Numerical Study of Coupled One-dimensional and Two-dimensional Hydrodynamic and Water Quality Model for Complex Lake and River Network Areas",
- Alhashimi, M.A.S., Mustafa, S.A., 2012, " PREDICTION OF WATER QUALITY INDEX FOR EUPHRATES RIVER-IRAQ", journal for environment and water.

REFERENCES

- Lima, R.D., 2020, " External control and automatic calibration of the HEC-RAS NSM-I water quality model", This manuscript is a non-peer reviewed preprint uploaded to EarthArXiv as an openaccess contribution.
- Alanbari, A.M., Alqizweeni, S.S., Abdalwahed, A.R., 2017, " Assessing of Water Quality of Al-Kufa River for Drinking Water using WQI and GIS", Journal of Current Engineering and Technology E-ISSN 2277 – 4106, P-ISSN 2347 – 5161.
- Taralgatti, D.P., Pawar, S.R., Pawar, S.G., 2020, " Water Quality Modeling of Bhima River by using HEC-RAS Software", Journal of Engineering and Advanced Technology (IJEAT) ISSN: 2249 – 8958, Volume-9 Issue-3.
- AHMED, H.A., 2010, " USING HEC-RAS AND QUAL2E TO ASSESS JOHOR RIVER WATER QUALITY", .
- Ferreira, M.D., Gomes, j., 2017, " Verification of Saint-Venant equations solution based on the lax diffusive method for flow routing in natural channels", Content may be subject to copyright DOI:10.1590/2318-0331.011716104.
- Al-Husseiny, A.A.A.K.F., Al-Mansori, J.N., Al-Kizwini, S.R., 2019, " MODELING AND SIMULATION OF POLLUTANTS TRANSPORT IN HILLA RIVER", A THESIS , University of Babylon Collage of Engineering Environmental Department.
- Khodair, A.A., Obead, H.I., 2017, " Design and Implementation of Remote Controller to Modeling the Dynamic Wave of Flood in Meandering Rivers", A Thesis Submitted to the College of Engineering University of Babylon.

REFERENCES

- Abida,H. , Ellouze , M,. Mahjoub , M., 2005 ," Flood routing of regulated flows in Medjerda River-Tunisia", Journal of Hydro informatics, Vol.(7), No.(3),IAHR-IWA Joint Committee on Hydroinformatics, IWA Publishing.
- Aldrighetti , E., 2007,"Computational hydraulic techniques for the Saint Venant Equations in arbitrarily shaped geometry" Ph.D. thesis, Dipartimento di Matematica, Dottorato di Ricerca in Matematica.
- AL-Fahdawi,S.A., 2009,"Numerical modeling of flood wave behavior with meandering effects (Euphrates River, Haditha Hit". B.Sc. Thesis, Building and Construction Engineering Department, University of Technology, Iraq.
- Amein, M., Fang, C.S., (1970)," Implicit flood routing in natural channels", Journal hydraulic division, ASCE, Vol.(96),No.HY-12, pp,2481-2500.
- Barkau, R. L., 1992,"One-dimensional unsteady flow through a full network of open channels", User's manual, Report CDP-66, Hydrological Engineering Center, US Army Corps of Engineers, Davis, CA.
- Bedford, K.W., Sykes, R.M., Libicki ,C., 1983," Dynamic Advective Water Quality Model for Rivers", Journal of Environmental Engineering, Vol.(109), No.(3).
- Chalfen , M. and Niemiec , A., 1986,"Analytical and numerical solution of Saint-Venant equations", Journal of Hydrology, Vol.(86)

  ,Issues 1-2, pp.1-13, Elsevier B.V.
- Chow,V. T., Maidment, D.R, and Mays,L.W., 1988,"Applied hydrology", McGraw-Hill,New York.

REFERENCES

- Chow, V.T., 1959,"Open-channel hydraulics", McGraw-Hill book company, New York.
- Contractor, D.N., and King, P.H., 1980," Stream flow and water quality modeling of the Chowan River ",Virginia Water Resources Research Center, 119, Bulletin, TD201, Vol.(57), No.(119).
- Fenton, J. D., 2002,"The application of numerical methods and mathematics to hydrography", 11th Australasian Hydrographic Conference. Sydney.
- French, R.H., Krenkel, P.A., 1980, " Effectiveness of River Models", Water Resources and Technology, Vol.(13), pp,99-113.
- Gunduz,O., 2004,"Coupled Flow and Contaminant Transport Modeling In Large Watersheds ", Ph.D. Thesis, Civil and Environmental Engineering, Georgia Institute of Technology.
- Gupta, B.L., 2007, "Water resources systems and management", 2nd Edition, Standard publishers ,Delhi.
- Heatherman, W., 2008, "Flood Routing on Small Streams: A Review of Muskingum-Cunge, Cascading Reservoirs, And Full Dynamic Solutions", Ph.D. thesis, Civil Engineering and the Graduate Faculty of the University of Kansas.
- Henderson, F.M., 1966, "Open Channel Flow", Macmillan Publishing Company, New York.
- Hubert, C., 2004, "The Hydraulics of Open Channel Flow", Butterworth-Heinemann, 2nd Edition, Linacre House, Jordan Hill, Oxford, Elsevier Ltd.
- Jayawardena,A.W., 2014," Environmental and Hydrological Systems Modeling ", CRC Press.
- Koussis, A.D., Mazi, K., Lykoudis, S., Argiriou A. A., 2012, " Reverse Flood Routing with The Inverted Muskingum Storage Routing Scheme". Natural Hazards Earth System Science.,

Vol.(12),
pp.217–227.

- Mahessar, A.A., Qureshi, A., Baloch, A., 2013, "Numerical Study on Flood Routing in Indus River ". International Water Technology Journal , IWTJ ,Vol.(3), No.(1).
- Maidment, D.R., 2002, "Handbook of Hydrology", McGraw-Hill, New York.
- Moghaddam, M.A., Firoozi, B., 2011, "Development of Dynamic Flood Wave Routing in Natural Rivers through Implicit Numerical Method ", American Journal of Scientific Research, Issue(14),pp.6-17.
- Naggar,O.M., 2004," Decision Support Systems in Water Management", Proceedings of the Eighth International Water Technology Conference, IWTC8 2004, Alexandria, Egypt.
- Price, R.K., 1974," Comparison of Four Numerical Methods for Flood Routing", Proceedings of the American Society of Civil Engineers, Journal of Hydraulics Division, Vol.(100), No.(HY7), pp.879- 899.
- Renjie, X., Ben, C. Y., 1994,"Significance of Averaging Coefficients in Open Channel Flow Equations", Journal of Hydraulic Engineering, Vol.(120), No.(169).
- Saavedra, J. L., Martínez, R. G., 2003," Dynamic Wave Study of Flow in Tidal Channel System of San Juan River" Journal of Hydraulic Engineering, Vol.(129), No.(519.)
- Sahib, J. H., 2013, " Inverse Routing for Operation and Control of Gates Stroke for Al-Kufa Barrage", M.Sc. thesis, College of Engineering, University of Kufa, Iraq.
- Snead, D.B., 2000, "Development and application of Unsteady Flood Models using Geographic Information Systems", M.Sc.

thesis, Faculty of the Civil Engineering Department, University of Texas, USA.

- U.S. Army Corps of Engineers, 2010," HEC-RAS, River Analysis System User's Manual ", Hydraulic Engineering Center, New York.
- Al-Eoubaidy, K.A., 1998, “Dispersion of Pollutants in Tigris River Using Finite Difference and Finite Element Method” The Sc. J. of Tikrit University, Vol. 5, No. 2, PP. 45-56.
- Al-Eoubaidy, K.A., 1999, “Water Quality Modeling Euphrates Rivers” Ph.D. Thesis, College of Eng., University of Baghdad.
- Fisher, Hugo, B., 1967, “Analytical Prediction of longitudinal Dispersion Coefficients in Natural Streams” The Twelfth International Association for Hydraulic Research, Vol. 4, b.
- Petrus, G.B., 1990, “Numerical Modeling of pollution transport in Rivers Including Density Effects “ M.Sc. Thesis, College of Eng. University of Baghdad.
- Vasiliev, O.F., 1965, “Methods for the Calculation of Shock waves in Open Channels” in Proc., 11th Congress IAHR, Leningrad, U.S.S.R. Paper 3.44.
- Al-Thamiry, H.A., 1997, “numerical Modeling of Salt-Intrusion in Shatt Ai-Arab” M.Sc. Thesis, College of Eng. Univ. of Baghdad.
- Taef Zuhair, 2000, “Water Quality Modeling in Diyala River” M.Sc. Thesis, College of Eng., University of Al- Mustansiriyah.
- Strelkoff, T., 1969, “ The One-Dimensional Equation of Open Channel Flow” J. Hyd. Div., ASCE, Vol. 95, No. (Hy3), PP.861-874.
- Stoker, J.J., 1953, “Numerical Solution of Flood Prediction and River Regulation Problems” Rept. I, New York University, Institute of Mathematical Scie., Rept. No. IMM-200, New York.

REFERENCES

- Castellarin, A., Di Baldassarre, G., Bates, P. D., Brath, A., 2008," Optimal cross-section spacing in Preissmann scheme 1D hydrodynamic models", J. Hydr. Eng., 135(2), pp.96–105,.
- Parhi, P. K., Sankhua, R. N., Roy, G. P., 2012 "Calibration of Channel Roughness of Mahanadi River (India) Using HEC-RAS Model," Journal of Water Resources and Protection, Vol. 4, No. 10, pp. 847-850.
- Doherty, R., 2010 "Calibration of HEC-RAS Models for Rating Curve Development in Semi Arid Regions of Western Australia," AHA 2010 Conference, Perth.
- Hicks, F. E., Peacock, T., 2005, "Suitability ofHEC-RASfor Flood Forecasting", Canadian Water Resources Journal, CWRA, Vol. 30(2), pp. 159-174.
- Jain, S. K., Agarwal, P. K., Singh, V. P., 2007, " Hydrology and Water Resources of India", Springer Netherlands, Part-3, Vol. 57, pp. 561-565.
- Tunas, I .G., 2004, "Simulation Model of Flood Control System Using HEC-RAS and GIS", Yogyakarta : Master Thesis Universitas Gadjah Mada) [in Indonesian].
- Otieno, D., 2008,"Determination of some Physico—Chemical Parameters of the Nairobi River, Kenya," Journal of Applied Science Environmental Management, Vol. 12, No. 1, 2008, pp. 57-62.
- Shrestha, S., Kazama, F., 2007,"Assessment of Surface Water Quality using Multivariate Statistical Techniques:

REFERENCES

A Case Study of the Fuji River Basin, Japan," Environmental Modeling & Software, Vol. 22, No. 4, 2007, pp. 464-475.

- Shivani, S., Anulool, S.M. N., Tandon, P., 2011, "Evaluation of Effect of Drains on Water Quality of River Gomti in Lucknow City Using Multivariate Statistical Techniques," International Journal of Environmental Sciences, Vol. 2, No. 1, 2011, pp. 1-7.
- Ritesh, V., Swapnil, R.K., 2011, "Assessment of Water Quality using Cluster Analysis In Coastal region of Mumbai, India", Environmental Monitoring Asssessment (2011), 321-332.
- Rudi, R., Matjaz, C., Andrej, S., 1997, "Hydrodynamic and Water Quality Modeling: Case Studies", Ecological Modeling 101 (1997), 209-228.
- Al-Heety, E.A., Turky, A.M., Al-Othman, E.M., 2011, "Assessment of the Water Quality Index of Euphrates River between Heet and Ramadi Cities, Iraq". International Journal of Basic and Applied Sciences IJBAS-IJENS, Vol. 11, No. 06, pp. 38-47.
- Al-Mahmoud, H., Al-Sayaab, H., Al-Miahi, D., Mutasher, W., 2011, "One dimensional model to study hydrodynamics properties for north part of Shatt Al Arab River (south Iraq)", Basrah Journal of Scienec , 28(1)p.p.1-14.
- Abed, B. SH., 1998, "Development of Dynamic Water Quality Model for Tigris River within Baghdad City", Ph.D. Thesis. College of Engineering, University of Baghdad
- Al-Shami, A., Al-Ani, N., and Al-Shalchi, T. K., 2006,"Evaluation of Environmental Impact of Tigris River Pollution (between

REFERENCES

Jadirriya and Dora Bridges)", Journal of Engineering, Vol. 13, No. 3, Sep., pp. 844-861.

- Al-Sudani, H. A., 2014, " Two Dimensional Mathematical Model of Contamination Distribution In The Lower Reach of Diyala River", M.Sc. thesis. University of Al-Mustansiriyah College of Engineering.
- Al-Zboon, K. K. and Al-Suhaili, R. H., 2009, "Improvement of Water Quality in a Highly Polluted River in Jordan", Jordan Journal of Civil Engineering, Vol. 3, No. 3, pp. 283-293.
- Al-Zubaidi, A, H., 2008, "Two Dimensional Numerical Model For Simulation The Dispersion of Pollutants In Shatt Al-Hilla", College of Engineering, Babylon University.
- Antonio, A. L. and Rui, A. R., 2008, "Pollutant Dispersion Modelling for Portuguese River Water Uses Protection Linked to Tracer Dye Experimental Data",Wseas Transactions on Environment and Development, Issue 12, Vol. 4, Dec.
- Aswed, T. Z., 2000, "Water Quality Model in Diyala River", M.Sc. Thesis. College of Engineering, Al-Mustansiriyah University.
- Basuki, W., 2012, "The Influence of Hydrodynamics on Pollutant Dispersion in the River", International Journal Contemporary Mathematical Sciences, Vol. 7, No. 45, pp. 2229-2234.
- Chow, V. T., 1975, "Open Channel Hydraulic". Mc Graw-Hill, New York.
- Crabtree, R. W., Cluckie, I. D., Forster, C. F., Crokett, C. P., 1986, "A Comparison of Two River Quality Models", Journal of Water Research, Vol.20, No. 1, pp. 53-61.
- Czernuszenko, W., 1987, "Dispersion of Pollutants in Rivers". Journal of Hydrological Science, Vol. 32, pp. 3-13.

REFERENCES

- Dammuller, D. C., Bhallamudi, S. M., Chaudhry, M. H., 1989, “Modeling of Unsteady Flow in Curved Channel”.Journal of Hydaulic Engineering, ASCE, Vol. 115, No. 11, pp. 1479-1495.
- Elisabeta, C. A., Vasile, M. C., Paul, S. A., Andrezj, K., 2010, "Dynamic Simulation of Someş River Pollution Using MATLAB and COMSOL Models", REV. CHIM. (Bucharest), Nr.11.
- Hashim, K. S., 2007, "Two-Dimensional Modeling of Water Quality in Shatt Al-Hilla",Ph.D. Thesis. Environmental Engineering Department, University of Baghdad.
- Ismail, A. H., Abed, G. A., 2013,"BOD and DO Modeling for Tigris River at Baghdad City Portion Using QUAL2K Model", Journal of Kerbala University, Vol. 11, No. 3 Scientific.
- Joodi, A. S., 2001, "Study of Thermal Pollution for Heated Water Released from Al-Doura Power Station to Tigris River", M.Sc. Thesis. Environmental Engineering Department, Al-Mustansiriyah University.
- Kashefipour, M. S., Falconer, R. A., 2002,"Longitudinal Dispersion Coefficients in Natural Channels”, Water Resources Research, Vol. 36, No. 6, pp. 1596–1608.
- Kefay, E., 2000,“Development of an Unsteady State Analytical Solution Surface Water Quality as an Environmental Tool”, Ph.D. Thesis. Italy.
- Keith, W. B., Robert, M. S., 1983,“Dynamic Advective Water Quality Model for Rivers”, Environmental Engineering Journal, Vol. 109, No. 3, Jan.
- Kudair, K. M., 1999,“A Finite Element Model to Simulate Pollutants Transport in Shatt Al-Basrah Canal and Khour Al-Zubair Estuary”, Ph.D. Thesis. College of Engineering, University of Baghdad.

REFERENCES

- Launder, B. E. Spalding, D. B., 1972,"Lectures in Mathematical Models of Turbulence", Academic Press.
- Liu, H., 1977, "Predicting Dispersion Coefficient of Streams", Journal of Environmental Engineering Division, ASCE, Vol. 103, No. 1, pp. 59-69.
- Matt, C., 2009, "An Evaluation of Turbulence Models for the Numerical Study of Forced and Natural Convective Flow in Atria", M.Sc. Thesis. Queen's University, Canada.
- McQuivey, R. S., Keefer, T. N., 1974,"Simple Method for Predicting Dispersion in Streams", Journal of Environmental Engineering, ASCE, Vol. 100, pp. 997-1011.
- Meddah , S., Saidane, B. , Hadjel ,M., Hireche O., 2015, "Pollutant Dispersion Modeling in Natural Streams Using the Transmission Line Matrix Method", Journal of water- open access, University of Sciences and Technologies in Algeria, Vol. No.7,pp. 4932-4950.
- Ministry of Water Resources.(2020).Iraq.
- Narsilio G., Pivonka A., and Smith P., 2007, "Comparative study of methods used to estimate ionic diffusion coefficients using migration tests", Cement and Concrete Research., 37, 1152–1163.
- Pawel, M. R., Jaroslaw, J. N., Tomasz, D., 2004, "Transport of Pollution in the Rivers Flowing Through Wetland Areas", Journal of Hydraulic Research, Vol. 36, No. 2, pp. 269-279.
- Nemerow, N. L., 1974, "Scientific Stream Pollution Analysis", McGraw-Hill Book Company, New York, U.S.A.
- Petrus, G. B., 1990, "Numerical Modelling of Pollutants Transport in Rivers Including Density Effect", M.Sc. Thesis. Environmental Engineering Department, College of Engineering, University of Baghdad.

REFERENCES

- Qasim, F.A., 2004, " Analytical Water Quality Models for the River Tigres Atninevah Province", Ph. D Thesis. College of Engineering, Mosol University.
- Rahman M. K., Al-Kutti W. A., Shazali M. A. Baluch M. H., 2012, "Simulation of chloride migration in compression-induced damage in concrete", Journal of Materials in Civil Engineering, 14, 789-796.
- Razoky, M. Y., 1984, "Dispersion of Pollutants in Rivers near Drainage or Sewer Outfall", M.Sc. Thesis. College of Engineering, University of Baghdad
- Roberson, J.A., Crowe, C. T., 1997, "Engineering Fluid Mechanics", John Wiley and Sons, Inc. New York.
- Sahay, R. R. Dutta, S., 2009, "Prediction of Longitudinal Dispersion Coefficients in Natural Rivers Using Genetic Algorithm", Hydrology Resource, Vol. 40, No. 6, pp. 544-552.
- Sayre, W. W., 1975, "Dispersion of Mass in Open Channel Flow", Hydrology Papers, Colorado, No. 75, Aug.
- Schnoor, J. L., 1996, "Environmental Modelling Fate and Transport of Pollutant in Water, Air and Soil", John Willey and Sons, Inc.
- Shaker, A. S. M., 1985, "Numerical Modeling of Unsteady Flow in the Tigris-Diyala Confluence", M.Sc. Thesis. College of Engineering, University of Baghdad.
- Shazali M. A., Baluch M. H., Al-Gadhib A. H., 2006, "Predicting residual strength in unsaturated concrete exposed to sulfate attack", Journal of Materials in Civil Engineering, 18, 343-354.
- Thomas, N. K., Jobson, H. E., 1978, "River Transport Modeling for Unsteady Flows", Journal of the Hydraulic Division, Vol. 104, No. HY5, May, pp. 635-647.

REFERENCES

- Vasile, M. C., Elena, D. B., Paul, S., 2010, "Simulation and Control of Pollutant Propagation in Someş River Using COMSOL Multiphysics", 20th European Symposium on Computer Aided Process Engineering– ESCAPE20, Elsevier B.V.
- Wang, Z., Delestre,O., Hou,Q.D., Wei, J., Dang, J., 2016, "SPH Simulation of Pollutant Transport in Rivers", School of Computer Science and Technology, Tianjin University, Tianjin 300350, China Lab. J.A.
- Yvetta, V., 2000, "Numerical Prediction of Pollutant Dispersion in Upper Part of Ondava River", Journal of Hydraulic Division, Process ASCE, Vol. 93, pp. 201-212.
- Iraqi Ministry of Water Resources / Water Resources Directorate of Babylon ,(2020).
- The Iraqi Ministry of Water Resources / Meteorological Authority,(2020).
- Iraqi Ministry of Water Resources / General Authority for Survey,(2020).
- Iraqi Ministry of Water Resources / Directorate of Water Resources of Babylon / Al-Hindiya Barrage Project.
- Iraqi Ministry of Water Resources / Najaf Water Resources Directorate / Kufa Barrage Project.

APPENDIXS

APPENDIX- A

LABORATORY TESTS

A-1 Laboratory Test.

A-1-1 Temperature.

The temperature was measured directly from the source of the sample. Figure (A-1-1) shows how this was done.

Figure (A-1.1): ***Temperature measurement***

A-1-2 Acidity Function pH

The measurements were taken at the collection site. In order to calculate pH, you must first calibrate the instrument, then place the electrode in a well-mixed sample and read the pH directly from the pH meter, as shown in figure (A-1-2)

Figure (A-1.2): ***The pH meter***

A-1-3 Dissolved Oxygen (DO)

The physical, chemical, and natural forms in a water body influence dissolved down oxygen (DO) levels in natural and wastewaters. The

dissolved oxygen (DO) is a measure of the quality of water. Increased dissolved oxygen levels are beneficial to marine organisms for a variety of reasons. The DO is also essential in the precipitation of organic substances in water and their dissolution.

The Winkler strategy was utilized to assess the concentration of the dissolved down oxygen in water in this study about. Samples are collected in a 300 mL container, with special attention paid to the absence of air bubbles. Two milliliters of manganese sulphate, base iodide are added to the sample and shaken several times before left for 10 minutes to precipitate. Add two milliliters of concentrated sulfuric acid and shake the container, oxygen is installed (this process is done in the collection site). Titrate 203 mL of the sample against sodium thiosulfate using starch as an indicator before the solution color changes from blue to colorless to complete the measurement (Al-Tufaili,2015).

The (DO)mg/L = the volume of sodium thiosulfate. The steps of this method shown in Figure(A-1-3) and(A-1-4).

APPENDIXS

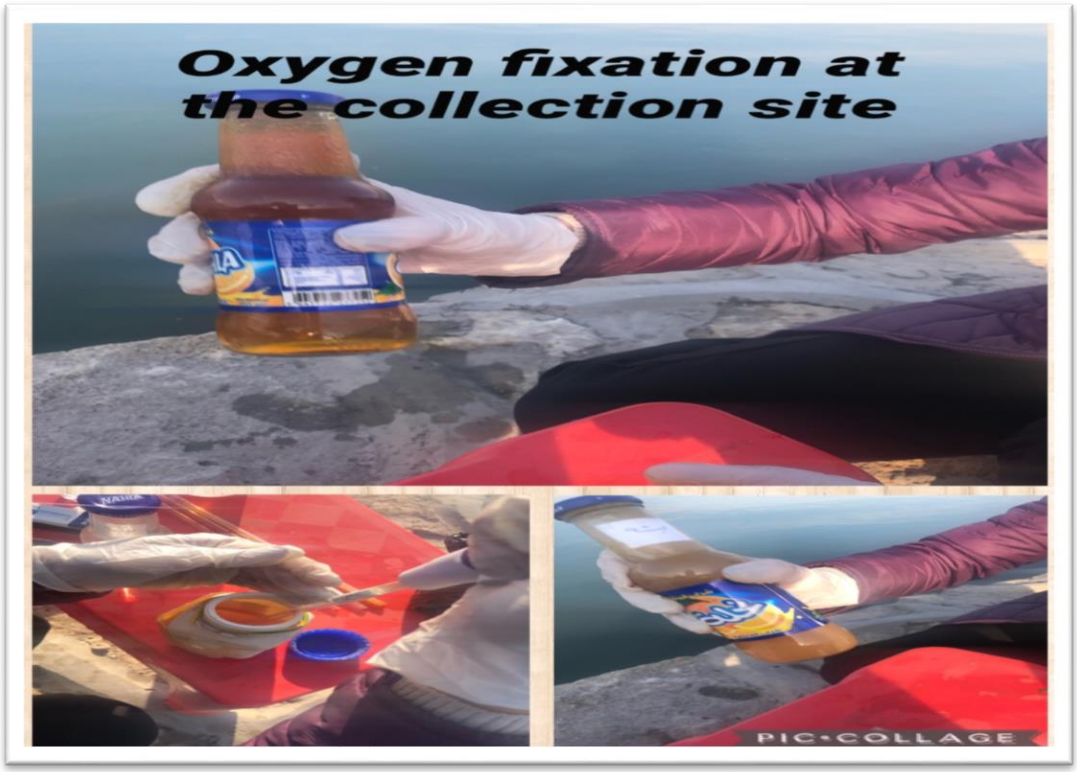

Figure (A-1.3): ***Oxygen fixation at collection site***

Figure (A-1.4): ***Do measurement***

A-1.4: Total dissolved solid. (TDS)

Total dissolved solids were tried with a two-in-one (TDS) squander water quality analyzer, the show HM computerized (COM-100).Measuring TDS entails calibrating the instrument by inserting an electrode in a well-mixed solution and then reading the TDS directly, as seen in Figueroa's diagram (A-1-5).

Figure (A-1.5): ***Total Dissolved Solid Meter***

APPENDIXS

APPENDIX- B

Table (B-1) Computed and observed stage hydrographs in section (65) for different value of manning

time(day)	Observed stage (1/1-30/6/2020)	Compn= (0.038-0.039)	Comp n= (0.04-0.047)	Comp n= (0.045-0.047)	Comp n= (0.047-0.049)	Comp n= (0.05-0.052)
1/1/2020	30	29.88	29.92	30.02	30.06	30.12
1/2/2020	30.03	29.91	29.95	30.05	30.09	30.15
1/3/2020	30.11	29.98	30.02	30.13	30.17	30.23
1/4/2020	30.19	30.06	30.1	30.21	30.25	30.32
1/5/2020	30.25	30.11	30.15	30.27	30.31	30.38
1/6/2020	30.29	30.14	30.19	30.31	30.36	30.43
1/7/2020	30.32	30.17	30.22	30.34	30.39	30.46
1/8/2020	30.32	30.17	30.23	30.35	30.4	30.47
1/9/2020	30.32	30.16	30.22	30.35	30.4	30.47
1/10/2020	30.31	30.16	30.21	30.34	30.4	30.47
1/11/2020	30.31	30.15	30.21	30.34	30.4	30.47
1/12/2020	30.31	30.15	30.21	30.34	30.39	30.47
1/13/2020	30.31	30.15	30.21	30.34	30.39	30.47
1/14/2020	30.31	30.15	30.21	30.34	30.39	30.47
1/15/2020	30.3	30.14	30.2	30.33	30.38	30.46
1/16/2020	30.29	30.13	30.19	30.32	30.37	30.45
1/17/2020	30.28	30.12	30.18	30.31	30.37	30.44
1/18/2020	30.27	30.12	30.17	30.31	30.36	30.44
1/19/2020	30.27	30.11	30.17	30.3	30.36	30.43
1/20/2020	30.24	30.09	30.15	30.28	30.33	30.41
1/21/2020	30.24	30.07	30.12	30.26	30.31	30.39
1/22/2020	30.21	30.06	30.11	30.24	30.3	30.37
1/23/2020	30.19	30.04	30.09	30.23	30.28	30.35
1/24/2020	30.17	30.02	30.07	30.2	30.25	30.33
1/25/2020	30.16	30.01	30.06	30.19	30.24	30.31

APPENDIXS

1/26/2020	30.15	30	30.05	30.18	30.23	30.3
1/27/2020	30.14	30	30.05	30.17	30.22	30.29
1/28/2020	30.15	30	30.05	30.17	30.22	30.29
1/29/2020	30.16	30.01	30.06	30.19	30.24	30.31
1/30/2020	30.18	30.03	30.08	30.2	30.25	30.32
1/31/2020	30.18	30.03	30.08	30.21	30.26	30.33
2/1/2020	30.18	30.03	30.08	30.21	30.26	30.33
2/2/2020	30.18	30.03	30.08	30.2	30.25	30.32
2/3/2020	30.18	30.03	30.08	30.2	30.25	30.32
2/4/2020	30.199	30.04	30.09	30.22	30.27	30.34
2/5/2020	30.2	30.05	30.1	30.23	30.28	30.35
2/6/2020	30.2	30.05	30.1	30.23	30.28	30.35
2/7/2020	30.21	30.06	30.11	30.23	30.28	30.36
2/8/2020	30.21	30.06	30.11	30.24	30.29	30.36
2/9/2020	30.21	30.06	30.11	30.24	30.29	30.36
2/10/2020	30.21	30.06	30.11	30.24	30.29	30.36
2/11/2020	30.2	30.05	30.1	30.23	30.28	30.35
2/12/2020	30.2	30.04	30.1	30.22	30.27	30.35
2/13/2020	30.19	30.04	30.09	30.22	30.27	30.34
2/14/2020	30.19	30.04	30.09	30.22	30.27	30.34
2/15/2020	30.2	30.05	30.1	30.22	30.27	30.35
2/16/2020	30.21	30.06	30.11	30.24	30.29	30.36
2/17/2020	30.22	30.07	30.12	30.25	30.3	30.38
2/18/2020	30.24	30.08	30.13	30.26	30.31	30.39
2/19/2020	30.24	30.09	30.14	30.27	30.32	30.39
2/20/2020	30.26	30.11	30.16	30.29	30.34	30.42
2/21/2020	30.29	30.13	30.19	30.32	30.37	30.44
2/22/2020	30.3	30.15	30.2	30.33	30.39	30.46
2/23/2020	30.3	30.14	30.2	30.33	30.38	30.46
2/24/2020	30.29	30.13	30.19	30.32	30.37	30.45
2/25/2020	30.27	30.11	30.17	30.3	30.35	30.43
2/26/2020	30.28	30.1	30.15	30.29	30.34	30.42
2/27/2020	30.28	30.1	30.16	30.29	30.34	30.42

APPENDIXS

2/28/2020	30.28	30.1	30.16	30.29	30.34	30.42
2/29/2020	30.28	30.1	30.16	30.29	30.34	30.42
3/1/2020	30.28	30.1	30.16	30.29	30.34	30.42
3/2/2020	30.28	30.1	30.16	30.29	30.34	30.42
3/3/2020	30.28	30.1	30.16	30.29	30.34	30.42
3/4/2020	30.28	30.1	30.16	30.29	30.34	30.42
3/5/2020	30.28	30.1	30.16	30.29	30.34	30.42
3/6/2020	30.28	30.1	30.16	30.29	30.34	30.42
3/7/2020	30.28	30.1	30.16	30.29	30.34	30.42
3/8/2020	30.28	30.1	30.16	30.29	30.34	30.42
3/9/2020	30.28	30.1	30.16	30.29	30.34	30.42
3/10/2020	30.28	30.1	30.16	30.29	30.34	30.42
3/11/2020	30.28	30.1	30.16	30.29	30.34	30.42
3/12/2020	30.28	30.1	30.16	30.29	30.34	30.42
3/13/2020	30.27	30.12	30.17	30.31	30.36	30.44
3/14/2020	30.29	30.14	30.19	30.33	30.38	30.46
3/15/2020	30.29	30.15	30.21	30.34	30.39	30.47
3/16/2020	30.33	30.18	30.23	30.37	30.42	30.5
3/17/2020	30.36	30.2	30.26	30.4	30.45	30.53
3/18/2020	30.38	30.22	30.28	30.42	30.47	30.55
3/19/2020	30.39	30.24	30.29	30.43	30.49	30.57
3/20/2020	30.4	30.24	30.3	30.44	30.5	30.58
3/21/2020	30.41	30.25	30.31	30.45	30.51	30.59
3/22/2020	30.42	30.26	30.32	30.46	30.51	30.59
3/23/2020	30.42	30.26	30.32	30.46	30.52	30.6
3/24/2020	30.42	30.26	30.32	30.46	30.52	30.6
3/25/2020	30.43	30.26	30.32	30.47	30.52	30.6
3/26/2020	30.42	30.26	30.32	30.46	30.52	30.6
3/27/2020	30.41	30.25	30.31	30.45	30.51	30.59
3/28/2020	30.41	30.25	30.31	30.45	30.51	30.59
3/29/2020	30.4	30.23	30.29	30.44	30.49	30.57
3/30/2020	30.38	30.21	30.27	30.42	30.47	30.55
3/31/2020	30.37	30.21	30.27	30.41	30.46	30.54

APPENDIXS

4/1/2020	30.37	30.21	30.27	30.41	30.46	30.54
4/2/2020	30.43	30.22	30.28	30.42	30.48	30.56
4/3/2020	30.43	30.23	30.29	30.43	30.49	30.57
4/4/2020	30.41	30.24	30.3	30.44	30.5	30.58
4/5/2020	30.41	30.25	30.31	30.45	30.51	30.59
4/6/2020	30.45	30.26	30.31	30.46	30.51	30.6
4/7/2020	30.45	30.26	30.32	30.46	30.52	30.6
4/8/2020	30.45	30.26	30.32	30.46	30.52	30.6
4/9/2020	30.45	30.26	30.32	30.47	30.52	30.6
4/10/2020	30.43	30.26	30.32	30.47	30.52	30.61
4/11/2020	30.41	30.24	30.3	30.45	30.5	30.58
4/12/2020	30.4	30.21	30.27	30.42	30.47	30.55
4/13/2020	30.36	30.19	30.25	30.4	30.45	30.53
4/14/2020	30.34	30.18	30.24	30.38	30.44	30.52
4/15/2020	30.32	30.16	30.22	30.36	30.42	30.5
4/16/2020	30.3	30.14	30.2	30.34	30.4	30.48
4/17/2020	30.3	30.14	30.2	30.34	30.39	30.47
4/18/2020	30.3	30.14	30.2	30.34	30.39	30.47
4/19/2020	30.3	30.14	30.2	30.34	30.39	30.47
4/20/2020	30.3	30.14	30.2	30.34	30.39	30.47
4/21/2020	30.29	30.13	30.19	30.32	30.38	30.45
4/22/2020	30.27	30.11	30.17	30.3	30.36	30.43
4/23/2020	30.27	30.1	30.15	30.29	30.34	30.42
4/24/2020	30.27	30.09	30.14	30.28	30.33	30.41
4/25/2020	30.27	30.08	30.14	30.27	30.32	30.4
4/26/2020	30.22	30.07	30.12	30.26	30.31	30.38
4/27/2020	30.21	30.05	30.11	30.24	30.29	30.37
4/28/2020	30.2	30.05	30.1	30.23	30.28	30.36
4/29/2020	30.2	30.04	30.09	30.22	30.27	30.35
4/30/2020	30.19	30.03	30.09	30.22	30.27	30.34
5/1/2020	30.18	30.03	30.08	30.21	30.26	30.34
5/2/2020	30.18	30.03	30.08	30.21	30.26	30.33
5/3/2020	30.15	30	30.05	30.18	30.23	30.3

APPENDIXS

5/4/2020	30.11	29.96	30.01	30.13	30.18	30.25
5/5/2020	30.1	29.93	29.98	30.1	30.15	30.22
5/6/2020	30.1	29.91	29.96	30.08	30.12	30.2
5/7/2020	30.04	29.9	29.94	30.06	30.11	30.18
5/8/2020	30.03	29.89	29.93	30.05	30.09	30.16
5/9/2020	30.02	29.88	29.93	30.04	30.08	30.15
5/10/2020	30.01	29.88	29.92	30.03	30.07	30.14
5/11/2020	30.01	29.87	29.92	30.02	30.07	30.13
5/12/2020	30	29.87	29.91	30.02	30.06	30.13
5/13/2020	30	29.87	29.91	30.02	30.06	30.13
5/14/2020	30	29.87	29.91	30.01	30.06	30.12
5/15/2020	30	29.87	29.91	30.01	30.06	30.12
5/16/2020	30	29.87	29.91	30.01	30.05	30.12
5/17/2020	30	29.87	29.91	30.01	30.05	30.12
5/18/2020	30	29.87	29.91	30.01	30.05	30.12
5/19/2020	30	29.88	29.92	30.02	30.06	30.12
5/20/2020	30.02	29.89	29.93	30.04	30.08	30.14
5/21/2020	30.05	29.92	29.97	30.07	30.11	30.17
5/22/2020	30.08	29.95	29.99	30.1	30.14	30.21
5/23/2020	30.1	29.97	30.01	30.12	30.16	30.23
5/24/2020	30.12	29.98	30.03	30.14	30.18	30.25
5/25/2020	30.14	30	30.04	30.15	30.2	30.27
5/26/2020	30.14	30	30.04	30.16	30.2	30.27
5/27/2020	30.13	29.99	30.03	30.15	30.2	30.26
5/28/2020	30.12	29.98	30.03	30.14	30.19	30.26
5/29/2020	30.13	29.99	30.04	30.15	30.2	30.27
5/30/2020	30.14	30	30.05	30.17	30.21	30.28
5/31/2020	30.15	30.01	30.06	30.17	30.22	30.29
6/1/2020	30.16	30.01	30.06	30.18	30.23	30.3
6/2/2020	30.16	30.01	30.06	30.18	30.23	30.3
6/3/2020	30.17	30.01	30.06	30.18	30.23	30.3
6/4/2020	30.17	30.01	30.06	30.18	30.23	30.3
6/5/2020	30.17	30.01	30.06	30.18	30.23	30.3

APPENDIXS

6/6/2020	30.17	30.01	30.06	30.18	30.23	30.3
6/7/2020	30.16	30.01	30.06	30.19	30.24	30.31
6/8/2020	30.16	30.02	30.07	30.19	30.24	30.31
6/9/2020	30.17	30.02	30.07	30.19	30.24	30.31
6/10/2020	30.17	30.02	30.07	30.19	30.24	30.31
6/11/2020	30.19	30.02	30.07	30.2	30.25	30.32
6/12/2020	30.19	30.02	30.07	30.2	30.25	30.32
6/13/2020	30.19	30.02	30.07	30.2	30.25	30.32
6/14/2020	30.19	30.02	30.07	30.2	30.25	30.32
6/15/2020	30.19	30.02	30.07	30.2	30.25	30.32
6/16/2020	30.19	30.02	30.07	30.2	30.25	30.32
6/17/2020	30.19	30.02	30.07	30.2	30.25	30.32
6/18/2020	30.19	30.02	30.07	30.2	30.25	30.32
6/19/2020	30.19	30.02	30.07	30.2	30.25	30.32
6/20/2020	30.19	30.02	30.07	30.2	30.25	30.32
6/21/2020	30.19	30.02	30.07	30.2	30.25	30.32
6/22/2020	30.19	30.02	30.07	30.2	30.25	30.32
6/23/2020	30.19	30.02	30.07	30.2	30.25	30.32
6/24/2020	30.2	30.02	30.07	30.2	30.25	30.32
6/25/2020	30.2	30.02	30.07	30.2	30.25	30.32
6/26/2020	30.2	30.02	30.07	30.2	30.25	30.32
6/27/2020	30.2	30.02	30.07	30.2	30.25	30.32
6/28/2020	30.2	30.02	30.07	30.2	30.25	30.32
6/29/2020	30.2	30.02	30.07	30.2	30.25	30.32
6/30/2020	30.2	30.02	30.07	30.2	30.25	30.32

APPENDIXS

Table (B-2) Simulation of Temp (Cº)

Length (m)	Temp (C°)	Length (m)	Temp (C°)
0	19.96	1000	17.57
1150	19.96	1000	17.5
1000	19.89	800.0001	17.44
900.0001	19.82	1000	17.38
1150	19.75	9550	17.02
1000	19.68	700	16.67
1000	19.61	900.0001	16.61
1000	19.54	950.0001	16.55
4000	19.37	850.0001	16.49
1000	19.2	1000	16.43
1000	19.13	950.0001	16.36
1000	19.06	1000	16.29
950.0001	19	1000	16.22
850.0001	18.94	950.0001	16.16
1000	18.87	1000	16.09
1000	18.8	1000	16.02
1000	18.74	1000	15.95
950.0001	18.67	900.0001	15.89
950.0001	18.6	1000	15.82
1000	18.54	1000	15.76
850.0001	18.47	900.0001	15.69
1000	18.41	1000	15.63
1000	18.34	1000	15.56
850.0001	18.28	1000	15.49
800.0001	18.22	900.0001	15.42
1000	18.16	850.0001	15.36
950.0001	18.09	1000	15.3
800.0001	18.03	950.0001	15.23
1000	17.97	950.0001	15.17
1000	17.9	1000	15.1
1000	17.84	1000	15.03
900.0001	17.77	0	15.03
1000	17.71	**/**	**/**
1000	17.64	**/**	**/**

APPENDIXS

Table (B-3) Simulated of PH (mg/l)

Length (m)	PH (mg/l)	Length (m)	PH (mg/l)
0	7.876	1000	8.22
1150	7.876	1000	8.23
1000	7.887	1000	8.24
900.0001	7.896	800.0001	8.249
1150	7.907	1000	8.258
1000	7.918	9550	8.311
1000	7.928	700	8.363
1000	7.938	900.0001	8.371
4000	7.963	950.0001	8.381
1000	7.988	850.0001	8.39
1000	7.998	1000	8.399
1000	8.009	950.0001	8.409
950.0001	8.018	1000	8.419
850.0001	8.028	1000	8.429
1000	8.037	950.0001	8.439
1000	8.047	1000	8.449
1000	8.057	1000	8.459
950.0001	8.067	1000	8.469
950.0001	8.077	900.0001	8.478
1000	8.086	1000	8.488
850.0001	8.096	1000	8.498
1000	8.105	900.0001	8.508
1000	8.115	1000	8.517
850.0001	8.125	1000	8.528
800.0001	8.133	1000	8.538
1000	8.142	900.0001	8.547
950.0001	8.152	850.0001	8.556
800.0001	8.161	1000	8.565
1000	8.17	950.0001	8.575
1000	8.18	950.0001	8.585
1000	8.19	1000	8.595
900.0001	8.2	1000	8.605
1000	8.209	0	8.605

APPENDIXS

Table (B-4) simulated of DO (mg/l)

Length (m)	DO(mg/l)	Length (m)	DO(mg/l)
0	3.547	1000	3.973
1150	3.547	1000	3.985
1000	3.56	800.0001	3.996
900.0001	3.572	1000	4.007
1150	3.584	9550	4.071
1000	3.597	700	4.133
1000	3.609	900.0001	4.143
1000	3.622	950.0001	4.154
4000	3.652	850.0001	4.165
1000	3.682	1000	4.176
1000	3.695	950.0001	4.188
1000	3.707	1000	4.2
950.0001	3.719	1000	4.212
850.0001	3.729	950.0001	4.224
1000	3.741	1000	4.236
1000	3.753	1000	4.248
1000	3.765	1000	4.26
950.0001	3.777	900.0001	4.272
950.0001	3.789	1000	4.283
1000	3.8	1000	4.296
850.0001	3.812	900.0001	4.307
1000	3.823	1000	4.319
1000	3.835	1000	4.331
850.0001	3.846	1000	4.343
800.0001	3.856	900.0001	4.355
1000	3.867	850.0001	4.365
950.0001	3.879	1000	4.376
800.0001	3.89	950.0001	4.388
1000	3.901	950.0001	4.4
1000	3.913	1000	4.412
1000	3.925	1000	4.424
900.0001	3.937	0	4.424
1000	3.948	**/**	**/**
1000	3.96	**/**	**/**

APPENDIXS

Table (B-5) Simulated of TDS (mg/l)

Length (m)	TDS(mg/l)	Length (m)	TDS(mg/l)
0	989.3	1000	1006
1150	989.3	1000	1006
1000	989.8	800.0001	1006
900.0001	990.2	1000	1007
1150	990.7	9550	1009
1000	991.2	700	1012
1000	991.6	900.0001	1012
1000	992.1	950.0001	1012
4000	993.3	850.0001	1013
1000	994.4	1000	1013
1000	994.9	950.0001	1014
1000	995.4	1000	1014
950.0001	995.8	1000	1015
850.0001	996.2	950.0001	1015
1000	996.7	1000	1016
1000	997.1	1000	1016
1000	997.6	1000	1017
950.0001	998.1	900.0001	1017
950.0001	998.5	1000	1017
1000	998.9	1000	1018
850.0001	999.4	900.0001	1018
1000	999.8	1000	1019
1000	1000	1000	1019
850.0001	1001	1000	1020
800.0001	1001	900.0001	1020
1000	1002	850.0001	1021
950.0001	1002	1000	1021
800.0001	1002	950.0001	1021
1000	1003	950.0001	1022
1000	1003	1000	1022
1000	1004	1000	1023
900.0001	1004	0	1023
1000	1005	**/**	**/**
1000	1005	**/**	**/**

الخلاصة

تم استخدام برنامج HEC-RAS لتحليل التدفق غير المستقر أحادي البعد وتحليل جودة المياه لنهر الفرات (من قناطر الهندية إلى قناطر الكوفة). يمكن استخدام النموذج الهيدروليكي الذي تم تطويره هنا لتحليل ومراقبة وتخمين تدفقات الأنهار وكذلك يوفر وسيلة لفهم وتمثيل الخصائص الهيدروليكية للنهر بينما يمكن استخدام نموذج جودة المياه لتتبع مسار الملوثات على طول منطقة الدراسة .. اذ تم تطبيقه بنجاح على منطقة نهر الفرات ، والتي تتكون من امتداد رئيسي مكون من 65 مقطعًا عرضيًا. فيما يأتي الخطوات التي تم بموجبها إكمال العمل:

في الجانب الهيدروديناميكي وبأستخدام نموذج HEC-RAS تتم معايرة نموذج التوجيه المباشر لنهر الفرات خلال المدة (1/1ولغاية 6/30 لعام 2020). تعد دقة معامل الخشونة المحسوب لمانينغ (n) أمرًا في غاية الأهمية في توقع التنبؤات في العمل على أساس المرحلة المرصودة والبيانات التدفق. نتيجة لذلك ، قيم معامل الخشونة (0.045) و (0.047) هي الأمثل للقناة الرئيسية والسهل الفيضي ، على التوالي ، بالإضافة إلى عامل ترجيح الوقت (θ) ، والذي تم تقديمه هنا كقيمة واحد. لتحديد درجة الاتفاق بين النتائج المرصودة والمحسوبة ، تم استخدام المعلمات الإحصائية مثل جذر متوسط الخطأ التربيعي (RMSE) ومعامل التحديد (.R2= 0.056, 7.453)

لتحليل بيانات جودة المياه ، تم جمع عينات العمل الحقلي على مدى أربعة أشهر (كانون الثاني ، شباط ، اذار و نيسان) اذ كانت المعايير المدروسة لجودة المياه هي [درجة الحرارة (T) ، الحموضة (pH) ، المواد الصلبة الذائبة الكلية (TDS) ، الأوكسجين المذاب (Do)] وبعد ذلك تم إدخال هذه المعلمات إلى برنامج HEC-RSA ، بالإضافة إلى بيانات الأرصاد الجوية التي تم الحصول عليها من مديرية الأرصاد الجوية (بغداد). تمت مقارنة المعلمات المقاسة والمحسوبة لكل مكون ، وأظهرت النتائج توافقًا مقبولًا بين القيم المحسوبة والقيم المرصودة.

سجلت اعلى قيمة لدرجة حرارة الماء عند الساعة (T=34.1C° , 13:30 pm) . أعلى واقل قيمة للاوكسجين المذاب في الماء كانت عند الساعة (DO = 4.9 mg/l, 15:15pm)(DO = 2.45 mg/l, 18:45pm) على التوالي . أعلى واقل قيمة للرقم الهيدروجيني في الماء كانت عند الساعة (PH = 8.03 mg/l, 16:45 pm) (PH = 6.9 mg/l, 1:45Am) على التوالي . أعلى واقل قيمة للمواد الصلبة

الذائبة في الماء كانت عند الساعة (TDS = 1034 mg/l, 9:00 pm)(TDS = 736 mg/l, 1:30Am)
على التوالي.

جمهورية العراق
وزارة التعليم العالي والبحث العلمي
جامعة بابل
كلية الهندسة
قسم الهندسة البيئية

نمذجة هيدروديناميكية ونوعية الماء لنهر الفرات (من سدة الهندية الى سدة الكوفة)

رسالة

مقدمة الى قسم الهندسة البيئية كلية الهندسة

في جامعة بابل كجزء من متطلبات نيل

درجة الماجستير في الهندسة / الهندسة البيئية

من قبل

زينب ناظم هادي الحسيني
بكالوريوس هندسة بيئية, (2012)

اشراف

أ.د. نسرين جاسم حسين المنصوري

1443 AH **2021 AD**